Tubulin and Ivermectin Pharmacology in the Parasitic Nematode *Haemonchus contortus*

Shoaib Ashraf

Institute of Parasitology
McGill University
Montreal, Canada

December 2014

A thesis presented to the Faculty of Graduate Studies and Research in partial fulfillment of the requirements of the degree of Doctor of Philosophy

Abstract

Ivermectin (IVM) is a macrocyclic lactone (ML) endectocide. It acts on the glutamate gated chloride channels and causes paralysis and death of nematode parasites. It is used in veterinary and human health as well as in agriculture. *Haemonchus contortus* (*H. contortus*) is a very pathogenic nematode of livestock. Attempts to control it with anthelmintic pharmaceuticals, such as IVM, has rapidly led to the development of drug resistance against most of the known anthelmintics. *Caenorhabditis elegans* (*C. elegans*) is a free living nematode that can be easily grown and cultivated on culture plates. Both of these nematodes have proven excellent models to study drug resistance mechanisms. Observations that IVM selects on β-tubulin in some nematodes, including *H. contortus* led me to study recombinant *H. contortus* β- and α-tubulins, and microtubules formed when these tubulins polymerize. Unlike mammalian microtubules, we report that *H. contortus* microtubules do not depolymerize under cold conditions. This microtubule resistance to cold may help the free-living stages of this parasite to survive cold climatic conditions. Because of reports that IVM is selecting on nematode tubulin we investigated a possible direct relationship between IVM and tubulins. We demonstrate that IVM is binding at low micromolar concentrations to both *H. contortus* and mammalian tubulins in the taxol binding pocket and that this IVM-mediated effect is reversible. We also demonstrate that the single nucleotide polymorphisms (F200Y and F167Y) on the *H. contortus* β-tubulin, previously reported to increase in frequency with IVM selection, had no apparent effect on IVM binding. We did not find any significant differences in the binding of IVM and moxidectin, another ML, to *H. contortus* and mammalian tubulins. The amphids are sensory structures, rich in dendrites and microtubule bundles. The *C.*

elegans strains N2 (IVM susceptible) and IVR-10 (IVM resistant) were used for lipophilic dye filling and IVM uptake experiments. We found that the IVR-10 strain was dye filling defective, that is the fluorescent dye did not enter the nematode amphids to the same extent as in susceptible nematodes. We also found that IVM may enter through the amphidial pore. These studies provide novel information on nematode tubulins, the role of tubulin in IVM and ML pharmacology and the possible role of amphids and microtubules in IVM uptake in nematodes. The findings advance knowledge of IVM pharmacology and enable better understanding nematode biology.

Résumé

L'ivermectine (IVM) est une lactone macrocyclique (ML) endectocide. Elle agit sur les canaux chlorures glutamate-dépendants et entraîne la paralysie et la mort des parasites nématodes. L'IVM est aussi bien utilisée en médecine vétérinaire et humaine qu'en agriculture. *Haemonchus contortus* (*H. contortus*) est un nématode de bétail très pathogène. L'utilisation d'anthelminthiques, comme l'IVM, a été largement -préconisée pour contrôler ce parasite. La résistance à la plupart des anthelminthiques s'est rapidement développée. *Caenorhabditis elegans* (*C. elegans*) est un nématode libre qui peut facilement être cultivé sur des plaques de culture. Ces deux nématodes sont d'excellents modèles pour étudier les méchanismes de résistance aux médicaments. L'ivermectine sélectionne la ß-tubulin chez des nématodes notamment chez *H. contortus*. L'objectif de cette étude était d'étudier l'α- et la ß-tubuline recombinante d'*H. contortus* ainsi que les microtubules formées lors de la polymérisations de ces tubulines. Nous avons observé qu'à la différence des microtubules de mammifères, les microtubules d' *H. contortus* ne se dépolymérisaient pas avec le froid. Cette résistance au froid des microtubules pourrait aider les stades libres de ce parasite à survivre dans des conditions climatiques froides.

Nous avons aussi investigué la possible relation directe entre l'IVM et les tubulines. Nous avons démontré que l'IVM se fixait à faible concentration micromolaire aussi bien sur les tubulines *d'H. contortus* que sur les tubulines de mammifères au niveau de la zone de fixation du taxol et que cet effet était réversible. Nous avons aussi démontré que chez *H. contortus*, les polymorphismes mononucléotidiques (F200Y et F167Y), connus dans la sélection à l'IVM, n'avaient pas d'effet sur la fixation de l'ivermectine sur la ß-tubuline.

Nous n'avons pas trouvé de différences significatives entre la fixation de l'IVM et de la moxidectine (un autre ML) sur les tubulines d'*H. contortus* et de mammifères.

Les souches N2 (sensible à l'IVM) et IVR-10 (résistante à l'IVM) de *C. elegans* ont été utilisées lors d'expériences d'absorption de l'IVM et de remplissage avec des colorants lipophiles. Nous avons montré que la souche IVR-10 ne permettait pas à un colorant fluorescent de bien pénétrer par les amphides de ces nématodes résistants contrairement aux amphides des nématodes sensible à l'IVM. Nous avons observé que l'IVM pouvait entrer par les pores amphidiaux. Les amphides sont des structures sensorielles riches en dendrites et en faisceaux de microtubules. Ces études fournissent de nouvelles informations sur les tubulines des nématodes, le rôle des tubulines dans la pharmacologie de l'IVM et des MLs et le possible rôle des amphides et des microtubules dans l'absorption de l'IVM par les nématodes. Ces conclusions contribuent à une meilleure connaissance de la pharmacologie de l'IVM et une meilleure compréhension de la biologie des nématodes.

Acknowledgements

I would like to thank the creator for giving me the wisdom to grasp knowledge, for providing me with everything that I just wish, and for making me whatever I am. I want to thank my parents and siblings for providing a solid background which enables me to cope with the modern scientific era, and excel in life. I would like to thank my wife without whom it would have been difficult to manage things during my PhD. I want to thank my son Mohid who eased me during times of stress. I would like to express gratitude to my supervisor Dr. Roger Prichard for accepting me as a graduate student and for his valuable scientific approach. I would also like to thank him for his financial support. I wish that everyone can have a professor like him. I can never forget Ms Kathy Keller who contributed so much towards the successful completion of my project/thesis. I would also like to thank all my new and old lab-mates including Dr. Catherine, Dr. Ludmel, Dr. Vijay, Pablo, Durai, Marion, Phil, Dr. Virginie, Dr. Aissatou and others. I would like to thank Dr. Mark Hancock, Dr. Robin Beech, Dr. Jerry Aldridge, Dr. Armando Jardim, Dr. Tim Geary and Dr. Reza Salavati. I would like to thank Serge for his help in immunofluorescence, and Hamid, and Anwer for giving me such a nice company. I acknowledge the Professors, seniors, staff members and students of the Institute of Parasitology, McGill University, for creating such a friendly and excellent research environment. At last but not the least I would like to thank Shirley for her help and acknowledge the efforts by my dear friend Umer Naveed Ch who always supported me in scientific discussions, and all other friends who I have not mentioned for their supportive attitude.

Contribution of authors

The experiments were designed and carried out by S.A. (Shoaib Ashraf) under the supervision of Dr. Roger Prichard. He provided intellectual input, the laboratory space, financial support and resources to conduct the experiments. For Chapter II (manuscript I) and Chapter III (manuscript II), the electron microscopy was done at the Electron Microscopy Facility, McGill University by Jeannie Mui and S.A. For Chapter III (manuscript II) Dr. Robin Beech performed the molecular docking studies, and Dr. Mark Hancock performed the surface plasmon resonance work. Dr. Robin Beech also performed the molecular docking studies for Chapter IV (manuscript III), and Thangadurai Mani made editorial contributions throughout the thesis. This thesis inclusive of all chapters was written by S.A. with contributions from my supervisor, Dr. Roger Prichard.

Statement of originality

To the best of the author's knowledge the manuscripts obtained in this thesis contributed original material and advancement of knowledge to the field.

Manuscript I: S. Ashraf, R.K Prichard (2014). *Haemonchus contortus* microtubules are cold resistant. Molecular and Biochemical Parasitology, 193: 20-22

In this manuscript the authors describe the behavior of microtubules of *Haemonchus contortus* in vitro. The authors also describe the effects of various chemicals on these microtubules.

Manuscript II: S. Ashraf, R.N. Beech, M.A. Hancock, R.K. Prichard. Ivermectin exhibits potent anti-mitotic activity: from anti-parasitic drug to novel anti-cancer candidate. (Submitted to Biochemical Pharmacology)

In this manuscript the authors describe for the first time evidence of a direct interaction between ivermectin and parasitic and mammalian tubulins. They also demonstrate the effect of ivermectin on replication of HeLa cells.

Manuscript III. S. Ashraf, R.N. Beech, T. Mani, R.K. Prichard. Macrocyclic lactones and their relationship to the SNPs related to benzimidazole resistance. (Manuscript in preparation).

In this manuscript the authors describe the differences in polymerization dynamics between wild type and F167Y and F200Y mutant tubulins. The binding of ivermectin

with mutant tubulins has also been described. Finally differences between the binding of ivermectin and moxdectin with the mutant tubulins have also been studied.

Manuscript IV. S. Ashraf, R.K. Prichard. Amphids: A possible route of entry for ivermectin. (Manuscript in preparation)

In this manuscript the authors describe dye filling and ivermectin uptake experiments on ivermectin susceptible and resistant *Caenorrhabditis elegans* strains.

List of abbreviations

BSA, bovine serum albumin

BZ, benzimidazole

C_{max}, maximum plasma concentrations

cDNA, complementary deoxyribonucleic acid

DAPI, 4',6-diamidino-2-phenylindole

DMSO, Dimethyl sulphoxide

GABA, γ-aminobutyric acid

GluCl, glutamate-gated chloride channel

HeLa, Henrietta Lacks

IPTG, isopropyl-β-D-thiogalactoside

IVM, Ivermectin

Lev, levamisole

LGIC, ligand-gated ion channel

ML, Macrocyclic lactones

MSD, Merck Sharpe and Dohme

OD, optical density

PCR, polymerase chain reaction

PF23, Laboratory strain of *H. contortus* which is sensitive to ivermectin and moxidectin

SNP, single nucleotide polymorphism

SPR, surface plasmon resonance

WT, wild type

Table of Contents

List of Figures

Chapter II

Chapter III

Chapter IV

Chapter IV

Introduction

Ivermectin is a drug used globally against various important veterinary and human parasites. It is the anthelmintic most often purchased generating business in the billions of dollars over the last 25 years and has been given titles such as ‘miracle drug’ (Omura and Crump, 2004) and ‘wonder drug’ (Geary, 2005). It has been shown that ivermectin binds to the glutamate gated chloride channels and causes paralysis and death of the parasite (Cully et al., 1994; Hibbs and Gouaux, 2011). Many field studies have been conducted to detect the prevalence of resistance to this drug. However, much is to be done to understand the mechanism of development of resistance. Unlike benzimidazoles, resistance to ivermectin is believed to be multigenic. Ivermectin is successfully used to treat internal and external parasites. Ivermectin resistance have jeopardized the socioeconomic situation of farmers, owners of companion animals and humans suffering from ecto and endo parasites.

Haemonchus contortus is a parasite found in the abomasum of sheep, goats and cattle. It feeds on blood, causes production losses and even death of the young livestock or weak adults. This results in huge losses to the farmers if the disease that it causes, haemonchosis, is not adequately controlled. The methods most often used to treat haemonchosis is through chemical treatment with anthelmintic pharmaceuticals. The most frequently used drugs are ivermectin, other related macrocyclic lactones, benzimidazoles and levamisole. Extensive use of these drugs has led to drug resistance. Drug resistance in now a worldwide issue and is characterized by a decrease in drug efficacy. Nematodes tubulins are of interest because the evidence suggests they are

targets of BZ anthelmintics and there was evidence that MLs are also selecting on β-tubulin.

The first manuscript for my PhD is about tubulins of *Haemonchus contortus* i.e. polymerized *H. contortus* tubulin is resistant to cold temperatures. This may be one reason why these parasites, which were considered to be parasites of temperate areas, are also prevalent in areas of cold climate such as Canada i.e. these parasites survive cold conditions.

The second paper was to investigate whether tubulin has an ivermectin binding site. This hypothesis was built on the fact that a genetic association between ivermectin and β-tubulin was previously reported (Eng and Prichard, 2005; Eng et al., 2006; Bourguinat et al., 2007; de Lourdes Mottier and Prichard, 2008; Nana-Djeunga et al., 2012; Osei-Atweneboana et al., 2012). It gave a deeper insight into the mechanism of drug action and this will be beneficial to design strategies to delay the process of development of resistance to benzimidazoles and macrocyclic lactones. Once it was established that ivermectin binds with parasite tubulin the next step was to explore its possible effects on mammalian tubulin. The results suggest that ivermectin can indeed bind to both parasitic and mammalian tubulin and this may open new avenues for its use as an anti-cancer agent.

The third paper was an attempt to unveil the reason why polymorphisms are being selected in *H. contortus* β-tubulin by repeated ivermectin selection (Eng and Prichard, 2005; Eng et al., 2006; de Lourdes Mottier and Prichard, 2008). The first hypothesis was that single nucleotide polymorphisms (F200Y and F167Y) may alter tubulin dynamics and ivermectin binding to tubulin. The second hypothesis was to check

if there was a difference between moxidectin and ivermectin on polymerization of microtubules. Contrary to our results the single nucleotide polymorphisms did not have any effect on tubulin polymerization, furthermore ivermectin also bound to tubulin in the presence of these polymorphisms. The comparison of moxidectin and ivermectin however showed us different results between parasitic and mammalian tubulins.

The fourth paper was using *Caenorhabditis elegans* as a model to study the amphidial pore and amphidial neurons. We report that the amphids of an ivermectin resistant strain (IVR-10) are shortened which resulted in a dye filling defective phenotype. We also report the amphidial pore as a possible alternative route of entry for ivermectin.

Altogether my thesis is about the pharmacology of ivermectin and its relationship with tubulin and amphids in *Haemonchus contortus* and *Caenorhabditis elegans*.

Reference

Bourguinat, C., Pion, S.D., Kamgno, J., Gardon, J., Duke, B.O., Boussinesq, M., Prichard, R.K., 2007. Genetic selection of low fertile Onchocerca volvulus by ivermectin treatment. PLoS neglected tropical diseases 1, e72.

Cully, D.F., Vassilatis, D.K., Liu, K.K., Paress, P.S., Van der Ploeg, L.H., Schaeffer, J.M., Arena, J.P., 1994. Cloning of an avermectin-sensitive glutamate-gated chloride channel from Caenorhabditis elegans. Nature 371, 707-711.

de Lourdes Mottier, M., Prichard, R.K., 2008. Genetic analysis of a relationship between macrocyclic lactone and benzimidazole anthelmintic selection on Haemonchus contortus. Pharmacogenetics and genomics 18, 129-140.

Eng, J.K., Blackhall, W.J., Osei-Atweneboana, M.Y., Bourguinat, C., Galazzo, D., Beech, R.N., Unnasch, T.R., Awadzi, K., Lubega, G.W., Prichard, R.K., 2006. Ivermectin selection on beta-tubulin: evidence in Onchocerca volvulus and Haemonchus contortus. Molecular and biochemical parasitology 150, 229-235.

Eng, J.K., Prichard, R.K., 2005. A comparison of genetic polymorphism in populations of Onchocerca volvulus from untreated- and ivermectin-treated patients. Molecular and biochemical parasitology 142, 193-202.

Geary, T.G., 2005. Ivermectin 20 years on: maturation of a wonder drug. Trends in parasitology 21, 530-532.

Hibbs, R.E., Gouaux, E., 2011. Principles of activation and permeation in an anion-selective Cys-loop receptor. Nature 474, 54-60.

Nana-Djeunga, H., Bourguinat, C., Pion, S.D., Kamgno, J., Gardon, J., Njiokou, F., Boussinesq, M., Prichard, R.K., 2012. Single nucleotide polymorphisms in beta-tubulin selected in Onchocerca volvulus following repeated ivermectin treatment: possible indication of resistance selection. Molecular and biochemical parasitology 185, 10-18.

Omura, S., Crump, A., 2004. The life and times of ivermectin - a success story. Nature reviews. Microbiology 2, 984-989.

Osei-Atweneboana, M.Y., Boakye, D.A., Awadzi, K., Gyapong, J.O., Prichard, R.K., 2012. Genotypic analysis of β-tubulin in Onchocerca volvulus from communities and individuals showing poor parasitological response to ivermectin treatment. International journal for parasitology: Drugs and drug resistance 2, 20-28.

Chapter I

Literature review

1.1 Anthelmintics

Helminths are a major problem in reducing the productivity and health of livestock and humans. They are arguably of relatively greater importance for domestic animals than humans (Waller, 2003). Massive farming practices, access to infective stages while grazing make herbivores an easy prey for many helminths. As a consequence anthelmintics, which are drugs used to control helminths, comprise the largest sector of the animal pharmaceutical industry.

Three centuries ago treatment of parasites started with crude extracts of plants or metals which mechanically irritated worms away from their predilection sites or dislodged them by removing the mucous. Some commonly used remedies were: salt, turpentine oil, calomel, arsenic and aloes (Blane, 1826). In the next century (20^{th} century) the progress was slow with the introduction of nicotine sulphate and carbon tetrachloride. In 1940 and 1954 the first compounds, phenothiazine and piperazine, respectively appeared in the market with real activity against target parasite species. The discoveries of anthelmintics such as thiabendazole in 1960 and levamisole in 1980 were of greater significance with therapeutic doses at milligram per kg rather than gram per kg. In 1981 a step forward was made with the introduction of ivermectin in the animal health industry at a dosage of microgram per kg. Derquantel a nicotinic acetylcholine antagonist has also been recently introduced into the market (Robertson et al., 2002; Little et al., 2010). In 2008, a new class of anthelmintic called amino-acetonitrile derivatives (nicotinic acetylcholine receptor agonists) was introduced into the veterinary pharmaceutical industry (Kaminsky et al., 2008).

The major classes of broad spectrum anthelmintics include benzimidazoles (BZ), imidathiozoles (e.g. levamisole) and the tetrahydropyrimidines (e.g. pyrantel), and macrocyclic lactones (MLs). All these classes have different modes of action, with BZs acting on β-tubulin, imidathiozoles on nicotinic receptors and MLs on the ligand-gated-chloride channels. Some of the important BZs include albendazole, fenbendazole, mebendazole, ricobendazole, oxfendazole and oxibendazole. Most widely used imidathiozoles are levamisole and tetramisole. Commonly available MLs are: Avermectins (ivermectin, abamectin, eprinomectin, doramectin), milbemycins (moxidectin, milbemycin oxime). To increase the broad spectrum activity and delay the development of resistance different treatment regimes have been developed for the use of anthelmintics. For example combinations of MLs with BZs and rotation between MLs and BZs have been adopted for treatment of various infections in human and veterinary practice.

1.2 Benzimidazole (BZ)

BZs are extensively used in veterinary and human practice. Initial studies of the mechanism of action of BZ suggested generalized biochemical responses including its inhibitory effect on glucose uptake and glycogen storage. The first link between BZ and microtubules was established when ultra-structural studies in the intestinal cells of Ascaris and Syngamus revealed disruption of the microtubule network by mebendazole (Borgers et al., 1975). Subsequent studies were focused on the molecular basis of the mode of action. There has been a consensus that BZ drugs inhibit the formation of microtubules by directly binding to the β-tubulin monomer or α/β-dimer in helminths thus inhibiting its polymerization (Lubega and Prichard, 1990). This disruption leads

towards failure to transport secretary granules or enzymes within the cell and eventually results in lysis and cell death (Lacey, 1988). β-tubulin from *H. contortus* was amongst the first tubulin gene sequenced from a parasitic nematode (Geary et al., 1992). It is proposed and arguably agreed that the specific binding site of BZ is between the phenylalanine at position 167 and 200 of β-tubulin isotype1 (Prichard, 2001; Robinson et al., 2004).

The binding of BZs is believed to be near the colchicine binding site (1-36 and 216-243 in the β-tubulin) and near the GTP binding domain (the loops T1-T7 in β-tubulin are in direct contact with the nucleotides), it either interferes with nucleotide exchange or prevents the self-association of subunits onto the growing microtubules and stops the elongation of the polymer. This results in capping of the microtubule at the associating end while the microtubule continues to dissociate from the opposite end, with a net loss or depolymerization of microtubule (Lacey, 1990).

1.3 Discovery of ivermectin

Serendipity has an important role in scientific research so it proved in the case of the drug ivermectin. The discovery of ivermectin came through the collaboration between Kitasato Institute in Japan and the Merck, Sharpe and Dohme (MSD) research laboratories in the United States. As a result of this partnership, avermectin was identified in 1970s in Japan as a fermentation product of the actinomycete *Streptomyces avermetilis*. In 1979, the first papers were published on avermectins describing it as a ML with powerful anthelmintic activity. Early chromatographic studies revealed that avermectin contained a complex of four major components in varying proportions. The

major components comprised A1, A2, B1 and B2, each with two variants designated as "a" and "b" (A_{1a}, A_{1b}, A_{2a}, A_{2b}, B_{1a}, B_{1b}, B_{2a} and B_{2b}). The homologue "a" carried more potent anthelmintic activity than the corresponding "b" component. Among the 8 compounds B_{1a} and B_{1b} had the most potent anthelmintic activity and reduction of the double bond C_{22}–C_{23} increased its spectrum and safety. As a result the semisynthetic analogue 22, 23-dihydro B_1 complex containing a mixture of at least 80% avermectin B_{1a} and 20% avermectin B_{1b} was selected for commercial development and was given the generic name ivermectin.

In 1981 ivermectin was registered for use in veterinary medicine as an antiparasitic drug with activity against nematodes, fleas, lice, flies, ticks and mites. It is active against ecto- and endoparasites and is the first endectocide registered. It soon proved the most effective, broad spectrum anthelmintic ever developed and became the market leader within two years of its development. Currently it is being used in more than 46 countries generating annual sales of over US$ 2 billion. After five years of its introduction it was being used to treat approximately 320 million cattle, 151 million sheep, 5.7 million pigs and 21 million horses (TDR, 1995). When researchers at MSD demonstrated that ivermectin was effective against the horse nematode *Onchocerca cervicalis* work also began for its possible use against *Onchocerca volvulus* (causative agent of river blindness) in humans. In 1985 after extensive field trials the drug was approved for the treatment of river blindness (Omura and Crump, 2004). The application of ivermectin has not been limited to veterinary and human use, it is also being used as an agricultural pesticide.

Ivermectin has been in the market for almost a quarter of a century but in these 25-years much remains to be learned about how this drug works and how resistance develops and so has earned the title of a ‘wonder drug’ (Geary, 2005). Though being a broad spectrum endectocide it is not effective against cestodes and trematodes as these helminths lack ivermectin sensitive channels.

1.4 Mechanism of action

Ivermectin binds to the glutamate-gated chloride channels and causes hyperpolarization and leads to paralysis of the nematodes (Geary, 2005; Omura and Crump, 2004). Two main types of effects have been observed when ivermectin is applied to nematodes, that is, rapid paralysis of: pharyngeal pumping (~0.1 nM) and movement (~10 nM). As a result the worms are not able to feed or move and are eventually expelled out of the host. A third type of effect of ivermectin has been seen against nematode reproduction, that is, long lasting reduction in the production of new eggs or microfilariae probably because ivermectin may act on the GluCls present on the muscle of the uterus this prevents the release of eggs or microfilariae. The forth type of effect on the killing of microfilariae (mf) may be due to ivermectin acting on GluCl associated with the excretory cell/pore preventing release of proteins and having an effect on host immune response (Moreno et al., 2010) These four effects together predict that there are four possible mechanisms of ivermectin action (1) pharyngeal paralysis, (2) body muscle paralysis, (3) paralysis of the uterus (Wolstenholme and Rogers, 2005) (4) paralysis of the excretory pore/altered host immune regulation (Moreno et al., 2010).

Initial data suggests ivermectin acted on γ-amino-n-butyric acid (GABA) receptors as a GABA agonist, a neurotransmitter which opens chloride-channels and allows inflow of chloride ions resulting in induction of resting potential (Pony et al., 1980). The GABA receptors are present in both invertebrates and mammals and were thought to be the primary inhibitory neurotransmitter in the nematode somatic neuromuscular system. However, the dose required to achieve this effect was too high to be clinically relevant (100 µM), furthermore in some experiments ivermectin inhibited GABA receptor channels rather than opening them (Holden-Dye and Walker, 1990). These observations led the scientific community to search for alternative chloride-channels as likely targets for ivermectin. Later on it was proven by work from scientists of Merck that glutamate-gated-chloride channels are the primary targets for ivermectin in nematodes (Cully et al., 1994). These ligand-gated chloride channels are absent in vertebrates but have a major role in nematodes and arthropods. It is now accepted that the nematocidal activity of ivermectin is caused by paralysis of the parasite by binding to the glutamate-gated or GABA-gated chloride channels which irreversibly opens and causes hyperpolarization in the muscle and nerve cells (Feng et al., 2002). The crystal structure of ivermectin bound to the GluCls was recently resolved. In this model ivermectin bound between the M1 and M3 membrane spanning domains of adjacent subunits and thus opens the channel by pushing the membrane spanning regions of subunits apart (Hibbs and Gouaux, 2011).

1.5 Development of anthelmintic resistance

Resistance has been defined as a "reduction in the efficacy of a drug against a population of parasites which are usually susceptible to this drug by a specific dose or concentration" (Prichard et al., 1980) or "when a greater concentration of drug is required to reach a certain level of efficacy" (Wolstenholme et al., 2004). The wide spread use of anthelmintics began in 1961 after the introduction of BZs and the outcome of this massive chemical assault on helminths was inevitably resistance (Kaplan, 2004). The process has been particularly rapid in nematodes of small ruminants and now it has spread to an extent that it is of great concern throughout the world.

Nematode populations are diploid groups of organisms which breed sexually, appear to be genetically heterogeneous and thus respond to selection pressure such as anthelmintic drugs (Prichard, 2001). Anthelmintic resistance occurs when the worms that resist the treatment survive and susceptible worms die. Resistant worms mate and the frequency of alleles responsible for resistance increases (Prichard, 1990). With the passage of time due to continued selection pressure, resistance alleles dominate the population and eventually the outcome is failure of treatment. The rate at which resistance spreads in the parasite population is dependent on a number of factors including: drug pressure, the frequency of resistant alleles in the population, the dominance or recessiveness of genes, and gene flow (Grant, 1994). In addition, any fitness cost of resistance may influence the rate of development of resistance (Urdaneta-Marquez et al., 2014).

1.6 Resistance to benzimidazoles

Early observations on fungi suggest a relationship between mutation in β-tubulin and resistance to BZs. Later it was shown by Lubega and Prichard (1990) that binding characteristics of BZ with β-tubulin were different in resistant and susceptible parasites. They showed that more drug bound to BZ susceptible rather than to the BZ resistance worms. In field isolates, an allele in which single nucleotide polymorphisms (SNPs) replaced phenylalanine with tyrosine on β-tubulin isotype1 was more prevalent in the resistant as compared to the susceptible parasites (Beech et al., 1994). (Kwa et al., 1995) demonstrated using transgenic *Caenorhabditis elegans* (*C. elegans*) that Phe200Tyr was the only substitution required by the parasite to confer resistance against BZs. Subsequent to this, some studies have shown that SNPs in β-tubulin isotype1 (phenylalanine to tyrosine) at codon 167, and (glutamate to alanine) at codon 198 can also confer resistance to BZs (de Lourdes Mottier and Prichard, 2008; Ghisi et al., 2007; Prichard, 2001).

While BZ resistance seems to be mainly due to allelic changes in β-tubulin isotype1, there is evidence that efflux mechanisms involving P-glycoproteins or other ABC transporters, may contribute to benzimidazole resistance (Blackhall et al., 2008; Kerboeuf et al., 2003; Nare et al., 1994).

1.7 Resistance to ivermectin

Drug resistance to ivermectin has been reported in many parts of the world in parasites of livestock (Wolstenholme and Rogers, 2005; Wolstenholme and Kaplan, 2012) and humans (Osei-Atweneboana et al., 2007). As compared to BZs the mechanism of resistance to ivermectin seems to be more complex and polygenic which means the

drug selected population may have more than one mechanism of drug resistance. Some of the factors involved in ivermectin resistance are as below.

1.7.1 Ligand-gated ion channels

γ-aminobutyric acid-gated chloride channels (GABA-Cl) and glutamate-gated chloride channels (Glu-Cl) are members of the ligand-gated ion channel family (Clevland, 1996). GABA-Cls are present in both vertebrates and invertebrates, whereas Glu-Cls are present in invertebrates and have not yet been identified in any vertebrate species. Glu-Cls are composed of five subunits forming a ring shaped structure. The α-subunit of Glu-Cls has been proposed as the main target site of ivermectin and it has been observed that mutating three α-subunit genes (*avr-14*, *avr-15*, and *glc-1*) confers loss of susceptibility to ivermectin (Dent et al., 2000). The genetic selection for ligand-gated ion channels is also evident in ivermectin resistant populations of *H. contortus* (Blackhall et al., 2003).

1.7.2 P-glycoprotein (PGP)

P-glycoproteins (PGP) are ATP-binding cassette transport proteins which function as ATP-dependant transport pumps (Aouali et al., 2005). PGPs can bind to the neutral or positively charged hydrophobic drugs. The pump causes efflux of a diverse range of molecules from interior to the exterior of the cell membrane by utilizing ATP. PGP substrates are mostly lipophilic, amphiphatic and have a ring structure. Many of these properties are similar to ivermectin which makes it a candidate ligand for PGP.

Over expression of PGP has been observed in ivermectin selected *H. contortus* (Xu et al., 1998). There has also been supporting evidence that PGPs were involved in ivermectin resistance by showing allele selection in a PGP gene in ML selected *H. contortus* (Blackhall et al., 1998; Sangster et al., 1999). Interaction between the polylinker domain of PGP (ABCB1) and α- and β-tubulin has also been demonstrated (Georges, 2007). It has been thought that this interaction is part of a signaling pathway and any distortion in microtubules may lead to enhanced production of PGP as a general defense mechanism of the cell which eventually leads towards efflux of the drug (Georges, 2007). The fact that ivermectin and BZs select on some PGPs has important implications for the choice of anthelmintics in drug rotation or combination schemes to reduce the selection for anthelmintic resistance.

1.7.3 Tubulin and microtubules

Microtubules are hollow cylindrical filamentous structures present in most cells of eukaryotes with an approximate outer diameter of 25 nm and lumen diameter of 15 nm (Lacey and Gill, 1994). They are formed by different soluble subunits of α and β-tubulin separated by a protease sensitive site near residue 339 for α-tubulin and residue 281 for β- tubulin (Sullivan, 1988). The subunits have over 40% similarity in their nucleotide sequence. Each subunit is comprised of about 450 amino acids with a molecular weight of approximately 50 kDa (Lacey and Gill, 1994).

When tubulin subunits reach a certain threshold they associate in a head to-tail fashion to form linear hollow tube shaped structures called protofilaments which then associate through side-to-side lateral interactions to form microtubules (Aamodt and Culotti, 1986). The number of protofilaments that form microtubules in nematodes are 11

to 15 (Chalfie and Thomson, 1979). The assembly and disassembly of tubulin subunits require different processes such as binding, exchange of GTP and hydrolysis. During the elongation phase the tube is prevented from depolymerization by a GTP cap. The GTP-cap is removed after prolonged elongation which exposes the GDP bound to β-tubulin and results in depolymerization and growth ceases. Polymerization is resumed when the GDP is exchanged for GTP from the microtubule.

Microtubules are in dynamic equilibrium with the dimers, as soluble tubulin DIMERS are added and subtracted on opposite ends of the insoluble microtubule in a "treadmilling" fashion (Lacey, 1988). The equilibrium may be disturbed by changes in temperature or by endogenous co-factors, such as GTP, Mg^{2+}, Ca^{2+} and microtubule associated proteins (MAPs) (Lacey and Gill, 1994). Thus, by varying temperature and different co-factors, microtubules can be assembled and disassembled *in vitro* using purified recombinant tubulins (Oxberry et al., 2001).

Microtubules are involved in many cellular processes including cell signaling, extracellular secretion, cell division, intracellular transport, cell morphology, chromosomal segregation, and cell motility. As tubulin is virtually connected to every cellular organelle, this makes its normal functioning necessary for survival of the nematode (Aboobaker and Blaxter, 2003). Genetic and biochemical evidence suggest that β-tubulin has a more critical role in drug resistance than α-tubulin. β-tubulins are grouped into 6 isotype classes that are highly conserved in many vertebrates (Sullivan, 1988). In *H. contortus,* four β-tubulin DNA sequences (Laing et al., 2013; Saunders et al., 2013; Schwarz et al., 2013) and one α-tubulin DNA sequence have been isolated (Klein et al., 1992; Laing et al., 2013; Schwarz et al., 2013)**.** The dynamic structure of

tubulin has made it a target for the development of many antimitotic drugs like colchicine, taxol and vinblastine. BZs other than being known as an anthelmintic also possess antimitotic activity.

To-date there is a lack of evidence of any direct involvement of β-tubulin with ivermectin resistance. Blackhall (1999) identified changes in β-tubulin allele frequencies in ivermectin selected *H. contortus* as compared to the parent strain. PhD Thesis. He hypothesized that ivermectin selection on β-tubulin was because of its genetic linkage to another gene on the same chromosome involved in resistance.

Kneussel and Betz (2000) have provided evidence that microtubules were involved in anchoring GABA and glycine ion channels in the membrane of synaptic junctions. It is therefore possible that microtubules may play a similar role in localizing surface receptors involved in ivermectin binding (GluCl and GABA-Cl). Thus the selection of a particular gene product allele (GluCl and GABA-Cl) from ivermectin treated worms may cause selection for a particular β-tubulin allele.

Experimental data further suggest ivermectin was selecting for SNPs on β-tubulin isotype1. It is not known whether changes in β-tubulin isotype1 have to do something directly or indirectly with the mechanism of ivermectin resistance. Eng and Prichard (2005) have identified changes in allele frequency of β-tubulin in *Onchocerca volvulus* (*O. volvulus*) by RFLP and SSCP following multiple yearly treatment with ivermectin, furthermore they also reported ivermectin is selecting on β-tubulin in *H. contortus* (Eng et al., 2006). Sequencing of the two β-tubulin alleles have shown three amino acid substitutions in third α-helix (H3) M to A,V to I, V to L interacts with the M-loop of the adjacent β-tubulin in the formation of microtubules (Lowe et al., 2001).

Mutations in the H3 may change the overall stability of the microtubules and result in a resistant phenotype.

Despite distinct mechanisms of action of ivermectin and BZs, de Lourdes Mottier and Prichard(2008) have identified SNPs (TTC200TAC and TTC167TAC) in *H. contortus* ivermectin resistant laboratory strains never exposed to BZs. There has also been recent evidence of selection of ivermectin on β-tubulin in *O. volvulus* (Nana-Djeunga et al., 2012; Osei-Atweneboana et al., 2012). These unexpected observations cannot be due to bottlenecking as in bottlenecking, rare alleles are lost and the common alleles increase in frequency, which indicates that this may be due to drug selection. In association with ivermectin resistance, SNP Phe200Tyr has been found in higher frequency than SNP Phe167Tyr.

1.7.4 Amphids

Amphidial neurons are neurons present in the nematode and are required for chemosensing (Fujii et al., 2004). They are located in the anterior head of the nematode where they form an amphid pore supplied with dendritic processes. By the help of these processes the nematode can taste the environment. Amphids aid in finding suitable mates, avoiding toxic substances, such as drugs, and react to food (Ashton et al., 1999; Starich et al., 1995).

Experimental evidence with the gastro-intestinal nematodes suggest that one mode of entry of ivermectin is via the oral pharyngeal route. In *C. elegans* the drug targets the glutamate-gated chloride channel (Glu-Cl) and causes flaccid paralysis of the nematode (Cully et al., 1994). However, Smith and Campbell, (1996) demonstrated

suppression of pharyngeal pumping by temporarily inducing paralysis of *C. elegans* by soaking the worms in 0.15% 1-phenoxy-2-propanol. If the worms were then placed in ivermectin they remained paralyzed as compared to the control worms placed in water. These interesting findings suggest an alternative route of entry other than the oral pharyngeal route.

Possible alternative routes could be a cuticular uptake mechanism and/or uptake via the anterior amphidial neurons. The amphidial neurons present in nematodes are rich in microtubules and process back to the nerve ring and thus to neuromuscular sites where ligand-gated chloride channels are expressed. The nematode amphid sensory neurons are used for chemical and thermal signaling in *C. elegans* (Dent et al., 2000), *O. volvulus* (Strote et al., 1996) and *H. contortus* (Ashton et al., 1999). Since there is evidence that the amphids are used to taste the environment, it is therefore reasonable to think that any mutation in genes that regulate amphid development may render the worm less permeable to the drug and result in a drug resistant phenotype.

In *C. elegans* more than 13 dye-filling (*dyf*) mutants have been identified. They are named *dyf* because of their inability to take up the lipophilic dye fluoroisothiocyanate into the amphid via the amphid sensory endings. The phenotypic consequence of being a *dyf* mutant is that the amphid organ becomes highly disorganized which leads to a profound defect in behavior. The worm requires an intact amphid for drug avoidance and mating (Dent et al., 2000). It was observed that all *dyf* mutant *C. elegans* larvae were ivermectin resistant and determined that amphidial neurons played a significant role in determining ivermectin sensitivity (Starich et al., 1995). The same

hypothesis was further supported as amphidial defective *C. elegans* were able to grow in the presence of 5 ng/ml of ivermectin.

Altered, shortened and deranged amphidial dendrites have been demonstrated in *H. contortus* resistant to ivermectin compared to the wild type strains (Freeman et al., 2003). This is a similar phenotype identified in *dyf* mutants in *C. elegans* (De Riso et al., 1994). The authors suggested that these distorted and possible dysfunctional amphidial dendrites may hinder the uptake of ivermectin and prevent binding to its receptors which results in a resistant phenotype. *Dyf-7* is required in anchoring dendritic tips of amphids (Heiman and Shaham, 2009). Recently the *dyf-7* gene was identified as an important factor in ivermectin resistance (Urdaneta-Marquez et al., 2014). The authors found mutations in the *dyf-7* gene that resulted in a null protein in ivermectin selected *C. elegans* that were resistant to ivermectin, and genetic changes in macrocyclic resistant *H. contortus* from around the world. They were able to reverse ivermectin resistance in *C. elegans* when they replaced the mutant *dyf-7* gene with the wild type gene.

Kotze and Bagnall (2006) also suggested the possibility of drugs entering the parasite via a non-oral route following results from RNAi experiments against the β-tubulin gene in *H. contortus*. The results showed a decrease in the expression of the β-tubulin gene following RNAi in L3 larvae which, at this stage, have no functional feeding mouth.

1.8 *Haemonchus contortus* life cycle

H. contortus is an important nematode of livestock (sheep, goats and cattle) causing substantial loss particularly to the small ruminant industries. The red stomach

worm (wire worm or Barber's pole worm) belongs to the family Trichostrongylidae and feeds on blood by attaching to the abomasal mucosa (Nikolaou and Gasser, 2006). It causes aneamia, bottle jaw and in heavy infections, death of the infected animal. The life cycle starts with adult females laying eggs while residing in the abomasum.

The eggs, when laid are 76×46μm in size, oval in shape and 4-cell in number. In freshly deposited faeces, the eggs are at the 11-to-26-cell stage. By 10 hours the embryo grows three times in size. After 12 hours, the growth stops but the embryo exhibits increased activity. At 26°C and 100% humidity the eggs take 14-17 hours to hatch and convert into the L1 stage. L1 larvae develop into L2, L3, and L4 stages before reaching the adult stage. After copulation (with males) the adult females start laying eggs at 18 days post oral infection with L3, and can be fully gravid by day 33. The infective larval stage begins at L3 which is the stage at which the host accidentally takes the parasite and which develops into adult in the abomasum (Veglia, 1915) where they feed on blood (12 μl per day).

1.9 *Haemonchus contortus* as a model organism and resistance

H. contortus has always been ahead in developing resistance against potential anthelmintics. In the case of ivermectin, the first case was reported in 1988 in South Africa (van Wyk and Malan, 1988) and since than many studies have shown resistance in this parasite. It is one of the most widely used parasites to study the development of resistance and has proven an excellent model organism (Prichard, 2001). As it is a parasite of sheep and goats so it can be tracked in the natural host whereas it is more difficult in the case of other parasites of humans or cattle. It is closely related to

other parasitic species and can be used to mimic the mechanisms involved in drug resistance in other parasites (Kaplan, 2004).

The female *H. contortus* lays around 4500 eggs per day so it provides a lot of material to work with. The large size of the worm gives enough DNA on which many PCR based genotyping assays can be performed. It is possible to cryopreserve the L3 larvae which can be used and stored for further analysis with little or no loss of viability and infectivity. It is also phylogenetically related to *C. elegans* which can be used for extrapolation of the experimental data. The whole genome has recently been sequenced, (Liang et al., 2014), but much of the genome remains unannotated. There is a large community of biologists using this nematode as a biological tool and hence it is one of the most attractive species used to study anthelmintic resistance (Gilleard, 2006).

1.10 *Caenorhabditis elegans* as a model organism and resistance

C. elegans is an excellent model to study drug resistance in parasitic nematodes. Both *H. contortus* and *C. elegans* are in nematode clade V. *C. elegans* is a harmless free living organism that feeds on bacteria. It can easily be grown on agar inoculated with bacteria. The life cycle has four stages and is completed in 3-days except if dauer form develops. They are 1 mm in length, most of them are self-fertilizing hermaphrodites and lay around 300 eggs during their whole fertilization period. It was the first multicellular organism which has its whole genome sequenced. The 302 neurons, in *C. elegans*, including their connections have completely been mapped. As most of the anthelmintics act on the nervous system, this nematode is a very useful model to study the mode of

action of anthelmintics and mechanism of drug resistance. Different strains of *C. elegans* have been developed to study different physiological processes. IVR-10 is a strain that is resistant to 10 ng/ml ivermectin. It was generated by James and Davey (James and Davey, 2009) by exposure of *C. elegans* to sublethal doses of ivermectin over several generations.

References

Aamodt, E.J., Culotti, J.G., 1986. Microtubules and microtubule-associated proteins from the nematode Caenorhabditis elegans: periodic cross-links connect microtubules in vitro. The Journal of cell biology 103, 23-31.

Aboobaker, A.A., Blaxter, M.L., 2003. Use of RNA interference to investigate gene function in the human filarial nematode parasite Brugia malayi. Molecular and biochemical parasitology 129, 41-51.

Aouali, N., Eddabra, L., Macadre, J., Morjani, H., 2005. Immunosuppressors and reversion of multidrug-resistance. Critical reviews in oncology/hematology 56, 61-70.

Ashton, F.T., Li, J., Schad, G.A., 1999. Chemo- and thermosensory neurons: structure and function in animal parasitic nematodes. Veterinary parasitology 84, 297-316.

Beech, R.N., Prichard, R.K., Scott, M.E., 1994. Genetic variability of the beta-tubulin genes in benzimidazole-susceptible and -resistant strains of Haemonchus contortus. Genetics 138, 103-110.

Blackhall, W.J., Liu, H.Y., Xu, M., Prichard, R.K., Beech, R.N., 1998. Selection at a P-glycoprotein gene in ivermectin- and moxidectin-selected strains of Haemonchus contortus. Molecular and biochemical parasitology 95, 193-201.

Blackhall, W.J., Prichard, R.K., Beech, R.N., 2003. Selection at a gamma-aminobutyric acid receptor gene in Haemonchus contortus resistant to avermectins/milbemycins. Molecular and biochemical parasitology 131, 137-145.

Blackhall, W.J., Prichard, R.K., Beech, R.N., 2008. P-glycoprotein selection in strains of Haemonchus contortus resistant to benzimidazoles. Veterinary parasitology 152, 101-107.

Blane D. 1826. The Outlines of the Veterinary Art, 3rd edn, Compton and Ritchie Printers.

Borgers, M., De Nollin, S., De Brabander, M., Thienpont, D., 1975. Influence of the anthelmintic mebendazole on microtubules and intracellular organelle movement in nematode intestinal cells. American journal of veterinary research 36, 1153-1166.

Chalfie, M., Thomson, J.N., 1979. Organization of neuronal microtubules in the nematode Caenorhabditis elegans. The Journal of cell biology 82, 278-289.

Cully, D.F., Vassilatis, D.K., Liu, K.K., Paress, P.S., Van der Ploeg, L.H., Schaeffer, J.M., Arena, J.P., 1994. Cloning of an avermectin-sensitive glutamate-gated chloride channel from Caenorhabditis elegans. Nature 371, 707-711.

de Lourdes Mottier, M., Prichard, R.K., 2008. Genetic analysis of a relationship between macrocyclic lactone and benzimidazole anthelmintic selection on Haemonchus contortus. Pharmacogenetics and genomics 18, 129-140.

De Riso, L., Ristoratore, F., Sebastiano, M., Bazzicalupo, P., 1994. Amphid defective mutant of Caenorhabditis elegans. Genetica 94, 195-202.

Dent, J.A., Smith, M.M., Vassilatis, D.K., Avery, L., 2000. The genetics of ivermectin resistance in Caenorhabditis elegans. Proceedings of the National Academy of Sciences of the United States of America 97, 2674-2679.

Desai, A., Mitchison, T.J., 1997. Microtubule polymerization dynamics. Annual review of cell and developmental biology 13, 83-117.

Eng, J.K., Blackhall, W.J., Osei-Atweneboana, M.Y., Bourguinat, C., Galazzo, D., Beech, R.N., Unnasch, T.R., Awadzi, K., Lubega, G.W., Prichard, R.K., 2006. Ivermectin selection on beta-tubulin: evidence in Onchocerca volvulus and Haemonchus contortus. Molecular and biochemical parasitology 150, 229-235.

Eng, J.K., Prichard, R.K., 2005. A comparison of genetic polymorphism in populations of Onchocerca volvulus from untreated- and ivermectin-treated patients. Molecular and biochemical parasitology 142, 193-202.

Feng, X.P., Hayashi, J., Beech, R.N., Prichard, R.K., 2002. Study of the nematode putative GABA type-A receptor subunits: evidence for modulation by ivermectin. Journal of neurochemistry 83, 870-878.

Freeman, A.S., Nghiem, C., Li, J., Ashton, F.T., Guerrero, J., Shoop, W.L., Schad, G.A., 2003. Amphidial structure of ivermectin-resistant and susceptible laboratory and field strains of Haemonchus contortus. Veterinary parasitology 110, 217-226.

Fujii, M., Matsumoto, Y., Tanaka, N., Miki, K., Suzuki, T., Ishii, N., Ayusawa, D., 2004. Mutations in chemosensory cilia cause resistance to paraquat in nematode Caenorhabditis elegans. The Journal of biological chemistry 279, 20277-20282.

Geary, T.G., Nulf, S.C. Favreau, M.A., Tang, L., Prichard, R.K., Hatzenbuhler, N.T.,Shea, M.H., Alexander, S.J., Klein, R.D. (1992) Three β-tubulin cDNAs from the parasitic nematode Haemonchus contortus. Molecular and Biochemical Parasitology 50: 295-306.

Geary, T.G., 2005. Ivermectin 20 years on: maturation of a wonder drug. Trends in parasitology 21, 530-532.

Georges, E., 2007. The P-glycoprotein (ABCB1) linker domain encodes high-affinity binding sequences to alpha- and beta-tubulins. Biochemistry 46, 7337-7342.

Ghisi, M., Kaminsky, R., Maser, P., 2007. Phenotyping and genotyping of Haemonchus contortus isolates reveals a new putative candidate mutation for benzimidazole resistance in nematodes. Veterinary parasitology 144, 313-320.

Gilleard, J.S., 2006. Understanding anthelmintic resistance: the need for genomics and genetics. International journal for parasitology 36, 1227-1239.

Grant, W.N., 1994. Genetic variation in parasitic nematodes and its implications. International journal for parasitology 24, 821-830.

Heiman, M.G., Shaham, S., 2009. DEX-1 and DYF-7 establish sensory dendrite length by anchoring dendritic tips during cell migration. Cell 137, 344-355.

Hibbs, R.E., Gouaux, E., 2011. Principles of activation and permeation in an anion-selective Cys-loop receptor. Nature 474, 54-60.
Holden-Dye, L., Walker, R.J., 1990. Avermectin and avermectin derivatives are antagonists at the 4-aminobutyric acid (GABA) receptor on the somatic muscle cells of Ascaris; is this the site of anthelmintic action? Parasitology 101 Pt 2, 265-271.
James, C.E., Davey, M.W., 2009. Increased expression of ABC transport proteins is associated with ivermectin resistance in the model nematode Caenorhabditis elegans. International journal for parasitology 39, 213-220.

Kaminsky, R., Ducray, P., Jung, M., Clover, R., Rufener, L., Bouvier, J., Weber, S.S., Wenger, A., Wieland-Berghausen, S., Goebel, T., Gauvry, N., Pautrat, F., Skripsky, T., Froelich, O., Komoin-Oka, C., Westlund, B., Sluder, A., Maser, P., 2008. A new class of anthelmintics effective against drug-resistant nematodes. Nature 452, 176-180.
Kaplan, R.M., 2004. Drug resistance in nematodes of veterinary importance: a status report. Trends in parasitology 20, 477-481.
Kerboeuf, D., Blackhall, W., Kaminsky, R., von Samson-Himmelstjerna, G., 2003. P-glycoprotein in helminths: function and perspectives for anthelmintic treatment and reversal of resistance. International journal of antimicrobial agents 22, 332-346.
Klein, R.D., Nulf, S.C., Alexander-Bowman, S.J., Mainone, C.B., Winterrowd, C.A., Geary, T.G., 1992. Cloning of a cDNA encoding alpha-tubulin from Haemonchus contortus. Molecular and biochemical parasitology 56, 345-348.
Kneussel, M., Betz, H., 2000. Clustering of inhibitory neurotransmitter receptors at developing postsynaptic sites: the membrane activation model. Trends in neurosciences 23, 429-435.
Kotze, A.C., Bagnall, N.H., 2006. RNA interference in Haemonchus contortus: suppression of beta-tubulin gene expression in L3, L4 and adult worms in vitro. Molecular and biochemical parasitology 145, 101-110.
Kwa, M.S., Veenstra, J.G., Van Dijk, M., Roos, M.H., 1995. Beta-tubulin genes from the parasitic nematode Haemonchus contortus modulate drug resistance in Caenorhabditis elegans. Journal of molecular biology 246, 500-510.
Kwa MS, Veenstra JG, Roos MH (1994) Benzimidazole resistance in Haemonchus contortus is correlated with a conserved mutation at amino acid 200 in beta-tubulin isotype 1. Mol Biochem Parasitol 63: 299-303.
Lacey, E., 1988. The role of the cytoskeletal protein, tubulin, in the mode of action and mechanism of drug resistance to benzimidazoles. International journal for parasitology 18, 885-936.
Lacey, E., 1990. Mode of action of benzimidazoles. Parasitology today (Personal ed.) 6, 112-115.
Lacey, E., Gill, J.H., 1994. Biochemistry of benzimidazole resistance. Acta tropica 56, 245-262.
Laing, R., Kikuchi, T., Martinelli, A., Tsai, I.J., Beech, R.N., Redman, E., Holroyd, N., Bartley, D.J., Beasley, H., Britton, C., Curran, D., Devaney, E., Gilabert, A., Hunt, M., Jackson, F., Johnston, S.L., Kryukov, I., Li, K., Morrison, A.A., Reid, A.J., Sargison, N., Saunders, G.I., Wasmuth, J.D., Wolstenholme, A., Berriman,

M., Gilleard, J.S., Cotton, J.A., 2013. The genome and transcriptome of Haemonchus contortus, a key model parasite for drug and vaccine discovery. Genome biology 14, R88.

Little, P.R., Hodge, A., Watson, T.G., Seed, J.A., Maeder, S.J., 2010. Field efficacy and safety of an oral formulation of the novel combination anthelmintic, derquantel-abamectin, in sheep in New Zealand. N. Z.Vet. J. 58, 121–129

Lowe, J., Li, H., Downing, K.H., Nogales, E., 2001. Refined structure of alpha beta-tubulin at 3.5 A resolution. Journal of molecular biology 313, 1045-1057.

Lubega, G.W., Prichard, R.K., 1990. Specific interaction of benzimidazole anthelmintics with tubulin: high-affinity binding and benzimidazole resistance in Haemonchus contortus. Molecular and biochemical parasitology 38, 221-232.

Moreno, Y., Nabhan, J.F., Solomon, J., Mackenzie, C.D., Geary, T.G., 2010. Ivermectin disrupts the function of the excretory-secretory apparatus in microfilariae of Brugia malayi. Proceedings of the National Academy of Sciences of the United States of America 107, 20120-20125.

Nana-Djeunga, H., Bourguinat, C., Pion, S.D., Kamgno, J., Gardon, J., Njiokou, F., Boussinesq, M., Prichard, R.K., 2012. Single nucleotide polymorphisms in beta-tubulin selected in Onchocerca volvulus following repeated ivermectin treatment: possible indication of resistance selection. Molecular and biochemical parasitology 185, 10-18.

Nare, B., Liu, Z., Prichard, R.K., Georges, E., 1994. Benzimidazoles, potent anti-mitotic drugs: substrates for the P-glycoprotein transporter in multidrug-resistant cells. Biochemical pharmacology 48, 2215-2222.

Nikolaou, S., Gasser, R.B., 2006. Prospects for exploring molecular developmental processes in Haemonchus contortus. International journal for parasitology 36, 859-868.

Omura, S., Crump, A., 2004. The life and times of ivermectin - a success story. Nature reviews. Microbiology 2, 984-989.

Osei-Atweneboana, M.Y., Boakye, D.A., Awadzi, K., Gyapong, J.O., Prichard, R.K., 2012. Genotypic analysis of β-tubulin in Onchocerca volvulus from communities and individuals showing poor parasitological response to ivermectin treatment. International Journal for Parasitology: Drugs and Drug Resistance 2, 20-28.

Osei-Atweneboana, M.Y., Eng, J.K., Boakye, D.A., Gyapong, J.O., Prichard, R.K., 2007. Prevalence and intensity of Onchocerca volvulus infection and efficacy of ivermectin in endemic communities in Ghana: a two-phase epidemiological study. Lancet 369, 2021-2029.

Oxberry, M.E., Geary, T.G., Winterrowd, C.A., Prichard, R.K., 2001. Individual expression of recombinant alpha- and beta-tubulin from Haemonchus contortus: polymerization and drug effects. Protein expression and purification 21, 30-39.

Pony S.S., Wang C.C. and Fritz L.C. 1980. Studies on the mechanisms of action of avermectin B la: Stimulation of release of gamma amino butyric acid from brain synaptosomes. Journal of Neurochemistry, 34: 351-358.

Prichard, R., 2001. Genetic variability following selection of Haemonchus contortus with anthelmintics. Trends in parasitology 17, 445-453.

Prichard, R.K., 1990. Anthelmintic resistance in nematodes: extent, recent understanding and future directions for control and research. International journal for parasitology 20, 515-523.
Prichard, R.K., Hall, C.A., Kelly, J.D., Martin, I.C., Donald, A.D., 1980. The problem of anthelmintic resistance in nematodes. Australian veterinary journal 56, 239-251.
Robinson, M.W., McFerran, N., Trudgett, A., Hoey, L., Fairweather, I., 2004. A possible model of benzimidazole binding to beta-tubulin disclosed by invoking an inter-domain movement. Journal of molecular graphics & modelling 23, 275-284.
Sangster, N.C., Bannan, S.C., Weiss, A.S., Nulf, S.C., Klein, R.D., Geary, T.G., 1999. Haemonchus contortus: sequence heterogeneity of internucleotide binding domains from P-glycoproteins. Experimental parasitology 91, 250-257.
Saunders, G.I., Wasmuth, J.D., Beech, R., Laing, R., Hunt, M., Naghra, H., Cotton, J.A., Berriman, M., Britton, C., Gilleard, J.S., 2013. Characterization and comparative analysis of the complete Haemonchus contortus beta-tubulin gene family and implications for benzimidazole resistance in strongylid nematodes. International journal for parasitology 43, 465-475.
Schwarz, E.M., Korhonen, P.K., Campbell, B.E., Young, N.D., Jex, A.R., Jabbar, A., Hall, R.S., Mondal, A., Howe, A.C., Pell, J., Hofmann, A., Boag, P.R., Zhu, X.Q., Gregory, T.R., Loukas, A., Williams, B.A., Antoshechkin, I., Brown, C.T., Sternberg, P.W., Gasser, R.B., 2013. The genome and developmental transcriptome of the strongylid nematode Haemonchus contortus. Genome biology 14, R89.
Smith, H., Campbell, W.C., 1996. Effect of ivermectin on Caenorhabditis elegans larvae previously exposed to alcoholic immobilization. The Journal of parasitology 82, 187-188.
Starich, T.A., Herman, R.K., Kari, C.K., Yeh, W.H., Schackwitz, W.S., Schuyler, M.W., Collet, J., Thomas, J.H., Riddle, D.L., 1995. Mutations affecting the chemosensory neurons of Caenorhabditis elegans. Genetics 139, 171-188.
Strote, G., Bonow, I., Attah, S., 1996. The ultrastructure of the anterior end of male Onchocerca volvulus: papillae, amphids, nerve ring and first indication of an excretory system in the adult filarial worm. Parasitology 113 (Pt 1), 71-85.
Sullivan, K.F., 1988. Structure and utilization of tubulin isotypes. Annual review of cell biology 4, 687-716.
TDR WHO, Geneva, 1995. Twelfth Programme Report. Tropical Disease Research: progress 1975–94, highlights 1993–94.
Urdaneta-Marquez, L., Bae, S.H., Janukavicius, P., Beech, R., Dent, J., Prichard, R., 2014. A dyf-7 haplotype causes sensory neuron defects and is associated with macrocyclic lactone resistance worldwide in the nematode parasite Haemonchus contortus. International journal for parasitology 44, 1063-1071.
van Wyk, J.A., Malan, F.S., 1988. Resistance of field strains of Haemonchus contortus to ivermectin, closantel, rafoxanide and the benzimidazoles in South Africa. The Veterinary record 123, 226-228.
Waller P.J. 2003. The future of anthelmintics in sustainable parasite control programs for livestock. Helminthologia, 40: 97-102.

Wolstenholme, A.J., Fairweather, I., Prichard, R., von Samson-Himmelstjerna, G., Sangster, N.C., 2004. Drug resistance in veterinary helminths. Trends in parasitology 20, 469-476.

Wolstenholme A. J. and Kaplan R. M. 2012. Resistance to macrocyclic lactones. Curr. Pharm. Biotechnol. 13, 873–887.

Wolstenholme, A.J., Rogers, A.T., 2005. Glutamate-gated chloride channels and the mode of action of the avermectin/milbemycin anthelmintics. Parasitology 131 Suppl, S85-95.

Xu, M., Molento, M., Blackhall, W., Ribeiro, P., Beech, R., Prichard, R., 1998. Ivermectin resistance in nematodes may be caused by alteration of P-glycoprotein homolog. Molecular and biochemical parasitology 91, 327-335.

Connecting statement I

In chapter I we have reviewed the history of anthelmintics, the mode of action and resistance mechanisms of benzimidazoles and ivermectin and other macrocyclic lactones. We also discussed the structure of tubulin. In the chapter II (manuscript I) my objective was to produce sufficient *Haemonchus contortus* α- and β-tubulins by recombinant expression to allow polymerization and depolymerization studies to be conducted and to study the effect of ivermectin on the formation of microtubules. However, after a lot of effort and repeated experiments it was found that, unlike mammalian microtubules, the microtubules of *Haemonchus contortus* were not depolymerized by cold temperatures. This stability to cold may be a property of the nematode microtubules which allows survival of free-living stages during cold climatic conditions.

Chapter II

Manuscript I

Haemonchus contortus microtubules are cold resistant

Shoaib Ashraf, Roger K. Prichard

Molecular and Biochemical Parasitology, 193, 2-22

(2014)

Abstract

Haemonchus contortus is an important nematode of livestock that is present in most parts of the world. The life cycle comprises free living stages (egg, L1, L2 and L3 larvae), and parasitic stages (L4, adult and egg) in a ruminant. Microtubules are filamentous structures which are made from polymerization of α- and β-tubulin. In vitro polymerization of α- and β-tubulin can be achieved by increasing the temperature to 37^{o}C under certain conditions. As part of its normal functioning, in mammals, the microtubules can be depolymerized when the temperature is reduced to 0^{o}C. However, interestingly the microtubules of *Haemonchus contortus* are cold resistant i.e. they do not depolymerize at 0^{o}C. Moreover these microtubules did not depolymerize even in the presence of 5 mM $CaCl_2$ or 50 μM colchicine. These interesting findings may explain how larvae in the free living stages may survive cold temperatures over winter.

Keywords: *Haemonchus contortus;* Tubulin; Microtubules; Cold resistance

2.1. Introduction

Haemonchus contortus (*H. contortus*) is an important nematode of livestock (e.g., sheep and goats) which can cause substantial loss to livestock industries. It causes anemia, hypoproteinemia and sometimes death in the infected animal [1]. The life cycle starts with adult females laying eggs while residing in the abomasum. The eggs when laid are oval in shape and pass out of the animal in the feces. By 10 hours the embryo grows to three times its initial size and much cell division occurs which requires microtubules. After 12 hours the growth stops but the embryo exhibits increased activity and development continues. At 26°C and 100% humidity, the eggs take 14-17 hours to hatch and develop into L1 stage larvae [2]. L1 larvae develop on pasture into L2, L3, and following ingestion by a ruminant host, into the L4 stages before reaching the adult stage. After copulation the adult females start laying eggs, 18 days after oral infection with L3, and can be fully gravid by day 33. The infective larval stage is the L3 which is the stage at which the host inadvertently ingests the parasite and it develops into an adult in the abomasum where they feed on blood (up to 12 μl per day/adult) [1].

Microtubules are hollow cylindrical filamentous structures present in most cells of eukaryotes [3]. They are formed by different soluble subunits of α and β-tubulin [4]. When tubulin subunits reach a certain threshold they associate in a head to-tail fashion to form linear hollow tubular shaped structures called protofilaments which then associate through side-to-side lateral interactions to form microtubules [5]. Microtubules are in dynamic equilibrium, as soluble tubulin is added and subtracted on opposite ends of the insoluble microtubule in a “treadmilling” fashion [6]. The growth and shrinkage

(polymerization and depolymerization) of the microtubules is an ongoing process and requires GTP hydrolysis. This GTP hydrolysis converts the straight protofilament that favors polymerization to the curved state that favors depolymerization [7]. The equilibrium may be disturbed by changes in temperature or by endogenous co-factors, such as GTP, Mg^{2+}, Ca^{2+} and microtubule associated proteins (MAPs) [3]. Thus by varying temperature and different co-factors, microtubule assembly or disassembly can be promoted in vitro using purified recombinantly-derived tubulins [8].

Microtubules have varying degrees of stability when exposed to low temperatures. For example the microtubules found in the cytoplasm and the mitotic apparatus of mammalian cells rapidly depolymerize at 0^oC, and in the presence of drugs that induce disassembly, whereas the microtubules of the sea urchin are stable and do not depolymerize at 0^oC or in the presence of colchicine [9]. Variation in stability may be due to chemical differences in tubulins as different tubulin genes form different tubulin molecules, or may be due to different posttranslational modifications [10]. Cold labile microtubules rapidly depolymerize in the presence of milli molar concentrations of calcium whereas cold stable microtubules are insensitive to calcium [11]. Microtubules are involved in many cellular processes. As tubulin is virtually connected to every cellular organelle, this makes its normal functioning necessary for survival of the nematode [12]. In *H. contortus,* four β-tubulin cDNA sequences [13-15] and one α-tubulin cDNA sequence [14-16] have been identified**.**

2.2. Materials and Methods

In order to clone *H. contortus* tubulins, RNA was extracted from adult worms of the PF23 (PF) strain of *H. contortus* [17] and converted into cDNA using Trizol reagent (Invitrogen, Toronto, ON) and QuantiTect Reverse Transcription Kit (Qiagen, Toronto, ON). PF is a laboratory strain (P=parental strain; F23=23rd generation) never exposed to macrocyclic lactone or benzimidazole drug treatment. Kindly supplied by Fort Dodge Animal Health, New Jersey, USA. The full length sequences of α-tubulin (accession number L-02108) and β-tubulin isotype 1 genes (accession number M-76493) were cloned into pETM-10 (EMBL, Heidelberg, Germany). The vector was linearized by the 5´-*Nco*I and 3´-*BamH*I restriction enzymes (NEB, Toronto, ON). For α-tubulin, *BsmB*I (sense primer) and 3´-*BamH*I (anti-sense primer) restriction sites were used to clone the gene. 5´- TTTA**CGTCTC**CCATGAGGGAGGTGATTTCCATTCACATC -3´ sense primer and 5´- **GGATCC**GCGTCAATACTCATCGCCTTCCTCAC -3´ anti-sense primers were used for cloning. For β-tubulin, 5´-*BspH*I (forward primer) and 3´-*BamH*I (reverse primer) (Invitrogen, Toronto, ON) restriction sites were used to clone the gene. 5´-GAAA**TCATGA**GGGAAATCGTTCATGTGCAAG-3´ sense primer and 5´-TGAT**GGATCC**TTACTCCTCGGGATATGCCTC-3´ anti-sense primer were used for cloning. The cloned products were transformed into *E. coli* (XL1-Blue) (Stratagene, Mississauga, ON) and sequenced at Genome Quebec Innovation Centre, Montreal, Quebec. α- and β-tubulin isotype 1 were transformed into Rosetta 2 cells (Novagen, Madison, USA) for protein expression. All the proteins were grown in LB broth containing 50 μg/ml kanamycin and 1% maltose (Sigma Aldrich, Toronto, ON). Induction was with 1 mM final concentration isopropyl-β-D-thiogalactoside (IPTG) (Invitrogen, Toronto, ON) and incubation continued for 3 h at 37°C at 250 rpm. Cell

pellets were lysed by sonication for 42 cycles (15 s pulses with 15 s resting periods) on ice in binding/lysis buffer (50 mM NaH_2PO_4, 500 mM NaCl, 10 mM imidazole, pH 8.0) containing one Complete EDTA-free protease-inhibitor cocktail tablet (Roche Applied Science, Laval, QC). All the procedures were according the QIAexpressionist™ manual (Qiagen, Toronto, ON). The lysates were centrifuged at 20000 rpm and the soluble fraction was loaded onto disposable columns (Biorad, Mississauga, ON) containing 1 ml packed beads of Ni-NTA agarose (Qiagen, Laval, QC). The proteins were washed with wash buffer (50 mM NaH_2PO_4, 500 mM NaCl, 20 mM imidazole, pH 8.0) and eluted with elution buffer (50 mM NaH_2PO_4, 500 mM NaCl, 250 mM imidazole, pH 8.0). All the proteins were analyzed by 10 % sodium dodecyl sulfate polyacrylamide gel electrophoresis (SDS-PAGE) and Western blot using specific monoclonal antibodies against α- and β-tubulin isotype 1 (GE Healthcare, Baie-d'Urfé, QC). The recombinantly-derived proteins were concentrated using Amicon ultracentrifugal filter 30 MWCO (Millipore, Bedford, MA) and the buffer was exchanged for PBS (10 mM $Na_2HPO_4.H_20$, 2 mm KH2PO4, 137 mM NaCl, 2.7 mm KCl,, pH 7.5). Protein concentration was determined by the Bradford assay (Biorad, Mississauga, ON).

Twenty μM purified α-tubulin was mixed with 20 μM purified β-tubulin isotype 1 in polymerization buffer (0.1 M PIPES pH 6.8, 10% glycerol, 1 mM EGTA, 1 mM $MgCl_2$, 1 mM GTP) (Sigma Aldrich, Toronto, ON) to form microtubules. The extent of polymerization was monitored by taking optical densities using a UV spectrophotometer (Beckman Coulter DU-640 UV/VIS Scanning Spectrophotometer) at 340 nm at 37°C every 20 seconds for 1 hour [18]. To determine the effect on polymerization, similar procedures were performed in the presence of taxol (10 μM) (Sigma Aldrich, Toronto,

ON) or colchicine (50 - 100 μM) (Sigma Aldrich, Toronto, ON). Dimethyl sulphoxide (DMSO) was used as a solvent control (Sigma Aldrich, Toronto, ON). Polymerization products were used in the depolymerization studies. The microtubules were incubated on ice for 5 min after which optical densities were measured at 340 nm at 0°C every 15 seconds for 1 hour by using the UV spectrophotometer. Up to 5 mM $CaCl_2$ and up to 100 μM colchicine were used in the depolymerization experiments.

Twenty μM α- and β-tubulin isotype 1 were mixed and polymerized for 1 h at 37°C and then depolymerized for 1 h at 0^oC. The polymerized and depolymerized products were fixed in 0.4% gluteraldehyde for 1 min at room temperature. The samples were then adsorbed onto glow-discharged formvar-and carbon-coated grids. The samples were stained for 25 seconds with 2% uranyl acetate. The samples were then imaged by FEI Tecnai 12 TEM equipped with an AMT XR80C CCD camera.

2.3. Results and Discussion

The identities of recombinantly-derived *H. contortus* α-tubulin and β-tubulin isotype 1 were confirmed by SDS-PAGE and Western blot with specific antibodies. Functional analysis of the proteins was done via polymerization assays. The polymerization was inhibited in the presence of 100 μM colchicine and 10 μM taxol increased the extent of polymerization when compared to DMSO (solvent control) (data not shown). Structural analysis was performed with electron microscopy. Under polymerizing conditions, the recombinantly-derived proteins were producing elongated microtubule and ring structures (Figure. 2.1A). The extent of polymerization was increased when α- and β-tubulin proteins were incubated at 37^oC for 1h (Figure. 2.2A). Interestingly, once polymerized

the microtubules did not depolymerize into soluble tubulin subunits even if kept at 0^{o}C for 1 h (Fig. 1B, 2B). Nor did the microtubules depolymerize in the presence of 5 mM $CaCl_2$ or 50 µM colchicine.

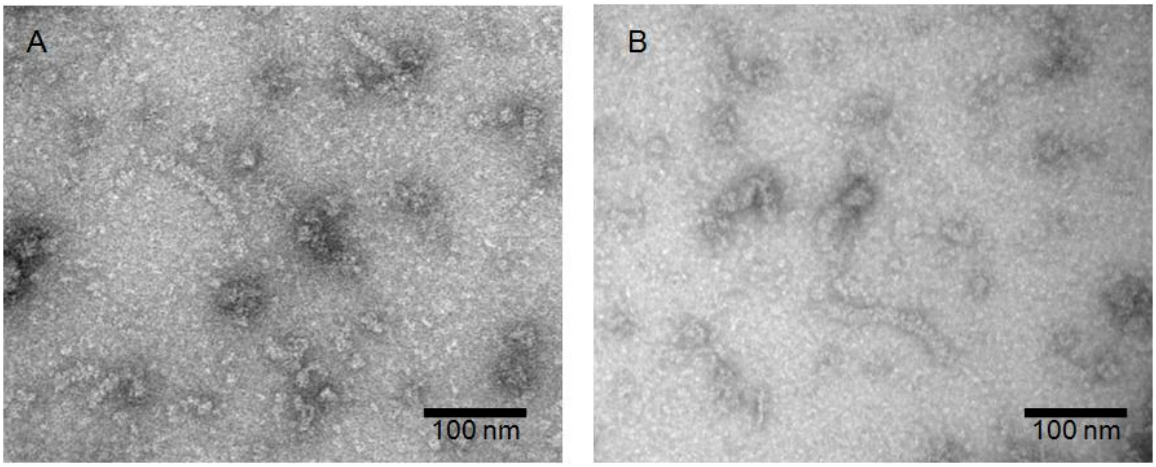

Figure. 2.1

Figure. 2.1. Electron microscopy of the microtubules. Twenty µM recombinantly-derived *H. contortus* α-tubulin and β-tubulin isotype 1, after polymerization for 1 h at 37^{o}C, showing elongated structures of microtubules (A), and following depolymerization conditions for 1 h at 0^{o}C (B).

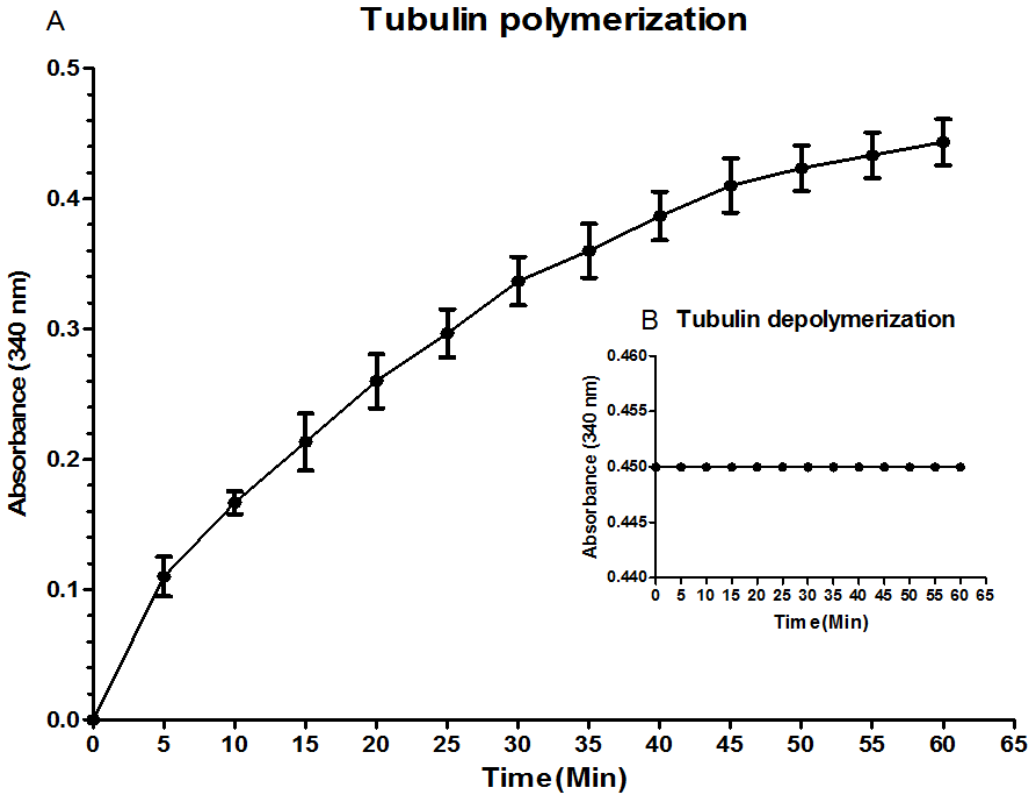

Figure. 2.2A, B

Figure. 2.2. Tubulin polymerization and depolymerization assays performed with 20 μM purified recombinantly-derived *H. contortus* α-tubulin and β-tubulin isotype 1. Tubulin polymerization, with an increase in absorbance, monitored at 340 nm (A). The microtubules did not depolymerize after incubation for 1 h at 0^{o}C (B).

The objective of the current study was to see if α- and β-tubulin isotype 1 were able to polymerize when incubated at 37^{o}C and to depolymerize when kept at 0^{o}C. For this recombinantly-derived *H. contortus* α- and β-tubulin were expressed in an *E. coli* expression system. Different functional and structural analyses were performed by turbidimetry and electron microscopy, respectively. Though the proteins behaved as expected in the polymerization assays, the *H. contortus* tubulins, once polymerized were stable. It is possible that the recombinantly-derived tubulins may behave differently from

the native *H. contortus* tubulins. The polymerization studies and electron microscopy both showed that the recombinantly-derived proteins were able to polymerize when incubated at 37^{o}C. However, they did not depolymerize at 0^{o}C. Interestingly these cold stable microtubules did not depolymerize when $CaCl_2$ was added up to 5 mM, or colchicine was added up to 50 µM. In vitro mammalian tubulins polymerize at 37^{o}C and rapidly depolymerize at 0^{o}C. However it was found that *H. contortus* microtubules did not depolymerize when incubated for up to 1 h at 0^{o}C. Interestingly, the microtubules in Antarctic fishes do not depolymerize at 0^{o}C [7]. Both *H. contortus* and Antarctic fish normally have phenylalanine (F) at position 200 on the β-tubulin protein. Detrich et al. (2000) postulate that the F at position 200 strengthens lateral interactions between protofilaments. They suggested that F at position 200 may make the structure more rigid and increase the energy activation barrier required for the hydrolysis-induced conformational changes (from straight to curved protofilaments). These conformational changes lead to depolymerization of the microtubules. The presence of F at position 200 may act as a surrogate taxol to stabilize the structure of tubulin and results in strong lateral interactions even at low temperatures which may prevent it from depolymerizing. This hypothesis is also in agreement with the life cycle of *H. contortus* which may explain why the free living stages of this parasite can survive at low temperatures [1]. We have done site-directed mutagenesis and have substituted F with tyrosine (Y) at position 200 on the β-tubulin protein. These mutant microtubules were also cold stable and did not depolymerize at 0^{o}C (data not shown). This finding suggests that the presence of F alone does not solely account for cold stability of *H. contortus* microtubules. Other factors involved in the cold stability of microtubules require further investigations.

2.4. Acknowledgements

This project received financial support from NSERC Canada, MDEIE-PSII and the FQRNT Centre for Host-Parasite Interactions, Quebec, Canada. We also wish to thank EMBL for the generous gift of pETM-10 expression vector and Kathy Keller for harvesting the parasites.

References

[1] Nikolaou S, Gasser RB. Prospects for exploring molecular developmental processes in *Haemonchus contortus*. International Journal for Parasitology, 2006;36:859-68.
[2] Veglia F. The anatomy and life-history of the Haemonchus contortus (Rud.). Rep. Dir. Vet. Res, 1915, 3–4, 347–500.
[3] Lacey E, Gill JH. Biochemistry of benzimidazole resistance. Acta Tropica, 1994;56:245-62.
[4] Sullivan KF. Structure and utilization of tubulin isotypes. Annual Review of Cell Biology, 1988;4:687-716.
[5] Aamodt EJ, Culotti JG. Microtubules and microtubule-associated proteins from the nematode *Caenorhabditis elegans*: periodic cross-links connect microtubules in vitro. Journal of Cell Biology, 1986;103:23-31.
[6] Lacey E. The role of the cytoskeletal protein, tubulin, in the mode of action and mechanism of drug resistance to benzimidazoles. International Journal for Parasitology, 1988;18:885-936.
[7] Detrich HW 3rd, Parker SK, Williams RC, Jr., Nogales E, Downing KH. Cold adaptation of microtubule assembly and dynamics. Structural interpretation of primary sequence changes present in the alpha- and beta-tubulins of Antarctic fishes. The Journal of Biological Chemistry, 2000;275:37038-47.
[8] Oxberry ME, Geary TG, Winterrowd CA, Prichard RK. Individual expression of recombinant alpha- and beta-tubulin from *Haemonchus contortus*: polymerization and drug effects. Protein Expression Purification, 2001;21:30-9.
[9] Snyder JA, McIntosh JR. Biochemistry and physiology of microtubules. Annual Review of Biochemistry, 1976;45:699-720.
[10] Webb BC, Wilson L. Cold-stable microtubules from brain. Biochemistry, 1980;19: 1993-2001.
[11] Job D, Rauch CT, Fischer EH, Margolis RL. Recycling of cold-stable microtubules: evidence that cold stability is due to substoichiometric polymer blocks. Biochemistry, 1982;21:509-15.

[12] Aboobaker AA, Blaxter ML. Use of RNA interference to investigate gene function in the human filarial nematode parasite *Brugia malayi*. Molecular and Biochemical Parasitology, 2003;129:41-51.
[13] Saunders GI, Wasmuth JD, Beech R, Laing R, Hunt M, Naghra H, et al. Characterization and comparative analysis of the complete *Haemonchus contortus* beta-tubulin gene family and implications for benzimidazole resistance in strongylid nematodes. International Journal for Parasitology, 2013;43:465-75.
[14] Laing R, Kikuchi T, Martinelli A, Tsai IJ, Beech RN, Redman E, et al. The genome and transcriptome of Haemonchus contortus, a key model parasite for drug and vaccine discovery. Genome biology. 2013;14:R88
[15] Schwarz EM, Korhonen PK, Campbell BE, Young ND, Jex AR, Jabbar A, et al. The genome and developmental transcriptome of the strongylid nematode Haemonchus contortus. Genome biology. 2013;14:R89.
[16] Klein RD, Nulf SC, Alexander-Bowman SJ, Mainone CB, Winterrowd CA, Geary TG. Cloning of a cDNA encoding alpha-tubulin from *Haemonchus contortus*. Molecular and Biochemical Parasitology, 1992;56:345-8.
[17] Ranjan S, Wang GT, Hirschlein C, Simkins KL. Selection for resistance to macrocyclic lactones by *Haemonchus contortus* in sheep. Veterinary Parasitology. 2002;103:109-17.
[18] Shelanski ML, Gaskin F, Cantor CR. Microtubule assembly in the absence of added nucleotides. Proceedings of the National Academy of Science of the United States of America, 1973;70:765-8.

Connecting statement II

In the previous chapter we reported that the microtubules of *Haemonchus contortus* are resistant to cold temperatures. Previous data from our and other labs have reported that ivermectin causes genetic selection on *H. contortus* β-tubulin. These findings led us to investigate whether ivermectin interacted directly with nematode tubulins and were the basis for chapter III (manuscript II). After optimizing the conditions for recombinant protein expression and purification we investigated a possible direct functional relationship between ivermectin and tubulin. In this manuscript we also report the effect of ivermectin on mammalian tubulin and replication of HeLa cells.

Chapter III

Manuscript II

Ivermectin exhibits potent anti-mitotic activity: from anti-parasitic drug to novel anti-cancer candidate

Shoaib Ashraf, Robin N. Beech, Mark A. Hancock and Roger K. Prichard

Submitted to Biochemical Pharmacology

Abstract

Tubulin/microtubules are a key target for many cancer therapies. Ivermectin (IVM) is a widely used anti-parasitic drug used in humans, livestock, companion animals, and agriculture that targets glutamate-gated chloride channels. Although a genetic association between β-tubulin and IVM has been previously reported, direct binding between IVM and tubulin has not been demonstrated to date. We now report that IVM exposure increased the polymerization of recombinant α- and β-tubulin from *Haemonchus contortus* (*H. contortus*), as well as protected these parasitic α- and β-tubulins from limited trypsin proteolysis. Direct binding between IVM and the tubulin monomers exhibited low micromolar affinities by surface plasmon resonance (SPR), and subsequent equilibrium dialysis indicated that IVM and taxol compete for binding to tubulin, consistent with our molecular modeling that predicted IVM interacts with the taxol binding pocket of both parasitic and mammalian tubulins. Based on this we also found that IVM increased the polymerization of and stabilized mammalian tubulin. IVM also prevented the replication of HeLa cells *in vitro* and this IVM-mediated effect was reversible. Collectively, our data indicate that IVM can bind to and stabilize microtubules (i.e. alter tubulin polymerization equilibrium) and this can then lead to mitotic arrest. Given that IVM is already approved for use in humans, the application of its anti-mitotic activity as an anti-cancer agent warrants further investigation.

Keywords: Ivermectin; Tubulin; Microtubule; Anti-mitotic; Anti-cancer

3.1. Introduction

Microtubules are composed of heterodimers of α- and β-tubulin and contribute to many cellular processes, including cell division [1]. Inhibiting microtubule function in actively dividing cells results in mitotic arrest and induces programmed cell death [2]. This, combined with the knowledge that the structure of tubulins is well-conserved across all species [3], makes tubulin an attractive target for the development of chemotherapeutics. Currently, there are two classes of anti-mitotic drugs that target microtubules: 1) microtubule stabilizing agents such as taxol and epothilone, and 2) microtubule destabilizing agents including colchicine and vinblastine [4]. The activity of these drugs is conferred through their interaction with distinct binding sites in tubulin and, although they offer immense therapeutic potential, their use as pharmacological agents is limited due to poor solubility and toxicity.

IVM is a macrocyclic lactone derived from avermectin [5]. It is used globally to treat parasitic infections of veterinary, human, and agricultural importance. IVM binds to glutamate-gated chloride channels on the surface of muscle and nerve cells of nematodes. This binding causes increased cell membrane permeability, resulting in hyperpolarization which leads to paralysis and ultimately death of the parasite [6, 7]. Previous studies have demonstrated that IVM treatment selectively increases the frequency of single nucleotide polymorphisms (F167Y and F200Y) in β-tubulin of parasitic nematodes, including *H. contortus* and *Onchocerca volvulus* [8-13], but the significance of this observation remains elusive.

While a direct interaction between tubulin and IVM has yet to be reported, several new aspects of this drug have been discovered recently. For example, anti-plasmodial, anti-viral, anti-mycobacterial and anti-leukemic effects of IVM have been described [14-17]. The pharmacology and safety of IVM in animals and humans is well established because of its long-standing use as an anti-parasitic drug. Typical therapeutic doses of IVM are 150-200 μg/kg in animals and humans, but administrations up to 1.6 mg/kg are well-tolerated [18]. In another study, healthy volunteers who received 30-120 mg of IVM orally three times per week experienced no negative side-effects [19]. The LD_{50} of IVM in rodents is 50 mg/kg [20], which is 250-fold more than its normal therapeutic dose (200 μg/kg). Our present study tested the hypothesis that IVM interacts directly with tubulin, thus providing anti-mitotic, anti-cancer potential. Here, we provide evidence of a direct interaction between IVM and tubulin at pharmacologically-relevant concentrations, which reversibly inhibited the replication of a transformed cell line *in vitro*. Our novel findings warrant further investigation of IVM as an anti-cancer therapeutic.

3.2. Materials and Methods

3.2.1. RNA extraction.

Adult worms from the PF strain [21] of *H. contortus* were stored at -80°C. This is a strain which was never exposed to MLs or BZs and is susceptible to IVM [21]. Total RNA was extracted from 15 – 20 worms using Trizol reagent as per instructions of the manufacturer (Invitrogen, Toronto, ON, Canada). cDNA was synthesized according to QuantiTect Reverse Transcription Kit (Qiagen, Toronto, ON, Canada).

3.2.2. Cloning of β-tubulin isotype 1.

The 1347 bp full length β-tubulin isotype 1 gene (accession number M-76493) was amplified using 5´-GAAA**TCATGA**GGGAAATCGTTCATGTGCAAG-3´ forward primer and 5´-TGAT**GGATCC**TTACTCCTCGGGATATGCCTC-3´ reverse primer. Two restriction sites, 5´-*BspH*I (forward primer) and 3´-*BamH*I (reverse primer) (Invitrogen, Toronto, ON) were introduced into the sequence. The PCR-amplified and double digested gene product was then introduced into expression vector pETM-10 (EMBL, Heidelberg, Germany), which was linearized using the 5´-*Nco*I and 3´-*BamH*I restriction enzymes (NEB, Toronto, ON, Canada). The complete construct was transformed into *Eschericia coli* (*E. coli*) (XL1-Blue) supercompetent cells (Stratagene, Mississauga, ON, Canada). The cloned product was then sequenced at McGill University/Genome Quebec Innovation Centre, Montreal, QC, Canada.

3.2.3. Cloning of α-tubulin.

To amplify the 1353 bp full length sequence of α-tubulin (accession number L-02108) 5´- TTTA**CGTCTC**CCATGAGGGAGGTGATTTCCATTCACATC -3´ sense primer and 5´- **GGATCC**GCGTCAATACTCATCGCCTTCCTCAC -3´ anti-sense primers (Invitrogen, Toronto, ON) were used. 5´-*BsmB*I (forward primer) and 3´-*BamH*I (reverse primer) restriction sites were used to clone the gene into pETM-10 (EMBL, Heidelberg, Germany) which was linearized by the 5´-*Nco*I and 3´-*BamH*I restriction enzymes (NEB, Toronto, ON). The cloned product was transformed into *E. coli* (XL1-Blue) supercompetent cells (Stratagene, Mississauga, ON) and confirmed by sequencing at Genome Quebec Innovation Centre, Montreal, QC.

3.2.4. Protein expression.

After validation of the sequences α- and β-tubulin isotype 1 were transformed into Rosetta 2 (Novagen, Madison, WI, USA) competent cells for protein expression. Both α- and β-tubulin isotype 1 were grown in 1 L LB broth containing 50 μg/ml kanamycin and 1% maltose (Sigma Aldrich, Toronto, ON). 1 mM final concentration isopropyl-β-D-thiogalactoside (IPTG) (Invitrogen, Toronto, ON) was added to induce cells and the incubation continued for 3 h at 37°C and 250 rpm agitation. Cell pellets were lysed by three freeze thaw cycles in liquid nitrogen followed by sonication for 32 cycles (15 s pulses with 15 s resting periods) on ice in binding/lysis buffer (50 mM NaH_2PO_4, 500 mM NaCl, 10 mM imidazole, pH 8.0) containing one Complete EDTA-free protease-inhibitor cocktail tablet (Roche Applied Science, Laval, QC, Canada). All the procedures were according to the QIAexpressionist™ (Qiagen, Toronto, ON, Canada).

3.2.5. Protein purification.

Cells were pelleted at 20000 rpm and the soluble fraction loaded onto disposable columns (Biorad, Mississauga, ON, Canada) containing 1 ml packed beads of Ni-NTA agarose (Qiagen, Toronto, ON, Canada). Following washes with the wash buffer (50 mM NaH_2PO_4, 500 mM NaCl, 20 mM imidazole, pH 8.0) proteins were eluted with the elution buffer (50 mM NaH_2PO_4, 500 mM NaCl, 250 mM imidazole, pH 8.0). All the samples were analyzed by 10 % tris-glycine sodium dodecyl sulfate polyacrylamide gel by electrophoresis (SDS-PAGE) and Western blotting using specific antibodies against α- and β-tubulin isotype 1 (GE Healthcare, Baie-d'Urfé, QC, Canada). All the recombinant proteins were concentrated and the buffer was exchanged for PBS (10 mM $Na_2HPO_4.H_20$, 2 mm KH_2PO_4, 137 mM NaCl, 2.7 mm KCl, pH 7.5) using Amicon

ultracentrifugal filter 30 MWCO (Millipore, Bedford, MA, USA). The concentration of the proteins was determined using the Bradford assay (Biorad, Mississauga, ON, Canada). Details of cloning, protein expression and purification can be found elsewhere [22].

3.2.6. Polymerization assay.

Recombinant tubulins were polymerized as α/β polymers to form microtubule-like polymers. 20 μM purified α-tubulin was mixed with 20 μM purified β-tubulin isotype 1 in polymerization buffer (0.1 M PIPES pH 6.8, 10% glycerol, 1 mM EGTA, 1 mM $MgCl_2$, 1 mM GTP) (Sigma Aldrich, Toronto, ON). The total volume was 1 ml and the procedure was done on ice. The samples were transferred to a 1 ml quartz cuvette (Beckman Coulter, Mississauga, ON) and the rate of polymerization was monitored by taking optical densities using a UV spectrophotometer (Beckman Coulter DU-640 UV/VIS Scanning Spectrophotometer) at 340 nm at 37°C every 20 seconds for 1 hour [23]. To determine the effect on polymerization, similar procedures were performed in the presence of IVM (3.75 μM, 7.5 μM, 15 μM, 22.5 μM and 30 μM) (Sigma Aldrich, Toronto, ON, Canada). Dimethyl sulphoxide (DMSO) was used as a solvent control, taxol (Sigma Aldrich, Toronto, ON), a drug used to stabilize polymerization was used as a positive control whereas colchicine (Sigma Aldrich, Toronto, ON), a drug used to inhibit polymerization was used as a negative control in the polymerization experiments [24]. The ratio of the final optical densities (ODs) of IVM versus DMSO was normalized against the final OD of DMSO and was expressed as increase relative to DMSO

(percentage). For the controls the absorbance was plotted against time and expressed as tubulin polymerization. For statistical analysis GraphPad Software Inc. V.5.00 was used.

3.2.7. Electron microscopy.

20 μM α- and β-tubulin isotype 1 were mixed and polymerized for 1 h at 37°C. The polymerized products were fixed in 0.4% gluteraldehyde for 1 min at room temperature. The samples were then adsorbed onto glow-discharged formvar-and carbon-coated grids. The samples were stained for 25 seconds with 2% uranyl acetate. The samples were then imaged by FEI Tecnai 12 transmission electron microscope equipped with an AMT XR80C CCD camera.

3.2.8. Limited trypsin proteolysis.

100 μg α- or β-tubulin isotype 1 was incubated with 30 μM IVM or DMSO (solvent control) for 30 min at 20°C prior to the addition of 1 μg sequencing grade modified trypsin (Promega, Ottowa, ON, Canada). Fifteen μl aliquots were removed at 0, 2, 5, 10, 15, 30 and 60 min and mixed with 10 μl of Complete EDTA-free protease-inhibitor cocktail tablet (Roche Applied Science, Laval, QC, Canada) (1 tablet/ml distilled water) to inactivate the trypsin prior to the addition of SDS-PAGE sample buffer. Samples were then analyzed on a 10% SDS-PAGE and stained with silver stain (Pierce, Ottawa, ON, Canada). The protein bands were then quantified using the NIH software ImageJ (version 1.46).

3.2.9. Surface plasmon resonance (SPR).

Binding of taxol (853 Da, positive control; 1 mM in 100% DMSO), and IVM (890 Da, test compound; 10 mM in 100% DMSO) to α- and β-tubulins (55 kDa monomer recombinant proteins from *H. contortus*) were examined using label-free, real-time BIACORE 3000 instrumentation (GE Healthcare Bio-Sciences AB, Uppsala, Sweden). Experiments were performed on research-grade CM5 sensor chips at 25°C using filtered (0.2 μm) and degassed HBS-EP+ running buffer (10 mM HEPES pH 7.4, 150 mM NaCl, 3.4 mM EDTA, 0.05% (v/v) Tween-20). Dimethylsulfoxide (DMSO) was from Sigma-Aldrich (St. Louis, MO, USA; catalog #D8418, <0.1% water), Pierce Gentle Elution was from Thermo Scientific (Rockford, IL, USA; catalog #21027), and detergents were from Anatrace (Maumee, OH, USA; Tween-20 #APT020 and Empigen #D350); all other chemicals were reagent-grade quality.

Using HBS-EP+ as the running buffer and similar to other tubulin-based SPR methods [25-28], α- and β-tubulin (60 μg/ml in 10 mM sodium acetate pH 4.0) were immobilized on separate flowcells using the Biacore Amine Coupling Kit (5,000 – 10,000 RU final); corresponding reference surfaces were prepared in the absence of any tubulin. Using HBS-EP+ (or PBS) supplemented with 5% (v/v) DMSO as the running buffer, standards and samples were prepared and analyzed according to Biacore bulletins #BR-2001-01 ("*Buffer and sample preparation for direct binding assay in DMSO using Biacore*") and #BR-2001-26 ("*Evaluation of small molecule assays in Biacore 2000/3000*"), respectively. Briefly, 8 DMSO standards (ranging from 4.5 – 5.8% (v/v) final concentration) were injected (25 μL/min x 2 min association + 30 sec dissociation) to generate daily solvent calibration curves. Samples were titrated (taxol, and IVM in 5% DMSO final concentration; 25 μL/min x 1 min association + 1 min dissociation) and

steady-state binding responses (report points near end of association phase) were subjected to DMSO solvent correction. Between sample injections, sensor chip surfaces were regenerated at 50 μL/min using two 30-second pulses of solution I (running buffer containing 1M NaCl) and solution II (Pierce Gentle Elution buffer containing 0.05% (v/v) Empigen).

SPR data was doubled-referenced [29] and is representative of duplicate injections acquired from two independent trials. For each replicate series, a buffer blank was injected first, the highest titrant concentration second, and serial dilutions followed (from the lowest to the highest concentration repeated); comparing responses between the two highest titrant injections verified consistent immobilized surface activity throughout each assay. Apparent equilibrium dissociation constants (K_D) were determined by global fitting of the DMSO-corrected data to a "steady-state affinity" model (BIAevaluation v4.1 software; GE Healthcare Bio-Sciences AB, Uppsala, Sweden). Theoretical binding maxima were predicted using the following equation: $R_{max} = (MW_A / MW_L) (R_L) (n)$; '$R_{max}$' is the maximal binding response (RU) at saturating compound concentration, 'MW_A' is the molecular weight (kDa) of the low molecular weight compound injected in solution, 'MW_L' is the molecular weight (kDa) of the immobilized tubulin monomer, 'R_L' is the amount (RU) of immobilized tubulin, 'n' is the predicted binding stoichiometry (e.g. 1:1).

3.2.10. Equilibrium dialysis.

10 μM α- or β-tubulin isotype 1 in PBS (10 mM $Na_2HPO_4.H_20$, 2 mm KH_2PO_4, 137 mM NaCl, 2.7 mm KCl,, pH 7.5) was used in the Equilibrium DispoDIALYZER, 10 kDa

(Harvard Apparatus, Holliston, MA, USA) to determine the binding site of IVM to tubulins and to validate the results from SPR. PBS with 20 μM BODIPY FL ivermectin, 20 μM BODIPY FL, 20 μM BODIPY FL ivermectin plus 50 μM Levamisole (Lev) and 20 μM BODIPY FL ivermectin with 10 μM DNase I (Roche Applied Science, Laval, QC) were used as controls whereas tubulin containing 20 μM BODIPY FL ivermectin, 20 μM BODIPY FL ivermectin plus 50 μM IVM or 20 μM BODIPY FL ivermectin (Molecular Probes, Toronto, ON, Canada) plus 50 μM taxol were used as test compounds. The incubation continued for 24 h at 4°C while shaking gently after which the fluorescence was measured from both the chambers. Readings were taken in a Varian Cary Eclipse fluorescence spectrophotometer (Agilent Technologies, Mississauga, ON, Canada) at room temperature. The excitation was set at 503 nm and scanned from 510 nm to 560 nm. The peak emission for BODIPY FL ivermectin was at 512 nm. Net fluorescence was calculated by subtracting the fluorescence readings from both dialysis chambers.

3.2.11. Molecular Modelling.

Homology models of α-β tubulin were prepared using the hm_build macro of YASARA v14.7.17 [30]. The structural templates were those of bovine or ovine α-β dimer bound to taxol (pdb: 1JFF) [31], zampanolide (pdb: 4I4T) [32] or colchicine (pdb: 3UT5) [33]. Protein sequences were aligned manually and trimmed to the length of the template. Quality of the final model was assessed by Z-score, a combination of 1D and 3D packing and dihedral angles, as calculated by YASARA. A value of 0 is equivalent to the mean value for experimentally verified structures deposited in the protein data bank

(PDB) with units scaled to the standard deviation of their distribution. The taxol structure was taken from the 1JFF pdb entry and IVM from the 3RIF pdb structure of ivermectin bound to the *C. elegans* GLC-1 glutamate-receptor [7]. Docking was carried out using Vina [34] as implemented in YASARA. The tubulin dimer was placed in a box that extended 10 Å beyond any atom of the protein to allow global docking with rigid protein and flexible ligand. One hundred docking runs were evaluated, based on the binding energy calculated by Vina. Docking poses within an RMSD of 5 Å were clustered. The final optimal binding pose was identified by local docking in a box extending 10 Å around the best global docking pose with one hundred docking runs.

3.2.12. Polymerization of mammalian tubulin.

The HTS-tubulin polymerization kit was used for the polymerization assay for mammalian tubulin (BK004, cytoskeleton, Denver, CO, USA). All the kit components were kept at 0^{o}C before starting the assay. The reaction started when the temperature was increased from 0^{o}C to 37^{o}C. Polymerization was monitored at 340 nm turbidometrically (Synergy HT Multimode plate reader (Biotek, Winooski, VT, USA). IVM was tested at concentrations of 3.75 µM, 7.5 µM, 15 µM, 22.5 µM and 30 µM. 10 µM taxol was used as positive control, 10 µM colchicine was used as a negative control and 2% DMSO was used as a solvent control (Sigma Aldrich, Toronto, ON)

3.2.13. Cells.

HeLa cells were provided by Dr Elias Georges, McGill University. HeLa cells were grown in alpha minimum essential media (α-MEM) supplemented with 10% fetal bovine serum (Invitrogen, Toronto, ON).

3.2.14. Immunofluorescence.

Microtubules were visualized by fluorescence microscopy. Briefly HeLa cells were grown on glass cover-slips. At least 24 h were allowed for the attachment of cells. Ten µM IVM, 0.1 µM taxol, 0.1 µM colchicine and 0.6% DMSO (Sigma Aldrich, Toronto, ON) were exposed to the cells for 24 h at 37^{o}C. Following this the cultures were left for 16 h at 4^{o}C during which the microtubules were allowed to depolymerize [35]. Cells were then fixed with 4% formaldehyde (Sigma Aldrich, Toronto, ON) for 10 min, washed with phosphate buffered saline (PBS, 137 mM NaCl, 10 mM Na_2PO_4, 20 mM KH_2PO_4, 27 mM KCl final concentrations) twice, and permeabalized with 100% methanol for 2 min. Non-specific proteins were blocked with 2% bovine serum albumin (BSA) (Sigma Aldrich, Toronto, ON) in PBS for 5 min. The primary antibody, anti-tubulin (AA4.3; DHSB, University of Iowa, IA) (1:100) was used and incubated overnight at 4^{o}C. After washing with 2% BSA/PBS three times, the secondary antibody, Alexa Fluor 568 donkey anti-mouse IgG (1:200) (Invitrogen, Molecular Probes, OR, USA), was incubated for 1 h in darkness. After three washes with 2% BSA/PBS, the nuclei were stained with DAPI (1:5000) (Molecular Probes) for 10 min. After a final rinse with PBS, the cover-slips were mounted in glycerol and the cells were examined using a Biorad Radiance 2100 confocal laser scanning microscope equipped with a Nikon E800 fluorescence microscope for confocal image acquisition and the LASERSHARP 2000 analyzing

software package. All the antibodies were diluted in PBS supplemented with 2% BSA; all procedures were at room temperature.

3.2.15. Cell multiplication.

HeLa cells were seeded in culture plates (Corning Inc., Corning, NY, USA). Thirty six h were allowed for the cells to attach and adapt to the environment. At this point the medium was replaced with α-MEM containing 0.6% DMSO, 0.1 µM IVM, 5 µM IVM or 10 µM IVM (Sigma Aldrich, Toronto, ON). Cells were detached with 0.25% trypsin-EDTA (Gibco, Life Technologies) counted with a Neubhar chamber at 12 h, 24 h, 36 h, 48 h and 60 h.

3.2.16. Reversibility of IVM effect.

Twelve well culture plates (Corning, NY, USA) were used to seed HeLa. The cells were allowed 36 h to attach and adapt to the environment after which the α-MEM was replaced with α-MEM containing 0.6% DMSO and 10 µM IVM. Following 18 h and 36 h the medium was replaced with α-MEM containing 0.6% DMSO and the incubation continued for a total of 60 h. The final 10 µM IVM exposure to cells was for 18 h, 36 h or 60 h. The final exposure for 0.6% DMSO was also 60 h. The cells were then trypsinized and counted in the Neubhar chamber.

3.2.17. Statistical analysis.

For the polymerization assay and equilibrium dialysis experiments, one way ANOVA and Tukey's Multiple comparison test were used. For limited trypsin proteolysis

experiments students T test was used. GraphPad Software Inc. V.5.00 was used for all the statistical analyses**.**

3.3. Results

3.3.1. IVM increases polymerization of *Haemonchus contortus* tubulin and protects tubulin from trypsin proteolysis.

The functional activity of the recombinant α- and β-tubulin from *H. contortus* was confirmed by testing the effects of taxol and colchicine on polymerization. As expected, 30 μM taxol increased the rate of tubulin polymerization, whereas it was inhibited by 200 μM colchicine (Figure 3.1A). The structural integrity of the polymerized recombinant tubulin was further confirmed using electron microscopy, and as expected, both ring and elongated microtubule-like structures were apparent (Figure 3.1B), further confirming the functional activity of the recombinant α- and β-tubulin. To test if IVM directly interacts with tubulin, we first examined the effect of IVM on *H. contortus* tubulin polymerization. In the presence of increasing IVM concentration, significant increases in the degree of tubulin polymerization were observed as compared to DMSO-treated controls (Figure 3.1C). Also indicative of an interaction between IVM and tubulin, we found that the presence of IVM significantly delayed trypsin-mediated proteolysis of β- (Figure 3.1D-E) and α-tubulin (Figure 3.1F-G) as compared to the DMSO-treated controls.

3.3.2. IVM binds directly to α- and β-tubulin and competes for taxol binding site.

Label-free, real-time SPR was utilized to test for direct interactions between IVM with immobilized α- and β-tubulin subunits from *H. contortus*. In terms of specificity,

significant binding responses were detected with IVM and taxol (positive control). In terms of binding kinetics and affinity, subsequent dose-dependent titrations (Figure 3.2A-D) for IVM and taxol binding to *H. contortus* tubulin were characterized by fast-on, fast-off kinetics. Consistent with mammalian tubulin, the overall affinity of taxol for β-tubulin (Figure 3.2B; K_D ~25 μM) was stronger compared to α-tubulin (Figure 3.2D; K_D >120 μM). Notably, IVM exhibited matching affinities for α- and β-tubulin (Figure 3.2A (K_D ~30 μM) and 3.2C (K_D ~33 μM), respectively) that were similar to the binding affinity of taxol for β-tubulin.

To cross-validate the SPR results and to identify the putative binding site for IVM on α- and β-tubulin, equilibrium dialysis with fluorescently (BODIPY)-labeled IVM (BFLIVM) was performed (Figure 3.2E-F). As anticipated, three negative controls (i.e. PBS plus 20 μM BFLIVM; α- or β-tubulin plus 20 μM BFL; 10 μM DNase I plus 20 μM BFLIVM) failed to exhibit significant differences in fluorescence between the samples retrieved from both chambers. Samples containing α- or β-tubulin plus 20 μM BFLIVM, however, exhibited significant increases in fluorescence from both chambers. Increased fluorescence due to the binding of BODIPY-labeled IVM to tubulin could be significantly diminished by the addition of non-fluorescent IVM as a competitor for β-tubulin (Figure 3.2E) and α-tubulin, (Figure 3.2F). Non-fluorescent taxol was also able to compete the interaction with β-tubulin; and α-tubulin, whereas non-fluorescent Lev was not. Overall, our equilibrium dialysis experiments indicate that the tubulin binding sites for IVM and taxol are overlapping.

3.3.3. Molecular modeling shows that IVM and taxol occupy the taxane binding pocket of β-tubulin.

To identify a putative IVM-binding site in tubulin, molecular dockings were generated based upon published (e.g. porcine crystal structure) and theoretical (*H. contortus*) models of tubulin. Optimized modeling quality was good/satisfactory, with Z scores of -1.442, -0.205 and -0.519 based on the 1JFF-AB (Hco-1JFF), 4I4T-CD (Hco-4I4T) and 3UT5-CD (Hco-3UT5) templates. Self-docking the ligand back onto the published structures produced optimized poses with RMSD values of 1.76, 1.55 and 0.33 for the 1JFF, 4I4T and 3UT5 structures respectively, thus validating the docking algorithm used. Docking IVM on to Hco-1JFF produced a best pose with a binding energy of -8.71 kcal/mol located within the taxane pocket occupied by taxol in the 1JFF structure (Figure 3.3A, 3D). Similarly, the best taxol pose had a binding energy of -9.87 kcal/mol, also within the taxane pocket (Figure 3.3B). Local docking of IVM to the taxane pocket of Hco-4I4T found a best pose with an energy of -8.00 kcal/mol compared to -7.44 kcal/mol for taxol. Docking to Hco-3UT5 found no pose within the taxane, colchicine, or any other pocket, but identified 12 poses that were distributed to various points on the structure surface. Docking IVM onto the bovine tubulin 1JFF structure also found a best pose within the taxane binding pocket, this time with energy of -9.01 kcal/mol (Figure 3.3C).

3.3.4. Effect of IVM on mammalian tubulin and replication of HeLa cells.

Consistent with our *H. contortus* tubulin experiments, IVM also increased the degree of polymerization of mammalian tubulin when compared to DMSO only, as well as taxol (increased) and colchicine (decreased) polymerization controls (Figure 3.4A). To

study the effect of IVM on the stability of mammalian tubulin, HeLa cells were treated with fixed concentrations of IVM, taxol, colchicine, or vehicle (0.6 % DMSO only). The microtubule networks were visualized by immunofluorescence such that each treatment group was maintained at 37^{o}C for 22 h, followed by incubation at 4^{o}C for 16 h (i.e. temperature at which microtubules depolymerize and networks should not be visible via immunofluorescence unless stabilized by drug). As indicated by anti-α-tubulin staining, pronounced microtubule bundles were visible in IVM- and taxol-treated cells (Figure 3.4B); in contrast, filamentous microtubule structures were seldom visible in the colchicine- and DMSO-treated cells. IVM and taxol stabilized the microtubules against depolymerization at 4^{o}C, whereas the cells treated with colchicine and DMSO did not. To study its effect on replication, HeLa cells were treated with IVM (Figure 3.4C): at 0.1 µM IVM, no effect was observed and the cells multiplied at the same rate as the DMSO group; at 5 µM, the cells multiplied but at a reduced rate compared to DMSO; at 10 µM, cell replication completely stopped. To see if this effect was reversible, HeLa cells were then treated with 10 µM IVM for 18 h or 36 h, followed by removal of IVM and then the incubation was continued for a total of 60 h (in fresh media containing 0.6% DMSO). The controls included cells treated with 10 µM IVM for 60 h (negative) or cells treated with 0.6 % DMSO for 60 h (positive). Notably, the cells started to multiply again once the IVM was removed from the media (Figure 3.4D).

3.4. Discussion

The objective of this study was to establish if there is a direct interaction between IVM and tubulin/microtubules. Many reports have previously shown that IVM selects on

β-tubulin in *Onchocerca volvulus* [8, 10-13]. Single nucleotide polymorphisms (F167Y and F200Y) on the β-tubulin isotype 1 gene have been found in IVM-selected *H. contortus* strains never exposed to benzimidazoles [9, 10]. Though these authors have established that IVM is selecting on the β-tubulin isotype 1 gene, unresolved is the molecular mechanism(s) to explain the relationship between repeated IVM treatment and genetic selection on the β-tubulin gene.

In the current study, recombinant *H. contortus* α- and β-tubulin isotype 1 were expressed and purified from *E. coli*. Polymerization experiments were performed in the absence and presence and absence of IVM which revealed that it can increase the extent of polymerization and stability of microtubules. Since IVM protected α- and β-tubulin from trypsin proteolysis, this further indicated that IVM can bind directly to *H. contortus* tubulin.

While a direct interaction between IVM and tubulin has not been previously reported, our current SPR experiments now demonstrate that IVM can bind to both the α- and β-subunits of *H. contortus* tubulin with low micromolar affinity. While many groups have examined small molecules binding to tubulins by SPR to date, our results are unique as we immobilized the individual α- and β-subunits to SPR sensors, not intact α/β-tubulin heterodimers. Compared to the reported equilibrium dissociation constants (K_D) for taxol (K_D ~1 μM, [36]; K_D ~2 μM, [37]; K_D ~3 μM, [38]) and other compounds (e.g. 5HPP-33, K_D ~0.2 μM, [25]; BM6, K_D ~1.5 μM, [26]; C9, K_D ~21 μM, [27]; MT119, K_D ~11 μM, [28]) binding to mammalian α/β-tubulin heterodimers, our binding of IVM to the individual *H. contortus* α- and β- tubulins also exhibited low micromolar affinities.

Evidence of a direct IVM-tubulin interaction was also provided by equilibrium dialysis experiments where increased fluorescence (i.e. BODIPY-labeled IVM (BFLIVM) binding to α- and β-tubulins) was observed compared to controls. Moreover, the interaction was specific given that non-fluorescent IVM was able to compete the binding of BFLIVM. While the exact binding site for IVM has yet to be defined, we were able to show that taxol can compete with BFLIVM for binding to tubulin. Taxol binds to the M-loop at the site of lateral interactions between the α- and β-subunits of tubulin [39] and, although β-tubulin is a major target for taxol [40, 41], taxol binding to α-tubulin has also been reported [42-44]. Our current *H. contortus* findings indicate that IVM can bind to both α- and β-tubulin with micromolar affinity, and that IVM and taxol compete for the same binding site on tubulin.

Our molecular modeling for the interaction between IVM and the *H. contortus* α/β-tubulin heterodimer is consistent with the equilibrium dialysis experiments that indicated IVM and taxol compete for the same taxane binding pocket in tubulin. The structural rearrangement brought about by ligand binding is significant and likely plays a critical role in stabilizing the polymerized microtubule [32]. Crystal structure models with taxol or zampanolide bound to the taxane pocket have led to the prediction that IVM also binds within this pocket. Models in which colchicine was bound to tubulin have failed to favor IVM binding. Consistent with our polymerization assays (both parasitic and mammalian tubulin), our molecular modeling suggests that IVM binding induces the same type of structural rearrangements (i.e. increased stabilization of microtubules) as taxol and other related compounds.

To then test the effect of IVM on the stability of mammalian tubulin, the microtubules of HeLa cells did not disappear following exposure to IVM at cold temperature. This shows that IVM stabilized the microtubules and prevented them from depolymerization, thus mimicking the effects of taxol. Higher IVM concentrations (i.e. 10 μM) did not allow HeLa cells to multiply, thus indicating that the cells were in mitotic arrest. While the effects of IVM were reversible in the current study (i.e. cell growth resumed once it was removed), additional drug development to select for IVM candidates with lower dissociation rate constants (i.e. evolve from micromolar to nanomolar affinity) would lead to improved pharmacokinetics (i.e. increased half-life).

Our novel findings open the door to new avenues for anti-cancer therapeutic development – i.e. application of existing drugs with newly discovered anti-mitotic effects. Indeed, the pharmacology and toxicology of IVM have been investigated extensively as an anti-parasitic agent. For human onchocerciases, the maximum plasma concentrations (C_{max}) achieved for IVM was 52 ng/ml when given at 150 μg/kg dosage [45]. This concentration is much lower than the concentrations that are required to produce an anti-mitotic, anti-cancer effect which may account for why these effects were not previously reported. IVM is very lipophilic and concentrations in fatty tissues are typically much higher than in plasma. High concentrations of IVM, that could have anti-cancer effects, were previously well tolerated in animals and humans. For example the LD_{50} of IVM in various animals is over 20 mg/kg [20]. Doses up to 2 mg/kg IVM have been well tolerated by various individuals [19]. In addition, many reports of IVM over-dosage, without any side effects, also support the wide therapeutic window for this drug.

Furthermore, our current study may lead to revised strategies for anthelmintic treatment. For example, the commonly practiced treatment where there is rotation between IVM and the benzimidazoles, which act on tubulin polymerization, should be revisited as this may increase selection pressure for resistance to both anthelmintics. Since IVM has a very high therapeutic index [20], it may be considered as a potential anti-cancer agent. The current findings may also explain the previously reported anti-tumor effects of avermectins [46, 47]. IVM has also caused cell death of leukemia cells at micromolar concentrations [17]. The authors report that this cell death is due to chloride dependent membrane hyperpolarization, however it may be possible that the effect on tubulin acts synergistically, causing the cell death. Overall, we have established that IVM directly interacts with tubulins and, given the extensive safety and toxicity testing of IVM as an anti-parasitic drug, IVM could rapidly be assessed in experimental trials as an anti-cancer agent.

3.5. Acknowledgements

This project received financial support from NSERC; and the FQRNT Centre for Host-Parasite Interactions Quebec, Canada; the McGill SPR Facility thanks the Canada Foundation for Innovation (CFI); and Canadian Institutes of Health Research (CIHR) for infrastructure support. We wish to thank EMBL for the generous gift of the pETM-10 expression vector, the McGill EM facility, A. Kottarampatel for fluorescent spectroscopy, Kathy Keller for harvesting the parasites, Dr. Armando Jardim for helpful discussions and Dr Jerry Aldridge for help with drafting the manuscript and helpful discussions. We thank Dr Anne Lespine for the gift of Bodipy FL ivermectin.

References

[1] Jordan MA, Wilson L. Microtubules as a target for anticancer drugs. Nature reviews Cancer. 2004;4:253-65.
[2] Wood KW, Cornwell WD, Jackson JR. Past and future of the mitotic spindle as an oncology target. Current opinion in pharmacology. 2001;1:370-7.
[3] Little M, Seehaus T. Comparative analysis of tubulin sequences. Comparative biochemistry and physiology B, Comparative biochemistry. 1988;90:655-70.
[4] Kavallaris M. Microtubules and resistance to tubulin-binding agents. Nature reviews Cancer. 2010;10:194-204.
[5] Campbell WC, Fisher MH, Stapley EO, Albers-Schonberg G, Jacob TA. Ivermectin: a potent new antiparasitic agent. Science (New York, NY). 1983;221:823-8.
[6] Cully DF, Vassilatis DK, Liu KK, Paress PS, Van der Ploeg LH, Schaeffer JM, et al. Cloning of an avermectin-sensitive glutamate-gated chloride channel from Caenorhabditis elegans. Nature. 1994;371:707-11.
[7] Hibbs RE, Gouaux E. Principles of activation and permeation in an anion-selective Cys-loop receptor. Nature. 2011;474:54-60.
[8] Bourguinat C, Pion SD, Kamgno J, Gardon J, Duke BO, Boussinesq M, et al. Genetic selection of low fertile Onchocerca volvulus by ivermectin treatment. PLoS neglected tropical diseases. 2007;1:e72.
[9] de Lourdes Mottier M, Prichard RK. Genetic analysis of a relationship between macrocyclic lactone and benzimidazole anthelmintic selection on Haemonchus contortus. Pharmacogenetics and genomics. 2008;18:129-40.
[10] Eng JK, Blackhall WJ, Osei-Atweneboana MY, Bourguinat C, Galazzo D, Beech RN, et al. Ivermectin selection on beta-tubulin: evidence in Onchocerca volvulus and Haemonchus contortus. Molecular and biochemical parasitology. 2006;150:229-35.
[11] Eng JK, Prichard RK. A comparison of genetic polymorphism in populations of Onchocerca volvulus from untreated- and ivermectin-treated patients. Molecular and biochemical parasitology. 2005;142:193-202.
[12] Nana-Djeunga H, Bourguinat C, Pion SD, Kamgno J, Gardon J, Njiokou F, et al. Single nucleotide polymorphisms in beta-tubulin selected in Onchocerca volvulus following repeated ivermectin treatment: possible indication of resistance selection. Molecular and biochemical parasitology. 2012;185:10-8.
[13] Osei-Atweneboana MY, Boakye DA, Awadzi K, Gyapong JO, Prichard RK. Genotypic analysis of β-tubulin in Onchocerca volvulus from communities and individuals showing poor parasitological response to ivermectin treatment. International Journal for Parasitology: Drugs and Drug Resistance. 2012;2:20-8.
[14] Kobylinski KC, Foy BD, Richardson JH. Ivermectin inhibits the sporogony of Plasmodium falciparum in Anopheles gambiae. Malaria journal. 2012;11:381.
[15] Lim LE, Vilcheze C, Ng C, Jacobs WR, Jr., Ramon-Garcia S, Thompson CJ. Anthelmintic avermectins kill Mycobacterium tuberculosis, including multidrug-resistant clinical strains. Antimicrobial agents and chemotherapy. 2013;57:1040-6.
[16] Mastrangelo E, Pezzullo M, De Burghgraeve T, Kaptein S, Pastorino B, Dallmeier K, et al. Ivermectin is a potent inhibitor of flavivirus replication specifically targeting

NS3 helicase activity: new prospects for an old drug. The Journal of antimicrobial chemotherapy. 2012;67:1884-94.
[17] Sharmeen S, Skrtic M, Sukhai MA, Hurren R, Gronda M, Wang X, et al. The antiparasitic agent ivermectin induces chloride-dependent membrane hyperpolarization and cell death in leukemia cells. Blood. 2010;116:3593-603.
[18] Costa JL, Diazgranados JA. Ivermectin for spasticity in spinal-cord injury. Lancet. 1994;343:739.
[19] Guzzo CA, Furtek CI, Porras AG, Chen C, Tipping R, Clineschmidt CM, et al. Safety, tolerability, and pharmacokinetics of escalating high doses of ivermectin in healthy adult subjects. Journal of clinical pharmacology. 2002;42:1122-33.
[20] Dadarkar SS, Deore MD, Gatne MM. Comparative evaluation of acute toxicity of ivermectin by two methods after single subcutaneous administration in rats. Regulatory toxicology and pharmacology : RTP. 2007;47:257-60.
[21] Ranjan S, Wang GT, Hirschlein C, Simkins KL. Selection for resistance to macrocyclic lactones by Haemonchus contortus in sheep. Veterinary parasitology. 2002;103:109-17.
[22] Ashraf S, Prichard RK. Haemonchus contortus microtubules are cold resistant. Molecular and biochemical parasitology. 2014;193:20-2.
[23] Shelanski ML, Gaskin F, Cantor CR. Microtubule assembly in the absence of added nucleotides. Proceedings of the National Academy of Sciences of the United States of America. 1973;70:765-8.
[24] Hait WN, Rubin E, Alli E, Goodin S. Tubulin targeting agents. Update on cancer therapeutics. 2007;2:1-18.
[25] Aoyama H, Noguchi T, Misawa T, Nakamura T, Miyachi H, Hashimoto Y, et al. Development of tubulin-polymerization inhibitors based on the thalidomide skeleton. Chemical & pharmaceutical bulletin. 2007;55:944-9.
[26] Li W, Shao Y, Hu L, Zhang X, Chen Y, Tong L, et al. BM6, a new semi-synthetic vinca alkaloid, exhibits its potent in vivo anti-tumor activities via its high binding affinity for tubulin and improved pharmacokinetic profiles. Cancer biology & therapy. 2007;6:787-94.
[27] Ren X, Dai M, Lin LP, Li PK, Ding J. Anti-angiogenic and vascular disrupting effects of C9, a new microtubule-depolymerizing agent. British journal of pharmacology. 2009;156:1228-38.
[28] Zhang Z, Meng T, Yang N, Wang W, Xiong B, Chen Y, et al. MT119, a new planar-structured compound, targets the colchicine site of tubulin arresting mitosis and inhibiting tumor cell proliferation. International journal of cancer Journal international du cancer. 2011;129:214-24.
[29] Myszka DG. Improving biosensor analysis. Journal of molecular recognition : JMR. 1999;12:279-84.
[30] Krieger E, Koraimann G, Vriend G. Increasing the precision of comparative models with YASARA NOVA--a self-parameterizing force field. Proteins. 2002;47:393-402.
[31] Lowe J, Li H, Downing KH, Nogales E. Refined structure of alpha beta-tubulin at 3.5 A resolution. Journal of molecular biology. 2001;313:1045-57.
[32] Prota AE, Bargsten K, Zurwerra D, Field JJ, Diaz JF, Altmann KH, et al. Molecular mechanism of action of microtubule-stabilizing anticancer agents. Science (New York, NY). 2013;339:587-90.

[33] Ranaivoson FM, Gigant B, Berritt S, Joullie M, Knossow M. Structural plasticity of tubulin assembly probed by vinca-domain ligands. Acta crystallographica Section D, Biological crystallography. 2012;68:927-34.
[34] Trott O, Olson AJ. AutoDock Vina: improving the speed and accuracy of docking with a new scoring function, efficient optimization, and multithreading. Journal of computational chemistry. 2010;31:455-61.
[35] Schiff PB, Horwitz SB. Taxol stabilizes microtubules in mouse fibroblast cells. Proceedings of the National Academy of Sciences of the United States of America. 1980;77:1561-5.
[36] Parness J, Horwitz SB. Taxol binds to polymerized tubulin in vitro. The Journal of cell biology. 1981;91:479-87.
[37] Ross JL, Santangelo CD, Makrides V, Fygenson DK. Tau induces cooperative Taxol binding to microtubules. Proceedings of the National Academy of Sciences of the United States of America. 2004;101:12910-5.
[38] Khrapunovich-Baine M, Menon V, Verdier-Pinard P, Smith AB, 3rd, Angeletti RH, Fiser A, et al. Distinct pose of discodermolide in taxol binding pocket drives a complementary mode of microtubule stabilization. Biochemistry. 2009;48:11664-77.
[39] Nogales E. Structural insights into microtubule function. Annual review of biochemistry. 2000;69:277-302.
[40] Nogales E, Wolf SG, Downing KH. Structure of the alpha beta tubulin dimer by electron crystallography. Nature. 1998;391:199-203.
[41] Nogales E, Wolf SG, Khan IA, Luduena RF, Downing KH. Structure of tubulin at 6.5 A and location of the taxol-binding site. Nature. 1995;375:424-7.
[42] Banerjee A, Kasmala LT. Differential assembly kinetics of alpha-tubulin isoforms in the presence of paclitaxel. Biochemical and biophysical research communications. 1998;245:349-51.
[43] Dasgupta D, Park H, Harriman GC, Georg GI, Himes RH. Synthesis of a photoaffinity taxol analogue and its use in labeling tubulin. Journal of medicinal chemistry. 1994;37:2976-80.
[44] Loeb C, Combeau C, Ehret-Sabatier L, Breton-Gilet A, Faucher D, Rousseau B, et al. [3H](azidophenyl)ureido taxoid photolabels peptide amino acids 281-304 of alpha-tubulin. Biochemistry. 1997;36:3820-5.
[45] Baraka OZ, Mahmoud BM, Marschke CK, Geary TG, Homeida MM, Williams JF. Ivermectin distribution in the plasma and tissues of patients infected with Onchocerca volvulus. European journal of clinical pharmacology. 1996;50:407-10.
[46] Drinyaev VA, Mosin VA, Kruglyak EB, Novik TS, Sterlina TS, Ermakova NV, et al. Antitumor effect of avermectins. European journal of pharmacology. 2004;501:19-23.
[47] Korystov YN, Ermakova NV, Kublik LN, Levitman M, Shaposhnikova VV, Mosin VA, et al. Avermectins inhibit multidrug resistance of tumor cells. European journal of pharmacology. 2004;493:57-64.

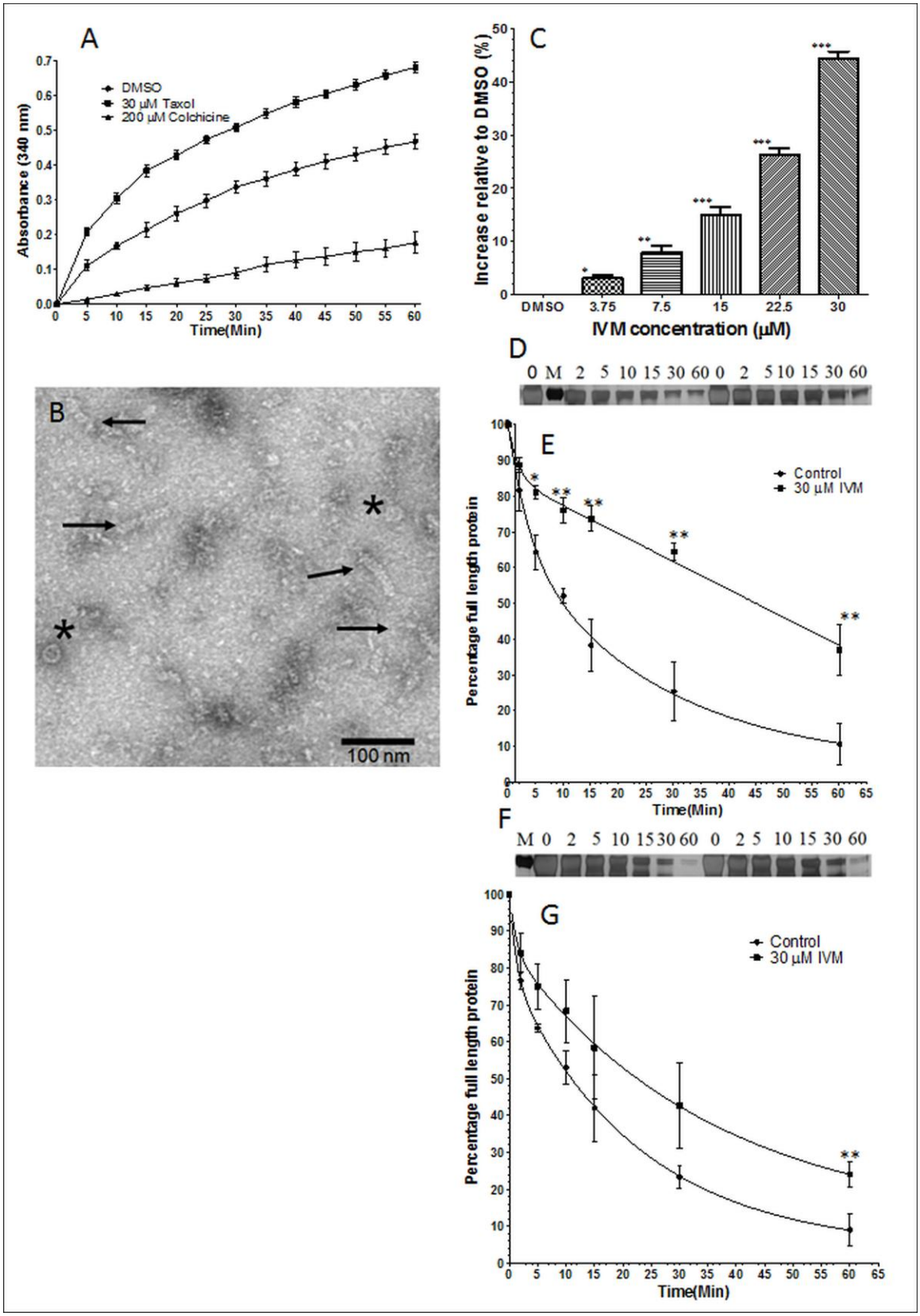
A
DMSO
30 μM Taxol
200 μM Colchicine
Absorbance (340 nm)
Time(Min)
B
100 nm
C
Increase relative to DMSO (%)
DMSO
3.75
7.5
15
22.5
30
IVM concentration (μM)
D
0 M 2 5 10 15 30 60 0 2 5 10 15 30 60
E
Control
30 μM IVM
Percentage full length protein
Time(Min)
F
M 0 2 5 10 15 30 60 0 2 5 10 15 30 60
G
Control
30 μM IVM
Percentage full length protein
Time(Min)

Figure 3.1

Figure 3.1 – Tubulin polymerization, electron microscopy, **the effect of IVM on *Haemonchus contortus* tubulin polymerization and limited trypsin proteolysis.** (A) Tubulin polymerization assay performed with 20 μM purified recombinant *H. contortus* α-tubulin and 20 μM purified recombinant *H. contortus* β-tubulin isotype 1. Two percent DMSO was added as a solvent control, 30 μM taxol was used as a positive control, whereas 200 μM colchicine was used as a negative control. (B) Electron microscopy of the polymerized tubulin. Twenty μM α-tubulin and β-tubulin isotype 1 showing both ring (asterisk) and elongated (arrow) structures of microtubules. Percent increases in tubulin polymerization. (C) The effect of IVM (3.75 – 30 μM) on polymerization of 20 μM α-tubulin and 20 μM β-tubulin isotype 1, relative to 2% DMSO control. The concentration-dependent increased polymerization was significantly different from the DMSO-treated control (one-way ANOVA and Tukey's multiple comparison tests). (D, E) Limited trypsin proteolysis of β-tubulin isotype 1, and (F, G) α-tubulin; in both cases, digestion was significantly delayed (Student's t test) in the presence of 30 μM IVM, as assessed by 10% SDS-PAGE with silver staining (lane M = 55 kDa marker; lanes 1-7 = 0, 2, 5, 10, 15, 30, 60 min with 2% DMS0; lanes 8-14 = 0, 2, 5, 10, 15, 30, 60 min with 30 μM IVM in 2% DMSO) (*P<0.05, **P= 0.01-0.05, ***P< 0.01, n=3).

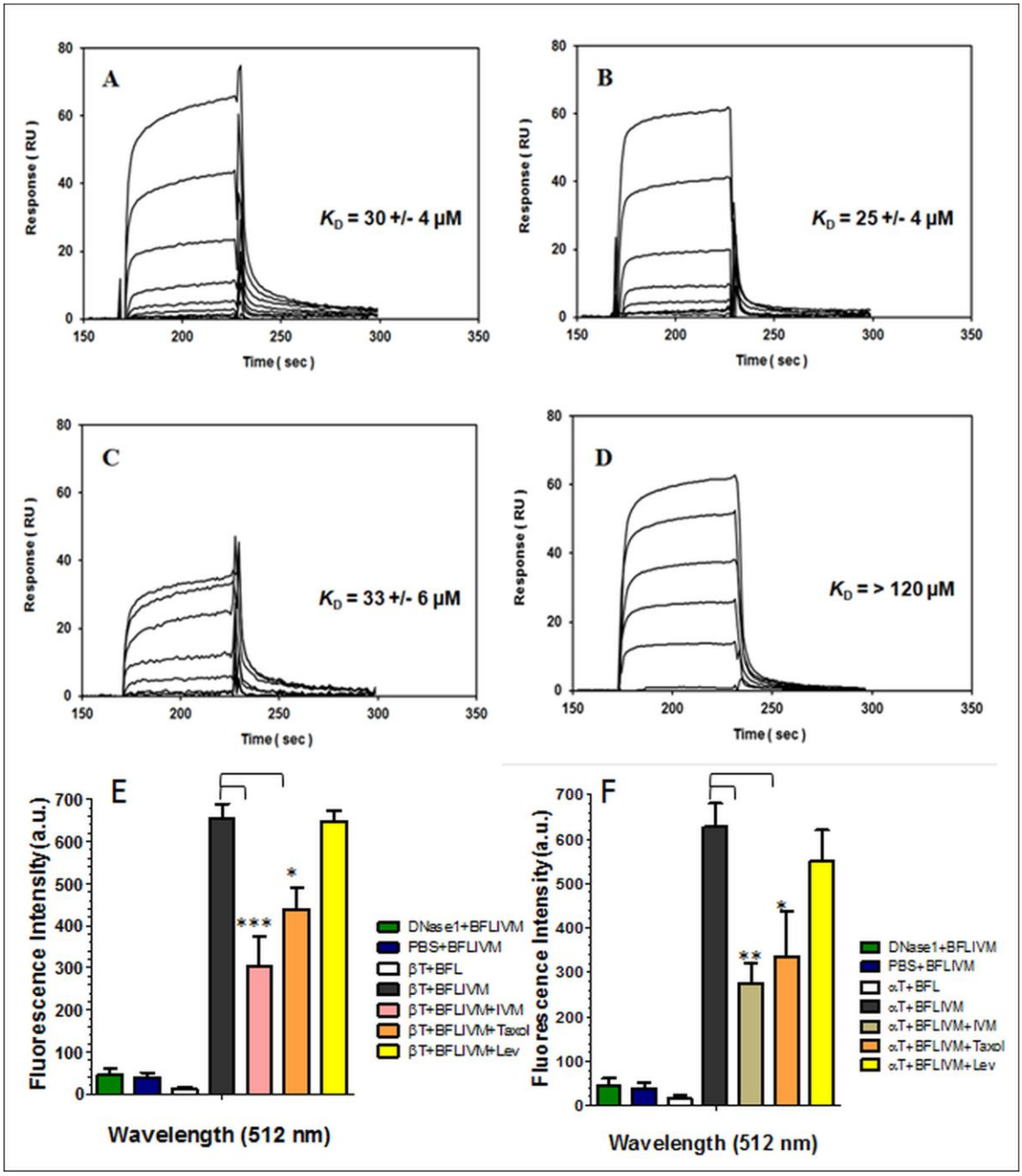

Figure 3.2

Figure 3.2 – IVM binds to *Haemonchus contortus* tubulin and competes for taxol binding site. Representative kinetics for compounds (in 5% DMSO) binding to amine-coupled tubulins (~5,000 RU each) at 25 µL/min (1 min association + 1 min dissociation), as assessed by SPR: (A) β-tubulin + IVM (0-100 µM, 2-fold serial); (B) β-

tubulin + taxol (0-75 µM, 2-fold serial); (C) α-tubulin + IVM (0-100 µM, 2-fold serial); (D) α-tubulin + taxol (0, 2, 10, 20, 30, 40, 50 µM). After DMSO solvent correction, SPR titration series were analyzed globally (BIAevaluation "steady-state affinity" model) to generate the inset equilibrium dissociation constants (average K_D +/- standard error; n = 4). To test where IVM binds on tubulin, β- (E), and α-tubulin (F) were dialyzed against BODIPY-labelled IVM (BFLIVM) in the absence and presence of non-fluorescent IVM, taxol, and levamisole (50 µM each); Non-fluorescent IVM and taxol significantly reduced the fluorescence as compared to BFLIVM for α- and β-tubulin (one-way ANOVA and Tukey's multiple comparison tests) (*P<0.05, **P= 0.01-0.05, ***P< 0.01, n=3).

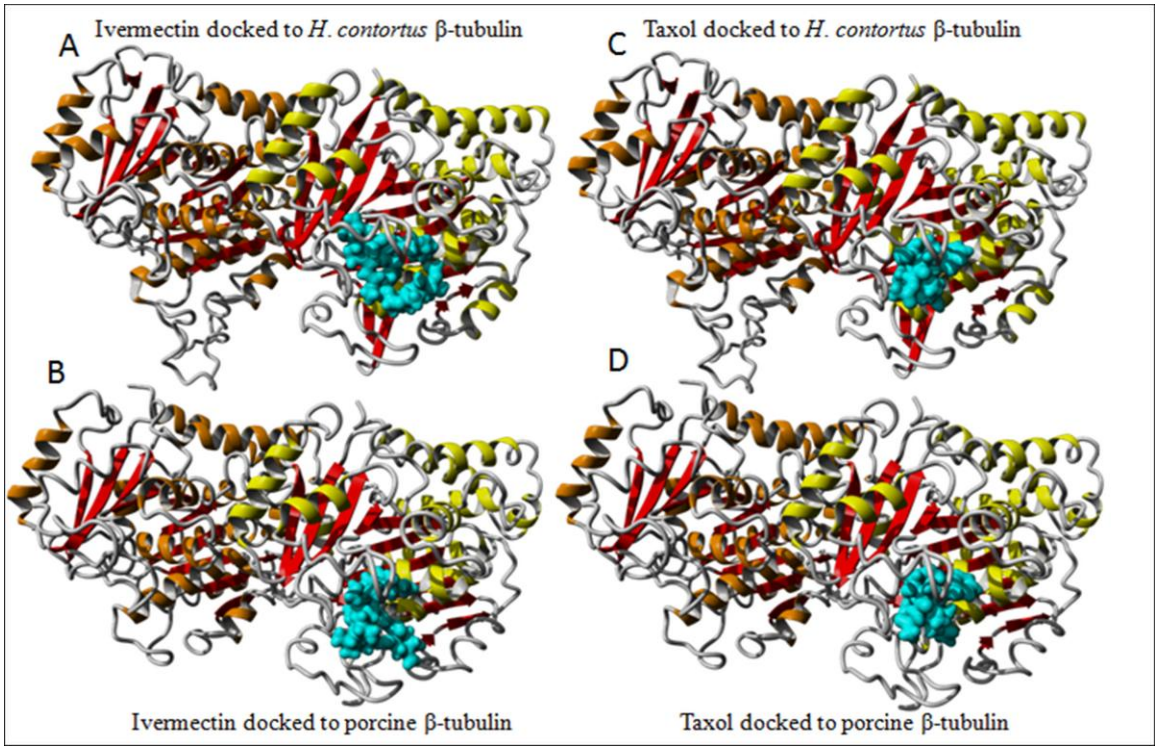

Figure 3.3

Figure 3.3 – Docking IVM and taxol with tubulin dimers *in silico*. Structural models of an α-β-tubulin dimer are shown with highest scoring binding poses for bound ligands. Protein secondary structure is shown as a cartoon with the α-subunit to the left. Bound ligands are shown as space filled models in blue. (A) Refined homology model of *H. contortus* α- and isotype-1 β-tubulin bound to IVM. (B) The porcine α-β dimer crystal structure (PDB 1JFF: C, D) showing IVM docked *in silico*. (C) The *H. contortus* refined model bound to taxol. (D) The porcine dimer showing the experimentally determined position of taxol in the crystal structure. In each case the highest scoring poses for IVM or taxol are found within the taxane binding pocket.

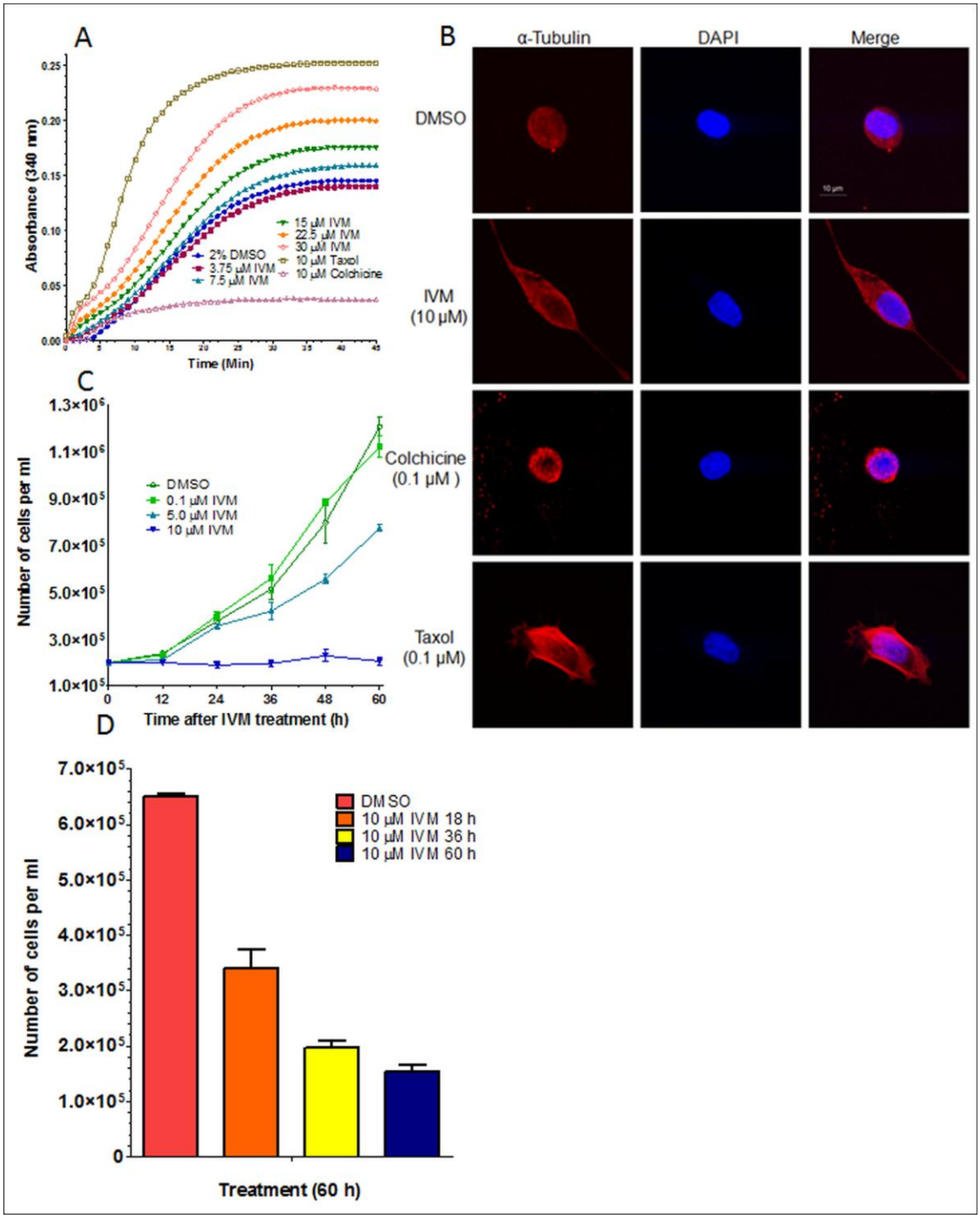

Figure 3.4

Figure 3.4 – Polymerization of mammalian tubulin and effect of IVM on HeLa cells. (A) Increases (IVM, taxol) and decreases (colchicine) in polymerization of porcine tubulin as compared to the DMSO-treated controls; data is representative of three

individual experiments. (B) IVM and taxol stabilize microtubules against depolymerization at 4^{o}C, as evinced by long microtubule bundles; microtubules were depolymerized in the presence of 0.6% DMSO or colchicine, as evidenced by significantly lack of filamentous structures. (C) variable effect of IVM on HeLa cell replication (i.e., no effect at 0.1 μM as compared to 0.6% DMSO control; cell multiplication was significantly reduced rate by 5 μM IVM; inhibition of cell multiplication occurred at 10 μM IVM); slopes were analyzed by linear regression analysis, $P<0.05$ (GraphPad Software Inc. V.5.00). (D) HeLa cells were treated with 10 μM IVM (or 0.6% DMSO only) for 18 or 36 h, followed by additional 60 h incubations with fresh media only (i.e. recovery phase); post-recovery increases in cell replication were significant compared to cells treated with 10 μM IVM for 60 h ($P<0.05$; one-way ANOVA and Tukey's multiple comparison tests).

Connecting statement III

In the previous chapter we report a specific interaction between ivermectin and tubulin. Interestingly previous reports have suggested that ivermectin was selecting for *H. contortus* β-tubulin containing the SNP 200Y or 167Y. It was therefore of interest to determine whether the F200Y or F167Y SNPs affected the relationship between ivermectin and tubulin. Furthermore, as moxidectin is also another macrocyclic lactone with some different properties to ivermectin, it was also of interest to investigate whether there were any differences in the binding of moxidectin and ivermectin to tubulin.

Chapter IV

Manuscript III

Macrocyclic lactones and their relationship to the SNPs related to benzimidazole resistance

Shoaib Ashraf, Robin N. Beech, Thangadurai Mani and Roger K. Prichard

In preparation for Molecular and Biochemical Parasitology

Abstract

Haemonchus contortus is an abomasal nematode of ruminants that is widely present in across the world. Its ability to cause death of the infected animal and rapidly develop anthelmintic resistance makes it a dangerous pathogen. Ivermectin (IVM) and moxidectin (MOX) are macrocyclic lactones (MLs). They have been successfully used to treat parasitic nematodes over the last three decades. A genetic association between IVM selection and single nucleotide polymorphisms (SNPs) on the β-tubulin isotype 1 gene was reported in *H. contortus*. These SNPs result in replacing phenylalanine (F, TTC) with tyrosine (Y, TAC) at position 167 or 200 on the β-tubulin protein. Recently we reported a direct interaction of IVM with α- and β-tubulin. It was hypothesized that these SNPs may change tubulin dynamics and directly affect IVM binding. However contrary to our hypothesis no differences were observed in the polymerization of wild and mutant tubulins. Furthermore neither of the SNPs reduced IVM binding. Varying results were obtained in the degree of polymerization of parasitic and mammalian tubulin for IVM and MOX i.e., the extent of polymerization was more for IVM versus MOX for *Haemonchus* tubulin and vice versa for mammalian tubulin. Molecular modeling showed that IVM and MOX docked into the taxol binding pocket of both mammalian and parasitic wild type and mutant tubulins, however the binding was stronger for mammalian tubulin as compared to parasitic tubulin.

Keywords: *Haemonchus contortus,* **i**vermectin, moxidectin, tubulin, single nucleotide polymorphism

4.1. Introduction

H. contortus is a nematode of livestock causing substantial losses to the industry. It belongs to the family Trichostrongylidae and feeds on blood by attaching to the abomasal mucosa. It sucks about 12 µl of blood per day. It causes aneamia, bottle jaw and subsequently death of the infected animal [1]. The parasite has always taken a lead in developing resistance against potential anthelmintics [2]. It is one of the most widely used parasites to study the development of resistance and has been proven as an excellent model organism [3].

IVM is a macrocyclic lactone (ML) from the avermectin group isolated from *Streptomyces avermetilis* [4]. It has been successfully used to treat haemonchosis and onchocerciasis for almost three decades. Moxidectin (MOX) is another ML, but from the milbemycins group and was isolated from *Streptomyces cyaneogriseus*. IVM and MOX are collectively referred to as endectocides because of their activity against both ectoparasites and endoparasites. Both IVM and MOX have a 16-membered ML ring fused with both spiroketal and benzofurane. One mechanism of action of MLs is that they bind to the glutamate-gated chloride channels (GluCls) and cause paralysis of the parasite [5]. Although both MLs have a similar mode of action, there are some differences in the pharmacodynamics, pharmacokinetics and toxicity. IVM has a disaccharide attached to the 13-position and a secondary butyl or isopropyl in the 25-position, whereas MOX is protonated (unglycosylated) in the 13-position, has a substituted olefinic side chain at the 25 position and a methoxime moiety at the 23-position [6].

Recent data suggests that IVM resistant *H. contortus* strains had altered amphidial dendrites [7]. These amphidial dendrites are made of microtubules which

were disorganized in resistant strains [8]. There are a number of reports suggesting a genetic association between IVM selection and β-tubulin in *O. volvulus* [9-13], and in IVM resistant *H. contortus* strains [9, 14]. These SNPs resulted in a single amino acid substitution from F to Y at position 167 and 200 of the β-tubulin isotype 1 protein. It is of interest that these SNPs were previously associated with benzimidazole (BZ) resistance. However in these studies of ML selected parasites showing these genetic changes, some of the parasite strains had never been exposed to BZs [14].

One of the differences between β-tubulin of *H. contortus* and mammalian tubulin is that the former has a F at the position 200 whereas the latter has a Y at this position. Recently, it has been established that IVM binds to α- and β-tubulin at micromolar affinities and stabilizes the microtubules (Ashraf et al., unpublished). It can be hypothesized that due to this interaction SNPs are being selected which results in reduced IVM binding and may ultimately lead to a BZ resistant phenotype. It was therefore of interest to investigate whether these SNPs resulted in altered IVM binding. It was also of interest to investigate the differences, if any, in the binding of IVM and MOX to both mammalian and *H. contortus* tubulin.

4.2. Materials and Methods

2.1. RNA extraction. Fifteen to twenty adults from the PF strain of *H. contortus* were collected and RNA was extracted and converted into cDNA using Trizol reagent (Invitrogen, Toronto, ON) and QuantiTect Reverse Transcription Kit (Qiagen, Toronto, ON) kits.

4.2.2. Cloning of α-tubulin. The full length sequence of α-tubulin (accession number L-02108) was cloned into the 6xHis-tagged vector pETM-10 (EMBL, Heidelberg,

Germany). The vector was linearized with 5´-*Nco*I and 3´-*BamH*I restriction enzymes (NEB, Toronto, ON). *BsmB*I (sense primer) and 3´-*BamH*I (anti-sense primer) restriction sites were used to clone the gene. 5´-TTTACGTCTCCCATGAGGGAGGTGATTTCCATTCACATC -3´ sense primer and 5´- GGATCCGCGTCAATACTCATCGCCTTCCTCAC -3´ anti-sense primers were used for cloning. The cloned product was transformed into *E. coli* (XL1-Blue) (Stratagene, Mississauga, ON) and sequenced at Genome Quebec Innovation Centre, Montreal, Quebec.

4.2.3. Cloning of β-tubulin isotype 1. The full length sequence of β-tubulin isotype 1 gene (accession number M-76493) was cloned into the 6xHis-tagged vector pETM-10. The vector was linearized by the 5´-*Nco*I and 3´-*BamH*I restriction enzymes. 5´-*BspH*I (forward primer) and 3´-*BamH*I (reverse primer) (Invitrogen, Toronto, ON) restriction sites were used to clone the gene. 5´-GAAATCATGAGGGAAATCGTTCATGTGCAAG-3´ sense primer and 5´-TGATGGATCCTTACTCCTCGGGATATGCCTC-3´ anti-sense primer were used for cloning. The cloned product was transformed into *E. coli* (XL1-Blue) and sequenced at the Genome Quebec Innovation Centre.

4.2.4. Mutagenesis of β-tubulin isotype 1. Site-directed-mutagenesis was performed to create point mutations TTC200TAC and TTC167TAC on β-tubulin isotype 1 gene. These SNPs replaced F with Y. For mutagenesis at amino acid position 200 the following primers were used: sense primer: 5'-GTAGAGAACACCGATGAAACATACTGTATTGACAACGAAG-3' antisense primer: 5'-CTTCGTTGTCAATACAGTATGTTTCATCGGTGTTCTCTAC-3'. For amino acid

167 the following primers were used: forward primer: 5'-ATAGAATTATGGCTTCGTACTCCGTTGTTCCATCACC-3' and reverse primer: 5'-GGTGATGGAACAACGGAGTACGAAGCCATAATTCTAT-3'. PCR reaction mix and thermal cycling conditions were according to QuickChange®II Site-Directed Mutagenesis Kit (Stratagene). The mutants were transformed into *E. coli* (XL1-Blue) supercompetent cells (Stratagene) and confirmed by sequencing at the Genome Quebec Innovation Centre.

4.2.5. Protein expression. α- and β-tubulin isotype 1 (WT and mutants) were transformed into Rosetta 2 (Novagen, Madison, USA) cells for protein expression. All the proteins were grown in LB broth containing 50 μg/ml kanamycin and 1% maltose (Sigma Aldrich, Toronto, ON). Induction was with 1 mM final concentration isopropyl-β-D-thiogalactoside (IPTG) (Invitrogen, Toronto, ON) and incubation continued for 3 h at 37°C at 250 rpm. Cell pellets were lysed by sonication for 42 cycles (15 s pulses with 15 s resting periods) on ice in binding/lysis buffer (50 mM NaH_2PO_4, 500 mM NaCl, 10 mM imidazole, pH 8.0) containing one Complete EDTA-free protease-inhibitor cocktail tablet (Roche Applied Science, Laval, QC). All the procedures were according to QIAexpressionist™ (Qiagen, Toronto, ON).

4.2.6. Protein purification. The lysates were centrifuged at 20000 rpm and the soluble fraction was loaded onto disposable columns (Biorad, Mississauga, ON) containing 1 ml packed beads of Ni-NTA agarose (Qiagen, Laval, QC). The proteins were washed with wash buffer (50 mM NaH_2PO_4, 500 mM NaCl, 20 mM imidazole, pH 8.0) and eluted with elution buffer (50 mM NaH_2PO_4, 500 mM NaCl, 250 mM imidazole, pH 8.0). All the proteins were analyzed by 10 % sodium dodecyl sulfate polyacrylamide gel by

electrophoresis (SDS-PAGE) and Western blot using specific monoclonal antibodies against α- and β-tubulin isotype 1 (AA4.3, E7, 1:50 Developmental Studies Hybridoma Bank, University of Iowa, USA). The proteins were concentrated using Amicon ultracentrifugal filter 30 MWCO (Millipore, Bedford, MA) and the buffer was exchanged for PBS (10 mM $Na_2HPO_4.H_20$, 2 mm KH2PO4, 137 mM NaCl, 2.7 mm KCl, pH 7.5). Protein concentration was determined by the Bradford assay (Biorad, Mississauga, ON). Details of protein expression and purification can found elsewhere [15].

4.2.7. Polymerization of parasite tubulin. 20 μM purified α-tubulin were mixed with 20 μM purified β-tubulin isotype 1 (WT and mutants) in polymerization buffer (0.1 M PIPES pH 6.8, 10% glycerol, 1 mM EGTA, 1 mM $MgCl_2$, 1 mM GTP) (Sigma Aldrich, Toronto, ON) to form microtubules. The extent of polymerization was monitored by taking optical densities using a UV spectrophotometer (Beckman Coulter DU-640 UV/VIS Scanning Spectrophotometer) at 340 nm at 37°C every 20 seconds for 1 hour [16]. To determine the effect on polymerization, similar procedures were performed in the presence of IVM (20 μM) (Sigma Aldrich, Toronto, ON). The ratio of IVM and DMSO was normalized against DMSO and was expressed as increase relative to DMSO (%). To compare the polymerization of MOX with IVM, 30 μM of each compound was tested. Two hundred μM colchicine was used as a negative control and 30 μM taxol was used as a positive control. Two percent dimethyl sulphoxide (DMSO) was used in all experiments as a solvent control (Sigma Aldrich).

4.2.8. Polymerization of mammalian tubulin. For polymerization of mammalian tubulin the HTS-tubulin polymerization kit (BK004, Cytoskeleton, USA) was used.

Polymerization was observed at 340 nm turbidometrically (Synergy HT Multimode plate reader, Biotek, USA). The reaction started when the temperature was increased from 0^{o}C to 37^{o}C. Thirty μM IVM, 30 μM MOX were used as the test compounds. Ten μM colchicine was used as negative control, 10 μM taxol was used as a positive control and 2% DMSO was used as a solvent control (Sigma Aldrich, Toronto, ON).

4.2.9. Equilibrium dialysis. β-tubulin isotype 1 (WT and mutants) in PBS (10 mM $Na_2HPO_4.H_20$, 2 mm KH_2PO_4, 137 mM NaCl, 2.7 mm KCl,, pH 7.5) were used in the Equilibrium DispoDIALYZER, 10 kDa (Harvard Apparatus, Massachusetts, USA) to determine if there is any difference in the binding between the WT and the mutants. PBS with 20 μM BODIPY FL ivermectin, 20 μM BODIPY FL, 20 μM BODIPY FL ivermectin plus 50 μM levamisole and 20 μM BODIPY FL ivermectin with 10 μM DNase I (Roche Applied Science, Laval, QC) were used as controls whereas tubulin containing 20 μM BODIPY FL ivermectin and 20 μM BODIPY FL ivermectin (Molecular Probes, Toronto, ON) plus 50 μM IVM were used as test compounds. The samples were incubated for 24 h at 4 °C while gentle shaking after which the fluorescence was measured from both the chambers. Readings were taken in a Varian Cary Eclipse fluorescence spectrophotometer (Agilent Technologies, ON, Mississauga) at room temperature. The excitation was set at 503 nm and scanned from 510 nm to 560 nm. The peak emission for BODIPY FL ivermectin was at 512 nm. Net fluorescence was calculated by subtracting the fluorescence readings from both dialysis chambers.

4.2.10. Molecular modeling. α- and β-tubulin sequences from *H. contortus* (accession numbers P50719 and AAA29170) [17, 18] and *Bos taurus* (PDB 1JFF Mol

C and D) [19] were aligned with the MAFFT plug-in of Geneious 7.12 (Biomatters Ltd) [20] and the alignment adjusted and trimmed manually. Homology models were prepared from using the hm_build.mcr macro of YASARA 14.7.17 [21]. Quality of the model was evaluated using the combined Z-score produced by the macro, a normalized distribution with a mean of 0 and standard deviation of 1, based on experimentally determined structures in the PDB database that includes 1D and 3D packing as well as an evaluation of dihedral geometry.

Structures of taxol (from PDB 1JFF), IVM (from PDB 3RIF) [22] and MOX (PubCem: CID_9571036) were cleaned and energy minimized using the em_runclean.mcr macro *in vacuo*. Docking was carried out using Vina [23] as implemented in YASARA 14.7.17 based on 100 docking runs in a cell extending twice the size of the ligand from the tubulin structure for global docking followed by local docking in a cell of 10 **Å** centred on the best global docking pose. Energy minimization of the locally docked poses was carried out using the em_runclean.mcr macro using the YASARA Forcefield to allow to some extent for the flexibility of tubulin known to occur on TAX binding [19].

4.3. Results

4.3.1 Expression of α- and β-tubulin wild type (WT) and mutant proteins and their polymerization in the presence and absence of IVM. The expression of recombinant *H. contortus* α-tubulin, β-tubulin isotype 1 (WT), β-tubulin isotype 1 (F200Y) and β-tubulin isotype 1 (F167Y) mutants were confirmed via SDS-PAGE

and Western blot using specific antibodies. After confirmation of the proteins, the degree of polymerization was compared between the WT and mutant proteins. No differences in the rates of polymerization were observed when the mutants (F200Y or F167Y) were compared with WT tubulin (Figure 1A). Twenty μM IVM increased the extent of polymerization and stabilized the polymers of both WT and mutant tubulin proteins (Figure 1B).

4.3.2. Equilibrium dialysis of β-tubulin (WT and mutants). Equilibrium dialysis with BODIPY FL ivermectin was performed to see if IVM bound to β-tubulin isotype 1 (WT, F200Y and F167Y mutants) in the presence of these SNPs. No differences between fluorescence intensities were observed between β-tubulin isotype 1 (WT), β-tubulin isotype 1 (F200Y) and β-tubulin isotype 1 (F167Y) (Figure 1C). The three controls, PBS plus 20 μM BODIPY FL ivermectin, β-tubulin (F200Y) or β-tubulin (F167Y) plus 20 μM BODIPY FL, and 10 μM DNase I plus 20 μM BODIPY FL ivermectin showed no significant differences between the samples retrieved from both the chambers, however the fourth control, with β-tubulin (F200Y) or β-tubulin (F167Y) plus 20 μM BODIPY FL ivermectin plus 50 μM levamisole gave significant differences between solutions from both chambers. The samples that contained β-tubulin (F200Y) or β-tubulin (F167Y) plus 20 μM BODIPY FL ivermectin showed significant differences between the solutions from both chambers. The increase in the fluorescence attributed to BODIPY FL ivermectin was significantly diminished by the addition of 50 μM non-fluorescent IVM as a competitor.

4.3.3. Comparison of polymerization of MOX and IVM in *H. contortus* and mammalian tubulin. Thirty μM of both IVM and MOX increased the degree of

polymerization of both *H. contortus* and mammalian tubulins. For *H. contortus* IVM increased polymerization more than MOX (Figure 3A), whereas for mammalian tubulin the polymerization was more with MOX as compared to IVM (Figure 4B). Colchicine inhibited whereas taxol increased the rate of polymerization.

4.3.4. Molecular modeling. The homology model of *H. contortus* tubulin, based on the 1JFF template (Hco-Tub$_{1JFF}$) was produced with a Z-score of -1.52. The *H. contortus* α-tubulin contained an insertion of 26 amino acids relative to the 1JFF template and this led to a disordered loop approximately 40 **Å** distant from the β-subunit that was removed before *in silico* docking. Local docking of the ligand back into the 1JFF structure produced a best ligand pose with an RSMD of 1.86, 0.53 and 1.62 compared to the structure file, validating the docking procedure. We have shown previously that IVM docks preferentially into the taxane binding site of Hco-Tub$_{1JFF}$ (Chapter 3) and here we found that MOX also produced a best pose within this site. The relative binding energies produced for local docking of IVM, MOX and TAX were 8.7, 9.0 and 9.9 kcal/mol respectively. The effect of introducing either the F167Y or F200Y substitutions into the *H. contortus* β-tubulin sequence was evaluated either by producing new homology models *de novo* or by making the individual substitutions to the original Hco-Tub$_{1JFF}$ model followed by local minimization in a water shell. In either case, all three ligands continued to produce best binding poses within the taxane pocket. Global docking also found that both IVM and MOX produced best poses within the taxane binding pocket of mammalian tubulin, with energies of 9.0 and 9.4 compared to 9.9 kcal/mol for TAX based on the 1JFF structure. This would suggest that the affinity of IVM and MOX is higher for mammalian than for the parasite

tubulin. Optimal binding poses for IVM and MOX for the Hco-Tub$_{1JFF}$ and 1JFF structures are shown in Figure 4.

4.4. Discussion

The objective of the current study was to see if the SNPs (F200Y and F167Y) in β-tubulin isotype 1 had any effect on IVM binding and to compare the effect of IVM and MOX on polymerization. For this, recombinant *H. contortus* α- and β-tubulin (WT and mutants) were expressed in an *E. coli* expression system. Different polymerization studies were performed followed by equilibrium dialysis and molecular modeling. The polymerization studies showed that there were no differences when the WT tubulins were compared with both the mutants. It has also been observed that IVM increased the extent of polymerization in the WT and the mutants.

The equilibrium dialysis experiments showed no differences between the binding of IVM with the wild and mutant tubulins. These findings suggest that the SNPs (F200Y and F167Y) have nothing to do directly with IVM binding. The polymerization experiments demonstrated varying results when IVM was compared with MOX. IVM increased the polymerization more than MOX in the case of *H. contortus* tubulin whereas for mammalian tubulin the polymerization was more for MOX as compared to IVM. However, these differences in polymerization kinetics need further investigations. The molecular docking studies showed that both IVM and MOX docked into the taxol binding pocket of parasitic and mammalian tubulin. IVM

docked even in the presence of the SNPs (F200Y and F167Y) indicating that they did not have any effect on IVM binding.

As tubulins are also structural and cargo proteins these SNPs could affect the functioning of receptors, such as ligand-gated ion channels, at the synaptic membranes which could alter neurotransmission and sensitivity towards IVM. Interestingly, the IVM resistant *H. contortus* have shortened amphids having disorganized tubulins [8], it would be of interest to see if these SNPs will cause structural and functional changes to the amphids. It has been hypothesized that the amphids played a significant role in determining IVM sensitivity [24] and recently it has been shown that genetic changes in the *dyf-7* gene found to be associated with IVM resistance in *H. contortus* from around the world, also alters dye uptake and amphid morphology in this nematode [7]. It can be hypothesized that structural changes in the amphids may be linked to SNPs in β-tubulin selected by repeated exposure to IVM. However, additional experiments are required to determine whether SNPs in β-tubulin and morphological changes in amphids may contribute to IVM resistance.

4.5. Acknowledgements

This project received financial support from NSERC and the FQRNT Centre for Host-Parasite Interactions Quebec, Canada. We also wish to thank EMBL for the generous gift of pETM-10 expression vector and Kathy Keller for the parasites.

References

[1] Nikolaou S, Gasser RB. Prospects for exploring molecular developmental processes in Haemonchus contortus. International journal for parasitology. 2006;36:859-68.
[2] Kaplan RM. Drug resistance in nematodes of veterinary importance: a status report. Trends in parasitology. 2004;20:477-81.
[3] Prichard R. Genetic variability following selection of Haemonchus contortus with anthelmintics. Trends in parasitology. 2001;17:445-53.
[4] Campbell WC, Fisher MH, Stapley EO, Albers-Schonberg G, Jacob TA. Ivermectin: a potent new antiparasitic agent. Science (New York, NY). 1983;221:823-8.
[5] Cully DF, Vassilatis DK, Liu KK, Paress PS, Van der Ploeg LH, Schaeffer JM, et al. Cloning of an avermectin-sensitive glutamate-gated chloride channel from Caenorhabditis elegans. Nature. 1994;371:707-11.
[6] Prichard R, Ménez C, Lespine A. Moxidectin and the avermectins: Consanguinity but not identity. International Journal for Parasitology: Drugs and Drug Resistance. 2012;2:134-53.
[7] Urdaneta-Marquez L, Bae SH, Janukavicius P, Beech R, Dent J, Prichard R. A dyf-7 haplotype causes sensory neuron defects and is associated with macrocyclic lactone resistance worldwide in the nematode parasite Haemonchus contortus. International journal for parasitology. 2014.
[8] Freeman AS, Nghiem C, Li J, Ashton FT, Guerrero J, Shoop WL, et al. Amphidial structure of ivermectin-resistant and susceptible laboratory and field strains of Haemonchus contortus. Veterinary parasitology. 2003;110:217-26.
[9] Eng JK, Prichard RK. A comparison of genetic polymorphism in populations of Onchocerca volvulus from untreated- and ivermectin-treated patients. Molecular and biochemical parasitology. 2005;142:193-202.
[10] Eng JK, Blackhall WJ, Osei-Atweneboana MY, Bourguinat C, Galazzo D, Beech RN, et al. Ivermectin selection on beta-tubulin: evidence in Onchocerca volvulus and Haemonchus contortus. Molecular and biochemical parasitology. 2006;150:229-35.
[11] Bourguinat C, Pion SD, Kamgno J, Gardon J, Duke BO, Boussinesq M, et al. Genetic selection of low fertile Onchocerca volvulus by ivermectin treatment. PLoS neglected tropical diseases. 2007;1:e72.
[12] Osei-Atweneboana MY, Boakye DA, Awadzi K, Gyapong JO, Prichard RK. Genotypic analysis of β-tubulin in Onchocerca volvulus from communities and individuals showing poor parasitological response to ivermectin treatment. International Journal for Parasitology: Drugs and Drug Resistance. 2012;2:20-8.
[13] Nana-Djeunga H, Bourguinat C, Pion SD, Kamgno J, Gardon J, Njiokou F, et al. Single nucleotide polymorphisms in beta-tubulin selected in Onchocerca volvulus following repeated ivermectin treatment: possible indication of resistance selection. Molecular and biochemical parasitology. 2012;185:10-8.
[14] de Lourdes Mottier M, Prichard RK. Genetic analysis of a relationship between macrocyclic lactone and benzimidazole anthelmintic selection on Haemonchus contortus. Pharmacogenetics and genomics. 2008;18:129-40.
[15] Ashraf S, Prichard RK. Haemonchus contortus microtubules are cold resistant. Molecular and biochemical parasitology. 2014;193:20-2.

[16] Shelanski ML, Gaskin F, Cantor CR. Microtubule assembly in the absence of added nucleotides. Proceedings of the National Academy of Sciences of the United States of America. 1973;70:765-8.
[17] Geary TG, Nulf SC, Favreau MA, Tang L, Prichard RK, Hatzenbuhler NT, et al. Three beta-tubulin cDNAs from the parasitic nematode Haemonchus contortus. Molecular and biochemical parasitology. 1992;50:295-306.
[18] Klein RD, Nulf SC, Alexander-Bowman SJ, Mainone CB, Winterrowd CA, Geary TG. Cloning of a cDNA encoding alpha-tubulin from Haemonchus contortus. Molecular and biochemical parasitology. 1992;56:345-8.
[19] Lowe J, Li H, Downing KH, Nogales E. Refined structure of alpha beta-tubulin at 3.5 A resolution. Journal of molecular biology. 2001;313:1045-57.
[20] Katoh K, Misawa K, Kuma K, Miyata T. MAFFT: a novel method for rapid multiple sequence alignment based on fast Fourier transform. Nucleic acids research. 2002;30:3059-66.
[21] Krieger E, Koraimann G, Vriend G. Increasing the precision of comparative models with YASARA NOVA--a self-parameterizing force field. Proteins. 2002;47:393-402.
[22] Hibbs RE, Gouaux E. Principles of activation and permeation in an anion-selective Cys-loop receptor. Nature. 2011;474:54-60.
[23] Trott O, Olson AJ. AutoDock Vina: improving the speed and accuracy of docking with a new scoring function, efficient optimization, and multithreading. Journal of computational chemistry. 2010;31:455-61.
[24] Starich TA, Herman RK, Kari CK, Yeh WH, Schackwitz WS, Schuyler MW, et al. Mutations affecting the chemosensory neurons of Caenorhabditis elegans. Genetics. 1995;139:171-88.

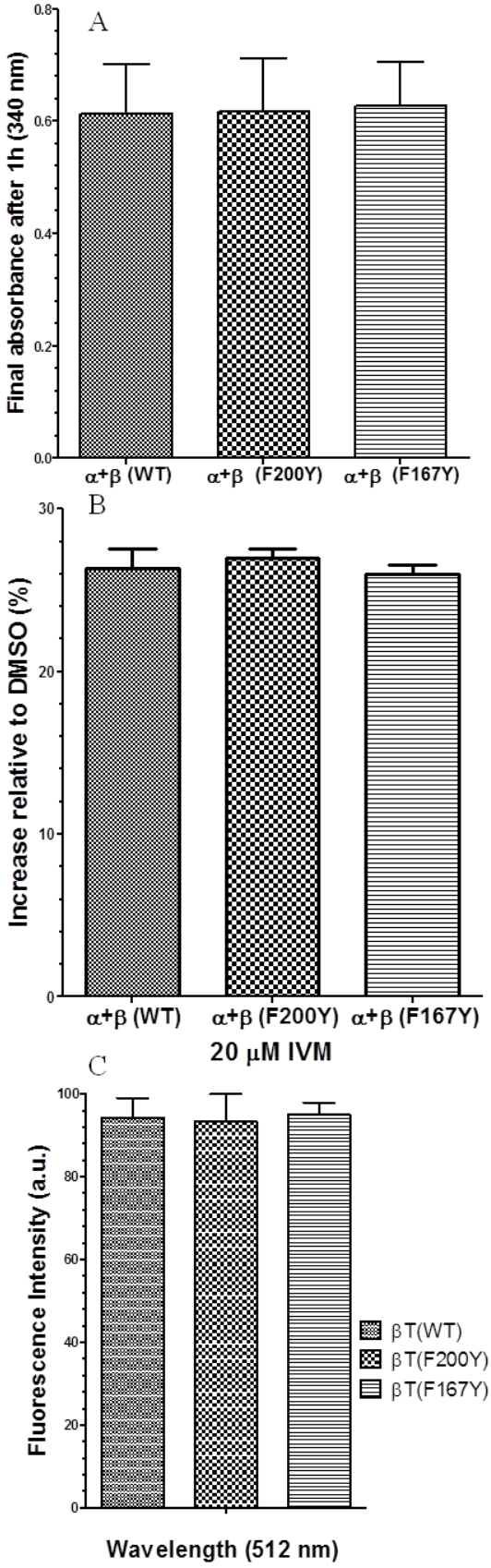
A
Final absorbance after 1h (340 nm)
0.0
0.2
0.4
0.6
0.8
α+β (WT)
α+β (F200Y)
α+β (F167Y)
B
Increase relative to DMSO (%)
0
10
20
30
α+β (WT)
α+β (F200Y)
α+β (F167Y)
20 μM IVM
C
Fluorescence Intensity (a.u.)
0
20
40
60
80
100
βT(WT)
βT(F200Y)
βT(F167Y)
Wavelength (512 nm)

Figure 4.1

Figure 4.1. Tubulin polymerization and equilibrium dialysis of WT and mutant tubulins. (A) Tubulin polymerization assay performed with 20 μM purified recombinant *H. contortus* α-tubulin, β-tubulin isotype 1 (WT), β-tubulin isotype 1 (F200Y) and β-tubulin isotype 1 (F167Y). No differences were observed between the extent of polymerization of the WT and mutant tubulins. (B) Effect of IVM on the degree of polymerization performed with 20 μM purified recombinant *H. contortus* α-tubulin, β-tubulin isotype 1 (WT), β-tubulin isotype 1 (F200Y) and β-tubulin isotype 1 (F167Y) expressed as increase relative to DMSO (%). IVM increased the degree of polymerization of the WT and mutant tubulins. There were no differences when WT were compared with the mutants (N=3). (C) Equilibrium dialysis of 20 μM BODIPY FL ivermectin with β-tubulin isotype 1 (WT), β-tubulin isotype 1 (F200Y) and β-tubulin isotype 1 (F167Y). No differences were observed when the fluorescence intensities were compared between the WT and mutants. (N=3).

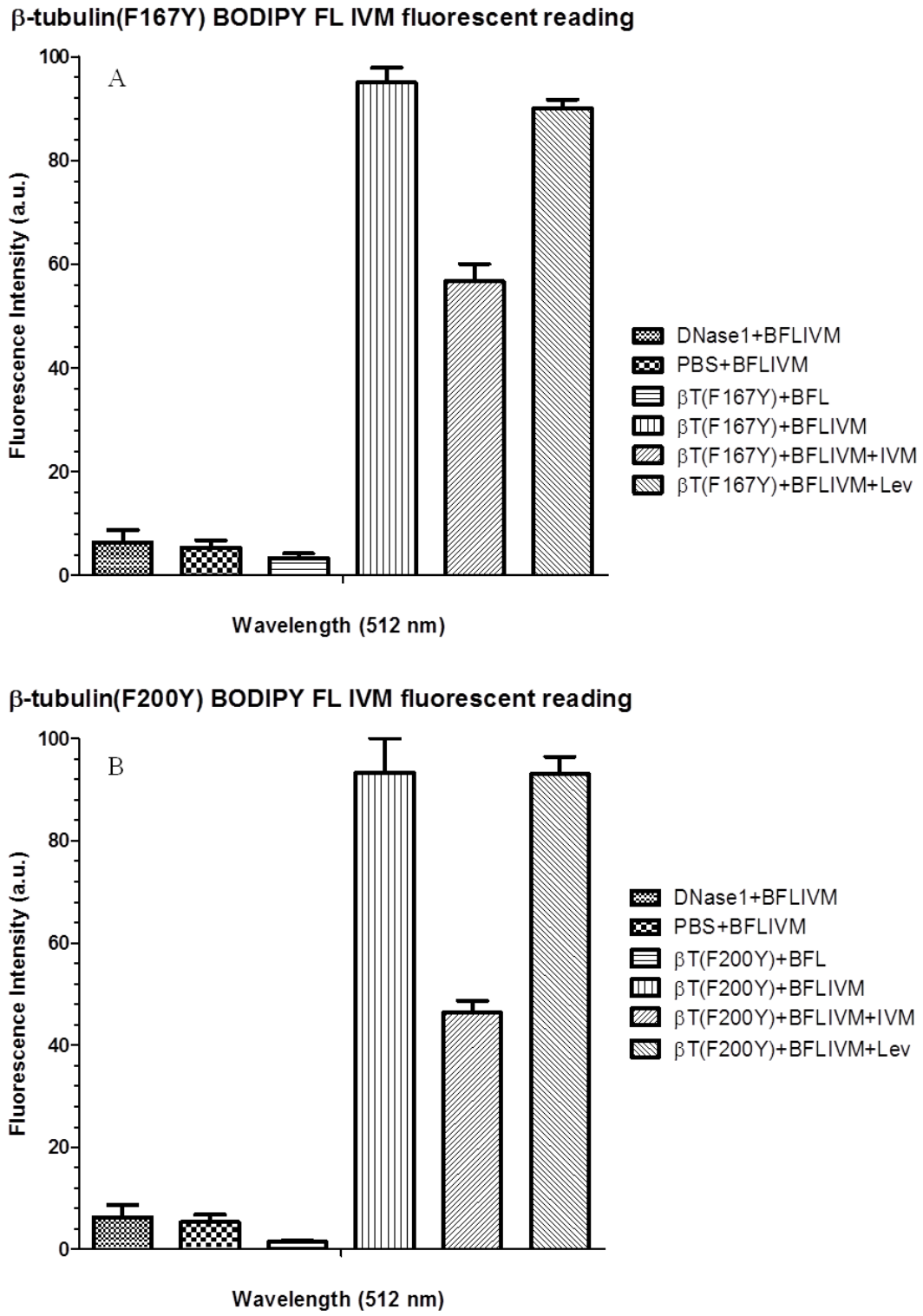
β-tubulin(F167Y) BODIPY FL IVM fluorescent reading
A
Fluorescence Intensity (a.u.)
100
80
60
40
20
0
Wavelength (512 nm)
DNase1+BFLIVM
PBS+BFLIVM
βT(F167Y)+BFL
βT(F167Y)+BFLIVM
βT(F167Y)+BFLIVM+IVM
βT(F167Y)+BFLIVM+Lev
β-tubulin(F200Y) BODIPY FL IVM fluorescent reading
B
Fluorescence Intensity (a.u.)
100
80
60
40
20
0
Wavelength (512 nm)
DNase1+BFLIVM
PBS+BFLIVM
βT(F200Y)+BFL
βT(F200Y)+BFLIVM
βT(F200Y)+BFLIVM+IVM
βT(F200Y)+BFLIVM+Lev

Figure 4.2

Figure 4.2. Equilibrium dialysis of BODIPY FL ivermectin with β-tubulin isotype 1 (F200Y) (A) and β-tubulin isotype 1 (F167Y) (B). Four controls were used, PBS dialyzed against 20 μM BODIPY FL ivermectin, 20 μM BODIPY FL ivermectin dialyzed against DNase I, BODIPY FL dialyzed against β-tubulin isotype 1 (F200Y) or β-tubulin isotype 1 (F167Y). Twenty μM BODIPY FL ivermectin dialyzed against β-tubulin isotype 1 (F200Y) and β-tubulin isotype 1 (F167Y) in competition with 50 μM levamisole. Twenty μM BODIPY FL ivermectin was also dialyzed against β-tubulin isotype 1 (F200Y) and β-tubulin isotype 1 (F167Y) in competition with 50 μM IVM (A, B). Non-fluorescent IVM significantly reduced the fluorescence as compared to BFLIVM for α- and β-tubulin (one-way ANOVA and Tukey's multiple comparison tests) (*P<0.05, **P= 0.01-0.05, ***P< 0.01, n=3).

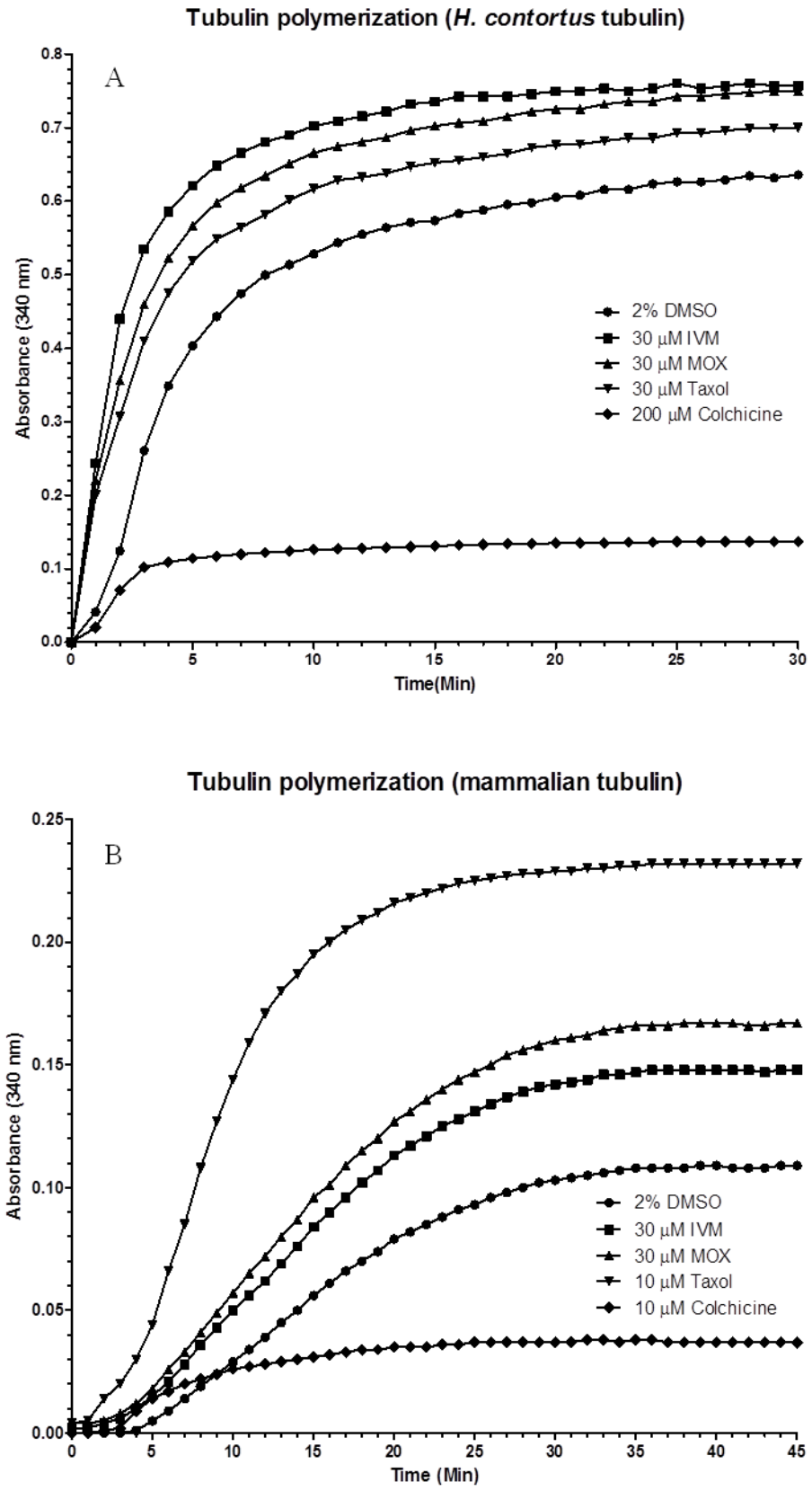
Tubulin polymerization (*H. contortus* tubulin)
A
Absorbance (340 nm)
Time(Min)
2% DMSO
30 µM IVM
30 µM MOX
30 µM Taxol
200 µM Colchicine
Tubulin polymerization (mammalian tubulin)
B
Absorbance (340 nm)
Time (Min)
2% DMSO
30 µM IVM
30 µM MOX
10 µM Taxol
10 µM Colchicine

Figure 4.3

Figure 4.3. Tubulin polymerization of *H. contortus* and mammalian tubulin, comparison between IVM and MOX. Thirty µM IVM increased the degree of polymerization more than 30 µM MOX for *H. contortus* tubulin (A) whereas 30 µM MOX increased the degree of polymerization more than 30 µM IVM for mammalian tubulin (B). Ten µM and 200 µM colchicine acted as a negative control and 10 µM and 30 µM taxol acted as a positive control for *H. contortus* and mammalian tubulin respectively. The graphs are representative of three individual experiments.

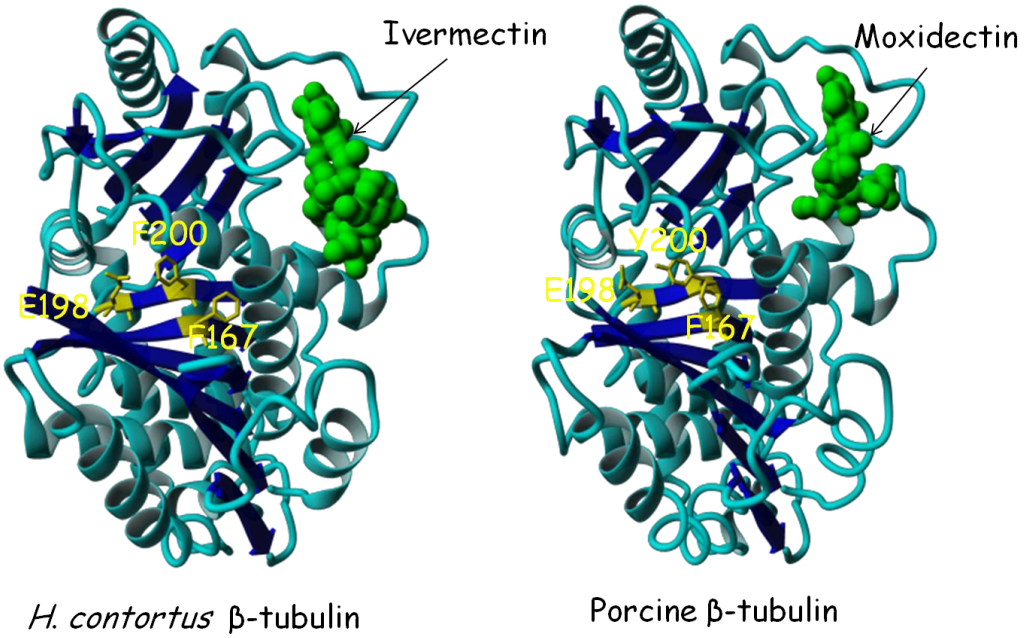

Figure 4.4

Figure 4.4. Optimal binding poses for a) IVM bound to Hco-Tub$_{1JFF}$ and b) MOX bound to 1JFF. Only the beta-tubulin subunit of the dimer is shown with IVM and MOX. The lactone ring of both molecules adopts the same orientation and in the case of IVM, the carbohydrate moieties face the exterior solvent.

Connecting statement IV

In chapter II we studied the structure of *H. contortus* microtubules. In chapter III and IV we established a functional relationship between ivermectin and wild type and mutant tubulin/microtubules. As the amphidial neurons in nematodes are highly abundant in microtubules, in chapter V we investigated whether the amphids are shortened, affecting lipophilic dye filling in ivermectin resistant and susceptible strains of *C. elegans*. We also performed experiments to analyze the possible role of the amphidial pores as a route of entry of ivermectin into nematodes.

Chapter V

Manuscript IV

Amphids: A possible route of entry for Ivermectin in nematodes

Shoaib Ashraf and Roger K. Prichard

In preparation for Veterinary Parasitology

Abstract

Amphids are sensory neurons that nematodes use to sense their environment. The IVR-10 strain is an ivermectin (IVM) resistant strain of *Caenorhabditis elegans* generated in the lab by repeated exposure to IVM. We found that the IVR-10 strain is dye filling defective which may be due to shortened amphids. The amphidial pore of the N2 Bristol strain fluoresced with an ivermectin antibody suggesting that ivermectin may enter the worms via the amphidial pore. The findings reiterate the importance of amphidial pore as a structure that is exposed to the chemical environment and may be a portal for drug entry.

Keywords: Amphids, amphidial pore, ivermectin, dye filling defective

5.1.Introduction

Amphids are chemosensary organs present in nematodes (Fujii et al., 2004). They are present in pairs on each side of the head. The socket cells form an amphidial pore on the anteriolateral surface. As a result there are two amphidial pores which are in close contact with the environment and are required for thermal and chemical cues (Ashton et al., 1999). Each neuron of the amphid usually has more than one receptor and the receptors for a given stimulus are usually present on more than one amphid (De Riso et al., 1994). Amphids help in avoiding toxic chemicals (Ashton et al., 1999). *Caenorhabditis elegans* (*C. elegans*) is a free living nematode that has been intensively studied. Its whole genome has been sequenced and annotated. It has 302 neurons and all of its neuronal connections have been identified (Kaletta and Hengartner, 2006). Since most anthelmintic drugs act on the nervous system it is an excellent model to study drug resistance mechanisms (Dent et al., 2000).

Lipophilic dyes such as 1,1'-Dioctadecyl-3,3,3',3'-Tetramethylindocarbocyanine Perchlorate (Dil), 3,3'-Dioctadecyloxacarbocyanine Perchlorate (DiO) or fluorescein isothiocyanate (FITC) (Molecular Probes, USA), etc., are normally taken up by the amphids. It is a very useful tool to visualize the morphology of the amphidial sensory neurons. More than 13 dye-filling (Dyf) defective mutants have been identified in *C. elegans*. They are named dyf because of their inability to take up these lipophilic dyes. As a result the dyf mutants have abnormal disorganized amphids. All the dyf mutants of *C. elegans* larvae (Starich et al., 1995) were resistant to ivermectin. They postulated that the amphids played an important role in determining ivermectin sensitivity, furthermore they also found that these *C. elegans* with defective amphids were able to grow in the

presence of 5 ng/ml of IVM. It has been shown that the *C. elegans* having dyf-7 mutations have defective amphids which results in a dyf phenotype (Urdaneta-Marquez et al., 2014).

5.2.Materials and Methods

5.2.1.Strains and culture conditions

The wild-type Bristol N2 and IVR-10 strains of *C. elegans* were a gift from Dr Catherine James from the University of Technology, Sydney, Australia (James and Davey, 2009). The N2 strain was grown on nematode growth media (NGM) with OP50 *Eschericia coli* (Brenner, 1974) and IVR-10 on NGM with OP50 supplemented with 10 ng/ml IVM. *C. elegans* were maintained while transferring old worms to a new NGM plate containing OP50 with or without IVM. The IVR-10 was generated by growing the N2 strain on increasing concentrations of IVM. Every week the *C. elegans* worms were transferred to new plates containing higher concentrations of IVM starting from 1 ng/ml until they were resistant to 10 ng/ml of IVM.

5.2.2.Dye-filling experiments

For dye filling the N2 and IVR-10 strains were used. Dil was used for the experiments. Briefly N2 and IVR-10 plates were rinsed with M9 buffer to get the *C. elegans* from the culture plates. The worms were collected in 1.5 ml eppendorf tubes and spun down at 2000 rpm for 5 min. The worms were washed two times with M9 buffer. Following this Dil was added at a concentration of 5 µg/ml in M9 (from 2 mg/ml stock in DMF (Dimethylformamide)). The incubation continued for 2 h at 20^0C with shaking at 100 rpm. After this the worms were spun down and washed once with M9 buffer. Then the worms were kept on ice for 30 min followed by mounting on glass slides.

5.2.3.Amphidial pore staining by ivermectin antibody

For the experiments done by the ivermectin antibody (Ivermectin-BTG antibody) the N2 and the IVR-10 strains were used. Briefly the N2 and the IVR-10 strains of *C. elegans* were cultured on NGM plates with OP50 containing 1 ng/ml and 5 ng/ml IVM for N2 and IVR-10 strains respectively for 3 h. M9 buffer was used to get the *C. elegans* wild type and mutant strains from the plates. The worms were washed three times with M9. Then the pellet was resuspended in 4% paraformaldehyde (PFA) and fixed for 5 h at 20^0C. The worms were then permeabilized overnight at 37^0C in permeabilization buffer (125 mM Tris-HCl, pH 6.9, 1% v/v Triton X-100, 5% v/v 2-β-mercaptoethanol) followed by three washes with PBS. Then the collagenase treatment (1 mM $CaCl_2$, 100 mM Tris-HCl pH 7.5, 1000 units of collagenase) was done followed by three washes with PBS. The worms were then incubated with the primary antibody i.e. the Sheep polyclonal ivermectin antibody (Abbiotec Cat No 252378) 1:150 (0.5% Triton X-100, 0.1% BSA, 0.05% sodium azide in PBS) overnight at 4^0C followed by one wash with PBS and one with T-PBS (0.1% Triton X-100). Then the worms were incubated in the secondary antibody (Alexa Fluor 594 donkey anti-sheep IgG) at 4^0C for 8 h. Then the worms were washed 5 times with T-PBS and observed under the microscope on glass slides.

5.3. Results

5.3.1. Dye-filling experiments

Amphids were clearly visible in the N2 strain (Fig. 1A). The majority of worms of the IVR-10 strain were dye-filling defective (Fig. 1B), however a few of them also took up the lipophilic dye, staining either one or both pairs of amphids indicating an incomplete phenotype.

5.3.2. Amphidial pore staining by ivermectin antibody

Ivermectin appeared to be taken up through the oropharyngeal route and via the amphidial pore in the wild type N2 strain of *C. elegans* (Fig 2A). This was shown by the presence of fluorescence in the oesophagus and the amphidial pore indicating that IVM does enter through the amphidial pore, whereas no or less fluorescence was visible in the IVR-10 strain (Fig 2B).

5.4. Discussion

The objective of the current study was to investigate if the IVR-10 strain has a dyf phenotype and to investigate the possibility of entry of IVM via the amphidial pore. It has been proposed that drugs like IVM target the glutamate-gated chloride channels (Glu-Cl) and cause flaccid paralysis of the nematode (Cully et al., 1994). Our current findings suggest that the IVR-10 strain is dye-filling defective and that this phenotype may be due to shortening of the amphids. The staining of the amphidial pore by the IVM antibody suggests that IVM may also enter through the amphidial pore. (Smith and Campbell, 1996) also suggested an alternative route of entry of IVM, other than the oral/pharyngeal route. They suppressed pharyngeal pumping of *C. elegans* with an alcohol and when the worms were placed in 50 µg/ml IVM they remained paralyzed. However, worms placed in water regained motility.

Amphids contain sensory neurons that are responsible for thermal and chemical signaling in *C. elegans* (Fujii et al., 2004), *Onchocerca volvulus* (Strote et al., 1996) and *H. contortus* (Ashton et al., 1999). The dyf-7 gene is involved in anchoring the tips of neuronal dendrites (Heiman and Shaham, 2009). Recently, Urdaneta-Marquez et al., (2014) demonstrated that the IVR-10 stain has a mutation in the *dyf-7* gene and that mutation results in a null protein. Furthermore, they were also able to reverse IVM

resistance by replacing the IVM resistant mutant *dyf-7* gene with the wild type. As amphids are required to 'taste' the environment, any alteration in the amphids may render the worm less permeable to IVM and result in a drug resistant phenotype.

5.5. Acknowledgements

This project received financial support from NSERC and the FQRNT Centre for Host-Parasite Interactions Quebec, Canada.

References

Ashton, F.T., Li, J., Schad, G.A., 1999. Chemo- and thermosensory neurons: structure and function in animal parasitic nematodes. Veterinary parasitology 84, 297-316.

Brenner, S., 1974. The genetics of Caenorhabditis elegans. Genetics 77, 71-94.

Cully, D.F., Vassilatis, D.K., Liu, K.K., Paress, P.S., Van der Ploeg, L.H., Schaeffer, J.M., Arena, J.P., 1994. Cloning of an avermectin-sensitive glutamate-gated chloride channel from Caenorhabditis elegans. Nature 371, 707-711.

De Riso, L., Ristoratore, F., Sebastiano, M., Bazzicalupo, P., 1994. Amphid defective mutant of Caenorhabditis elegans. Genetica 94, 195-202.

Dent, J.A., Smith, M.M., Vassilatis, D.K., Avery, L., 2000. The genetics of ivermectin resistance in Caenorhabditis elegans. Proceedings of the National Academy of Sciences of the United States of America 97, 2674-2679.

Fujii, M., Matsumoto, Y., Tanaka, N., Miki, K., Suzuki, T., Ishii, N., Ayusawa, D., 2004. Mutations in chemosensory cilia cause resistance to paraquat in nematode Caenorhabditis elegans. The Journal of biological chemistry 279, 20277-20282.

Heiman, M.G., Shaham, S., 2009. DEX-1 and DYF-7 establish sensory dendrite length by anchoring dendritic tips during cell migration. Cell 137, 344-355.

James, C.E., Davey, M.W., 2009. Increased expression of ABC transport proteins is associated with ivermectin resistance in the model nematode Caenorhabditis elegans. International journal for parasitology 39, 213-220.

Kaletta, T., Hengartner, M.O., 2006. Finding function in novel targets: C. elegans as a model organism. Nature reviews. Drug discovery 5, 387-398.

Smith, H., Campbell, W.C., 1996. Effect of ivermectin on Caenorhabditis elegans larvae previously exposed to alcoholic immobilization. The Journal of parasitology 82, 187-188.

Starich, T.A., Herman, R.K., Kari, C.K., Yeh, W.H., Schackwitz, W.S., Schuyler, M.W., Collet, J., Thomas, J.H., Riddle, D.L., 1995. Mutations affecting the chemosensory neurons of Caenorhabditis elegans. Genetics 139, 171-188.

Strote, G., Bonow, I., Attah, S., 1996. The ultrastructure of the anterior end of male Onchocerca volvulus: papillae, amphids, nerve ring and first indication of an excretory system in the adult filarial worm. Parasitology 113 (Pt 1), 71-85.

Urdaneta-Marquez, L., Bae, S.H., Janukavicius, P., Beech, R., Dent, J., Prichard, R., 2014. A dyf-7 haplotype causes sensory neuron defects and is associated with macrocyclic lactone resistance worldwide in the nematode parasite Haemonchus contortus. International journal for parasitology 44, 1063-1071.

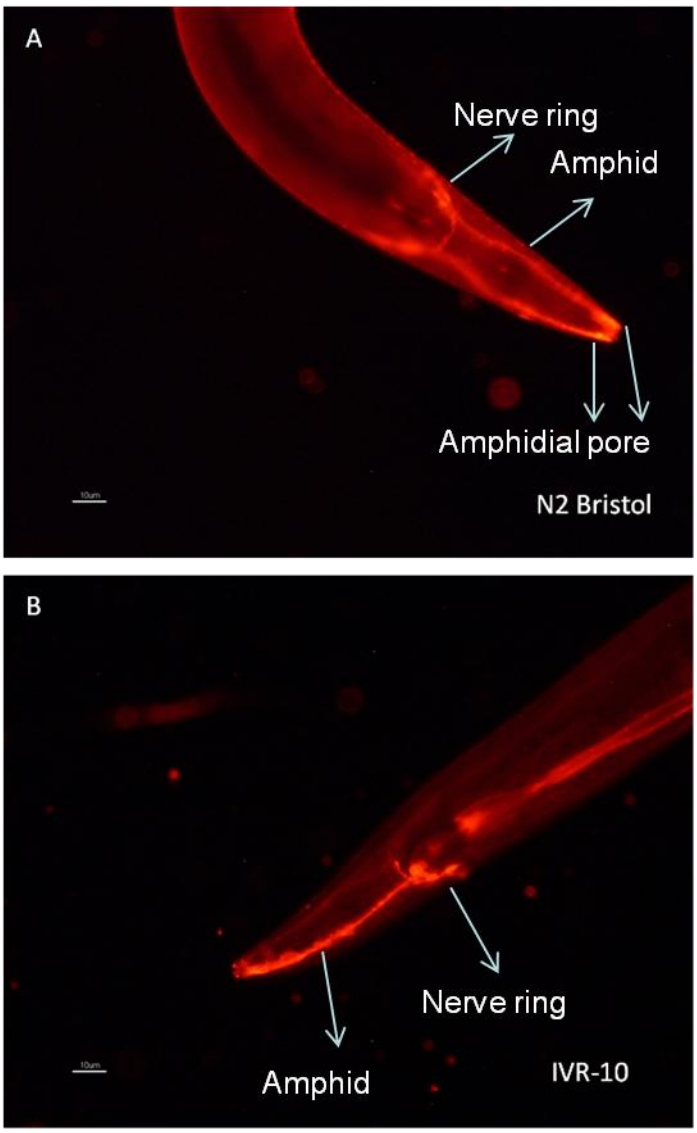

Figure 5.1

Figure 5.1. Dye filling experiments of N2 Bristol and IVR-10 strains of *C. elegans*. Both pairs of amphid of the N2 strain are clearly visible as they have taken up the lipophilic dye Dil (A). Only one amphid is visible in the IVR-10 strain showing a dyf phenotype(B).

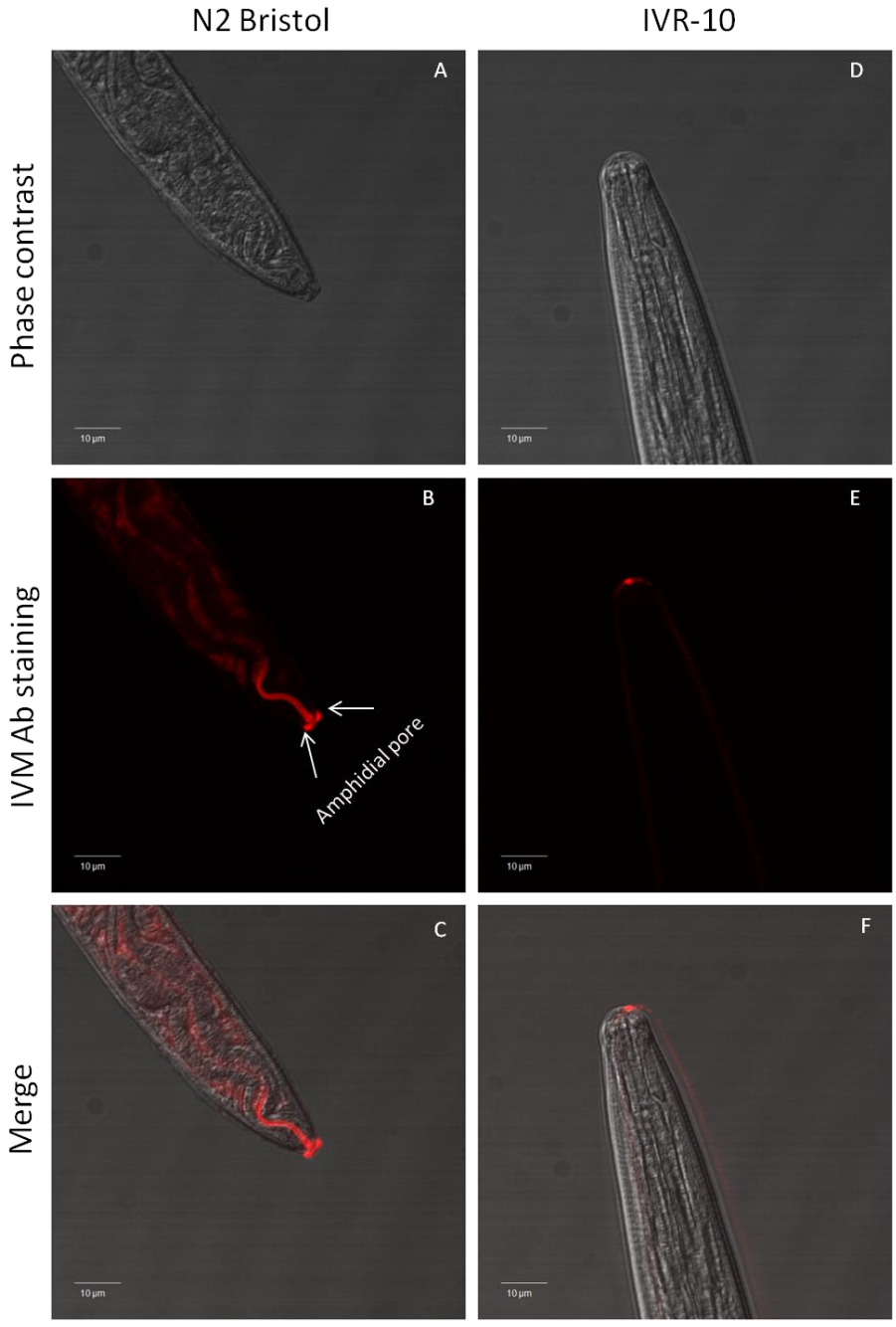

Figure 5.2

Figure 5.2. Amphidial pore staining of the N2 Bristol and the IVR-10 strains of *C. elegans* with an anti-ivermectin antibody. The amphidial pore is clearly visible in the N2 Bristol strain (A, B, C) indicating the uptake of ivermectin (IVM) via the amphidial pore. The

amphidial pore is not visible in the IVR-10 strain indicating that IVM did not enter in these worms through the amphidial pore (D, E, F).

Chapter VI

General Discussion

Ivermectin is a drug used all over the world to treat various ecto and endo parasites. Since its discovery only a few new anthelmintic classes have come to the market. Some of the few new drug classes include emodepside, derquentel and monepental. Ivermectin has the highest sales for an anthelmintic and generates billions of US dollars. The first report of ivermectin resistance came from South Africa, in *H. contortu*s, just 33-months after its launch (van Wyk and Malan, 1988). Ivermectin resistance has become a major problem. One can hypothesize that resistance to ivermectin in *H. contortu*s will follow similar patterns in other nematodes, including filarids and *C. elegans*. These resistance mechanisms may include: 1) decrease in the drug receptors, 2) increase in drug metabolism, 3) increase in drug efflux mechanisms by P-glycoproteins (Kerboeuf et al., 2003), 4) alteration in the drug binding site which results in reduce drug binding (Wolstenholme and Rogers, 2005), 5) decrease availability of the drug to the receptors e.g., by decreased uptake via the chemosensory pores (Freeman et al., 2003). It seems that resistance to ivermectin may involve multiple mechanisms (Prichard and Roulet, 2007). The basic phenotype of an organism depends upon its genotype. Ivermectin has been selecting on the ligand-gated-chloride channels (Njue et al., 2004) and p-glycoproteins (Xu et al., 1998). There has also been some evidence that illustrates the involvement of amphidial neurons in ivermectin resistance (Urdaneta-Marquez et al., 2014). Hence the situation of ivermectin resistance, unlike benzimidazole resistance, is quite complex. The situation for ivermectin selection has become even more complex; since 2005 a number of papers have reported that ivermectin is also selecting on β-tubulin. This recent paradigm led us to do some work on tubulin and ivermectin.

In this thesis, it was observed in chapter II, manuscript I, that microtubules from *H. contortus* are resistant to cold. In mammals, the tubulin subunits polymerize into microtubules when kept at 37^0C and they rapidly depolymerize/disassemble into tubulin subunits when kept at 0^0C. However, unlike mammals the microtubules of *H. contortus* did not depolymerize, i.e., they did not disassemble when kept for an hour at 0^0C. This is an interesting finding as this may allow the free-living stages of *H. contortus* to survive the cold climatic conditions in countries such as Canada. One difference between β-tubulin of *H. contortus* and mammalian tubulin is that the later has a tyrosine (Y) at the position 200 on this protein whereas the former has a phenylalanine (F). According to Detrich et al. (2000) this position is involved in lateral contacts between monomers. The "F" at this position stabilizes the dimers against depolymerization effects. *H. contortus* is characteristically a nematode of temperate areas and this may be the reason why this parasite was previously not considered of that much concern in northern parts of North America (Kaplan and Vidyashankar, 2012). Due to this characteristic of the parasite, little importance had been given to epidemiological surveys to this parasite in Canada. A recent study showed *H. contortus* infections in 100% of Ontario sheep flocks (Mederos et al., 2010., Falzon et al., 2013) and 70-80% of Quebec sheep flocks (Barrere et al., 2013) and has become the most common nematode parasite in sheep flocks in this country. The parasite along with having cold stable microtubules may survive over the winter by going into a dormant hypobiotic state in the host.

In Chapter III manuscript II, I explore the functional relationship between ivermectin and tubulin. For this, polymerization experiments were performed in the presence of ivermectin and it was observed that ivermectin increased the rate of polymerization hence

altering tubulin equilibrium. Other anticancer drugs such as taxol and epothilone also increase the rate of polymerization and thus kill the cells. Following polymerization trypsin proteolysis was performed and it was found that ivermectin delayed the limited trypsin proteolysis of both α- and β-tubulin. The rationale behind this approach was that when a drug and a proteolytic enzyme are added to a protein, the drug interacts with this protein, stabilizes and protects it from the enzymatic digestion of residues near the drug/protein binding site (Serrano et al., 1984). After this, surface plasmon resonance was done, which showed that indeed ivermectin was binding to both α- and β-tubulins.

To further validate our results and to map the binding site, I used equilibrium dialysis. For this a fluorescent labeled ivermectin (BODIPY FL ivermectin) was used. It was confirmed that BODIPY FL ivermectin bound to both α- and β-tubulin. DNase I showed no binding with BODIPY FL ivermectin, and levamisole (levamisole is another anthelmintic that targets nicotinic acetyl choline gated receptors (Fleming et al., 1997)) did not bind to either α- or β-tubulin. Non-fluorescent ivermectin competed with BODIPY FL ivermectin indicating that the binding was specific. Taxol also competed with BODIPY FL ivermectin indicating that their binding sites are overlapping. Interestingly this indicated that ivermectin is probably binding to the hydrophobic taxol binding pocket of both α- and β-tubulin. It is widely appreciated that taxol binds to β-tubulin, however evidence for binding to α-tubulin comes from experiments from Dasgupta et al. (1994) and Banerjee and Kasmala (1998). They concluded, by using taxol analogs in photo affinity labeling experiments and studying the in vitro assembly of α-tubulin isoforms, that taxol bound to the α-tubulin subunit. Interestingly, in our studies the K_D for recombinant *H. contortus* β-tubulin was ~25 μM whereas for α-tubulin it was

>120 μM. These results supported the fact that the primary site for taxol binding is on the β-tubulin protein in mammalian tubulin. These findings were also consistent with computer simulation/molecular docking which indicated that ivermectin was bound to the taxol binding pocket of tubulin. The model of *H. contortus* tubulin, based on the 3UT5 (Ranaivoson et al., 2012) crystal structure bound to colchicine produced no high affinity docking of either taxol or ivermectin to the taxol binding pocket. However, the 1JFF template (Lowe et al., 2001), in which the tubulin was bound to taxol, produced high affinity docking of both taxol and ivermectin to the taxol pocket. We were unable to reliably model the region of α-tubulin corresponding to the taxol binding pocket, due to an insertion of 26 amino acids in the parasite α-tubulin relative to the porcine template, and so have no basis for judging whether taxol or ivermectin could bind.

Once it was confirmed that ivermectin was binding to the parasitic recombinant tubulin we sought to investigate its possible effect on mammalian tubulins. For this I did polymerization assays with porcine tubulins and found that ivermectin was also increasing the degree of polymerization of mammalian tubulin. Following this the effect of ivermectin on the stability of microtubules was investigated in HeLa cells and we found that ivermectin was stabilizing the microtubules and preventing them from depolymerization due to cold temperature, an effect also shown by taxol. Finally it was concluded that the effects of ivermectin were reversible i.e. the cells resumed growth once ivermectin was removed from the media. It is important to note that these anti-mitotic effects of ivermectin were not in the nanomolar range. The plasma concentration of ivermectin was 52 ng/ml (C_{max}) when given at a dose of 150 μg/Kg (Baraka et al., 1996). This concentration is much lower than the concentrations showing an effect in our

experiments. However the LD_{50} of ivermectin is more than 20 mg/Kg (Dadarkar et al., 2007) which if used may give plasma concentrations in the micromolar range. Furthermore ivermectin is a very lipophilic drug (Prichard et al., 2012) and the neurons, which are fatty tissues, have a rich abundance of microtubules. Therefore, it is reasonable to think that the concentrations of ivermectin in neurons may be much higher than the plasma concentration. This finding, together with the known pharmacology and toxicology of ivermectin, warrants further investigation of this drug as a potential anti-cancer candidate if used at dose rates higher than those used for antiparasitic effects.

BZ resistance has been characterized by the presence of SNPs F200Y and F167Y on the β-tubulin protein. In *H. contortus* we, and other labs, have identified these SNPs in ivermectin resistant isolates never exposed to BZs or the frequency of these SNPs increased with repeated exposure to ivermectin, in the absence of BZ treatments. So we speculated that these SNPs may have a direct relationship with ivermectin effects. We hypothesized that these SNPs will result in different tubulin dynamics when compared to the wild type tubulins and that these SNPs may result in reduced ivermectin binding. For this in chapter four, manuscript III, I investigated the effects of the SNPs (F200Y and F167Y) on the polymerization of microtubules. Contrary to our hypothesis, the mutant and the wild tubulins polymerized at the same rates and the SNPs did not affect ivermectin binding. Ivermectin and moxidectin are both macrocyclic lactones. Ivermectin belongs to the avermectin group whereas moxidectin is from the milbemycin group. Both of these anthelmintics have a similar mode of action. However there are some differences in their structures, with ivermectin having a sugar moiety and moxidectin lacking it. Moxidectin has a partition co-efficient log P_{MOX}=6 whereas ivermectin has a log

P_{IVM}=4.8. This shows that moxidectin is much more lipophilic than ivermectin and hence has a higher retention time in fatty tissue and longer elimination half-life (Prichard et al., 2012). Apart from the structural differences, there have been reports of differences in their anthelmintic action. For example, studies on *C. elegans* have demonstrated that 9 nM ivermectin causes complete paralysis of the nematode, whereas 39 nM of moxidectin is required to get the same effects, furthermore the pharynx is more sensitive in the case of ivermectin as compared to moxidectin (Ardelli et al., 2009). It has also been suggested that ivermectin selects for resistance more rapidly than does moxidectin (Ranjan et al., 2002). Due to these similarities and differences between ivermectin and moxidectin, it was logical to investigate if tubulin also has a moxidectin binding site and, if so, are there any differences in the binding kinetics between the two. For this the effects of ivermectin and moxidectin were compared on tubulin polymerization of parasitic and mammalian tubulins. No significant differences were observed between ivermectin and moxidectin. However, varying results were obtained between mammalian and parasitic tubulin. Overall, our results suggest that ivermectin binds to α- and β-tubulin and that the SNPs (F200Y and F167Y) on β-tubulin have no direct effect on ivermectin binding. Moreover these SNPs did not alter tubulin dynamics. It can be hypothesized that there may be an indirect relationship between these SNPs and ivermectin; however this requires further investigations. Eng (PhD thesis, 2006) had found three amino acid substitutions in the helix-three domain on the β-tubulin protein of *Onchocerca volvulus* that had been under ivermectin selection for many years compared with β-tubulin from ivermectin naïve *O. volvulus*. This region interacts with the M-loop and is involved in making lateral contacts between monomers (Lowe et al., 2001). The region between amino acid 167 and 200 on

the β-tubulin protein provides monomer stability, so it can be speculated that any change in the structure may affect the overall morphology of the microtubules and perhaps, as a result affect the morphology of the amphid. Any changes corresponding to this region or to other neurons, may also effect the functioning of the ligand-gated chloride channels as microtubules are involved in anchoring receptors (Kneussel and Betz, 2000) which in turn can lead to impaired neurotransmission and could affect responses to ivermectin.

Lipophilic dyes can be taken up by nematodes through their receptor cilia. This is a technique frequently used to stain the chemosensory neurons of different worms. The worms having defective cilia are not able to take up these lipophilic dyes and are called dye filling defective (Hedgecock et al., 1985). In chapter five, manuscript IV, I have used *C. elegans* N2 and IVR-10 strains and found that the IVR-10 strain worms were defective in dye filling. The wild type N2 strain took up the lipophilic dye. As the amphids are required to taste the environment and avoid toxic substances the IVR-10 dye filling defective phenotype may be due to shortened amphids. This shortening of the amphids may be due to a number of reasons including mutations in the dyf-7 gene (Urdaneta-Marquez et al., 2014) or may be due to the presence of SNPs on tubulin. I also exposed the N2 and the IVR-10 strains of *C. elegans* to ivermectin and attempted to monitor its uptake via the amphids by using an ivermectin antibody. The amphidial pore fluoresced, indicating the presence of ivermectin in the pore. These results suggest that there may be an alternative route of entry of ivermectin, other than the oral-pharyngeal route, i.e., entry via the amphidial pore. Smith and Campbell (1996) also hypothesized a similar idea. They used *C. elegans* and paralyzed its pharynx by immersing the worms in alcohol. When they took out the nematodes and put them in 50 ng/ml ivermectin they remained

paralyzed, indicating ivermectin entered the worms despite having the pharynx paralyzed, as compared to the controls which regained motility when put in water.

There has been some evidence that the polylinker domain of P-glycoprotein can interact with tubulin (Georges, 2007). This interaction may be part of a signaling mechanism and any distortion in tubulin, for example the presence of SNPs, may affect the functioning of P-glycoprotein and could play a role in ivermectin resistance. Ivermectin has also proven as an excellent multidrug resistance reversing agent as it is a proven substrate for P-glycoproteins (Pouliot et al., 1997).

Taken together this thesis gives new information regarding the pharmacology of tubulin and its relationship to new pharmacological effects of ivermectin and possibly to ivermectin resistance. First it describes the behavior of recombinant tubulin proteins in vitro. Second it also established a new pharmacological effect of ivermectin and opens possible new avenues for considering ivermectin as an anti-cancer agent. Third it addresses the possibility that the β-tubulin SNPs (F167Y and F200Y) might have a direct relationship with ivermectin. Finally it showed that ivermectin may enter the nematodes through the amphidial pore. Overall the thesis has important implications for parasite control. In livestock there is a common practice of rotation of anthelmintics between BZs and macrocyclic lactones to delay the spread of resistance. The findings in the thesis suggest that this policy should be revisited as this may increase selection pressure on both anthelmintics. Similarly the combination of a BZ (e.g., albendazole) with ivermectin for lymphatic filariasis and livestock parasites also should be reconsidered. Previous studies have suggested that BZ resistance is irreversible (Elard et al., 1998), however a decrease in BZ resistance has been observed where levamisole was used to replace the BZ (Martin,

1987). It has been observed that in the case where ivermectin was given as a substitute drug for a BZ in a *H. contortus* population that was moderately BZ resistance, the level of BZ resistance worsened (Waller et al., 1989). These finding support our current understanding where we demonstrate that both ivermectin and BZ select on the same SNP sites in β-tubulin, and their combination may increase selection pressure.

References

Ardelli, B.F., Stitt, L.E., Tompkins, J.B., Prichard, R.K., 2009. A comparison of the effects of ivermectin and moxidectin on the nematode Caenorhabditis elegans. Veterinary parasitology 165, 96-108.

Banerjee, A., Kasmala, L.T., 1998. Differential assembly kinetics of alpha-tubulin isoforms in the presence of paclitaxel. Biochemical and biophysical research communications 245, 349-351.

Baraka OZ, Mahmoud BM, Marschke CK, Geary TG, Homeida MM and Williams JF (1996) Ivermectin distribution in the plasma and tissues of patients infected with Onchocerca volvulus. *European journal of clinical pharmacology* **50**(5): 407-410.

Barrère, V. Keller, K Samson-Himmelstjerna G V, Prichard R.K., 2013. Efficiency of a genetic test to detect benzimidazole resistant Haemonchus contortus nematodes in sheep farms in Quebec, Canada. Parasitology. International. 62: 464–470 (2013).

Dasgupta, D., Park, H., Harriman, G.C., Georg, G.I., Himes, R.H., 1994. Synthesis of a photoaffinity taxol analogue and its use in labeling tubulin. Journal of medicinal chemistry 37, 2976-2980.

Dadarkar SS, Deore MD and Gatne MM 2007. Comparative evaluation of acute toxicity of ivermectin by two methods after single subcutaneous administration in rats. *Regulatory toxicology and pharmacology : RTP* **47**(3): 257-260.

Detrich HW 3rd, Parker SK, Williams RC, Jr., Nogales E, Downing KH., 2000. Cold adaptation of microtubule assembly and dynamics. Structural interpretation of primary sequence changes present in the alpha- and beta-tubulins of Antarctic fishes. The Journal of Biological Chemistry, 275:37038-47.

Elard, L., Sauve, C., Humbert, J.F., 1998. Fitness of benzimidazole-resistant and -susceptible worms of Teladorsagia circumcincta, a nematode parasite of small ruminants. Parasitology 117 (Pt 6), 571-578.

Georges, E., 2007. The P-glycoprotein (ABCB1) linker domain encodes high-affinity binding sequences to alpha- and beta-tubulins. Biochemistry 46, 7337-7342.

Hedgecock, E.M., Culotti, J.G., Thomson, J.N., Perkins, L.A., 1985. Axonal guidance mutants of Caenorhabditis elegans identified by filling sensory neurons with fluorescein dyes. Developmental biology 111, 158-170.

Falzon, L.C., Menzies, P.I., Shakya, K.P., Jones-Bitton, A., Vanleeuwen, J., Avula, J., Stewart, H., Jansen, J.T., Taylor, M.A., Learmount, J., Peregrine, A.S., 2013.

Anthelmintic resistance in sheep flocks in Ontario, Canada. Vet. Parasitol. 193, 150–162.

Fleming, J.T.; Squire, M.D.; Barnes T.M.; Tornoe, C.; Matsuda, K.; Ahnn, J.; Fire, A. ; et al.,1997. *Caenorhabditis elegans* levamisole resistance genes lev-1,unc-29 and unc-38 encode functional nicotinic acetylcholine receptor subunits. *Journal of Neuroscience*, v. 17, p. 5843-5857.

Freeman, A.S., Nghiem, C., Li, J., Ashton, F.T., Guerrero, J., Shoop, W.L., Schad, G.A., 2003. Amphidial structure of ivermectin-resistant and susceptible laboratory and field strains of Haemonchus contortus. Veterinary parasitology 110, 217-226.

Kaplan, R.M., Vidyashankar, A.N., 2012. An inconvenient truth: global worming and anthelmintic resistance. Veterinary parasitology 186, 70-78.

Kerboeuf, D., Blackhall, W., Kaminsky, R., von Samson-Himmelstjerna, G., 2003. P-glycoprotein in helminths: function and perspectives for anthelmintic treatment and reversal of resistance. International journal of antimicrobial agents 22, 332-346.

Kneussel, M., Betz, H., 2000. Clustering of inhibitory neurotransmitter receptors at developing postsynaptic sites: the membrane activation model. Trends in neurosciences 23, 429-435.

Little, P.R., Hodge, A., Watson, T.G., Seed, J.A., Maeder, S.J., 2010. Field efficacy and safety of an oral formulation of the novel combination anthelmintic, derquantel-abamectin, in sheep in New Zealand. N. Z. Vet. J. 58, 121–129

Lowe J, Li H, Downing KH, Nogales E., 2001. Refined structure of alpha beta-tubulin at 3.5 A resolution. Journal of molecular biology, 313:1045-57.

Martin, P.J., 1987. Development and control of resistance to anthelmintics. International journal for parasitology 17, 493-501.

Mederos, A., Fernandez, S., VanLeeuwen, J., Peregrine, A.S., Kelton, D., Menzies, P., LeBoeuf, A., Martin, R., 2010. Prevalence and distribution of gastrointestinal nematodes on 32 organic and conventional commercial sheep farms in Ontario and Quebec, Canada (2006-2008). Veterinary parasitology 170, 244-252.

Njue, A.I.; Hayashi, J.; Kinne, L.; Fenge, X.P.; Prichard, R.K. 2004. Mutations in the extracellular domain of glutamte-gated chloride channel alpha3 and beta subunits from ivermectin-resistant *Cooperia oncophora* affect agonist sensitivity. *Journal of Neurochemistry*, v. 89, p. 1137-1147.

Pouliot, J.F., L'Heureux, F., Liu, Z., Prichard, R.K., Georges, E., 1997. Reversal of P-glycoprotein-associated multidrug resistance by ivermectin. Biochemical pharmacology 53, 17-25.

Prichard, R.K., Roulet, A., 2007. ABC transporters and beta-tubulin in macrocyclic lactone resistance: prospects for marker development. Parasitology 134, 1123-1132.

Prichard R, Ménez C and Lespine A (2012) Moxidectin and the avermectins: Consanguinity but not identity. *International Journal for Parasitology: Drugs and Drug Resistance* **2**: 134-153.

Ranaivoson FM, Gigant B, Berritt S, Joullie M, Knossow M (2012). Structural plasticity of tubulin assembly probed by vinca-domain ligands. Acta crystallographica Section D, Biological crystallography, 68:927-34.

Ranjan, S., Wang, G.T., Hirschlein, C., Simkins, K.L., 2002. Selection for resistance to macrocyclic lactones by Haemonchus contortus in sheep. Vet. Parasitol. 103, 109–117.

Serrano, L., Avila, J., Maccioni, R.B., 1984. Limited proteolysis of tubulin and the localization of the binding site for colchicine. The Journal of biological chemistry 259, 6607-6611.

Smith, H., Campbell, W.C., 1996. Effect of ivermectin on Caenorhabditis elegans larvae previously exposed to alcoholic immobilization. The Journal of parasitology 82, 187-188.

Starich, T.A., Herman, R.K., Kari, C.K., Yeh, W.H., Schackwitz, W.S., Schuyler, M.W., Collet, J., Thomas, J.H., Riddle, D.L., 1995. Mutations affecting the chemosensory neurons of Caenorhabditis elegans. Genetics 139, 171-188.

Urdaneta-Marquez, L., Bae, S.H., Janukavicius, P., Beech, R., Dent, J., Prichard, R., 2014. A dyf-7 haplotype causes sensory neuron defects and is associated with macrocyclic lactone resistance worldwide in the nematode parasite Haemonchus contortus. International journal for parasitology 44, 1063-1071.

van Wyk, J.A., Malan, F.S., 1988. Resistance of field strains of Haemonchus contortus to ivermectin, closantel, rafoxanide and the benzimidazoles in South Africa. The Veterinary record 123, 226-228.

Waller, P.J., Donald, A.D., Dobson, R.J., Lacey, E., Hennessy, D.R., Allerton, G.R., Prichard, R.K., 1989. Changes in anthelmintic resistance status of Haemonchus contortus and Trichostrongylus colubriformis exposed to different anthelmintic selection pressures in grazing sheep. International journal for parasitology 19, 99-110.

Wolstenholme, A.J., Rogers, A.T., 2005. Glutamate-gated chloride channels and the mode of action of the avermectin/milbemycin anthelmintics. Parasitology 131 Suppl, S85-95.

Xu, M., Molento, M., Blackhall, W., Ribeiro, P., Beech, R., Prichard, R., 1998. Ivermectin resistance in nematodes may be caused by alteration of P-glycoprotein homolog. Molecular and biochemical parasitology 91, 327-335.